Electronic Supplementary Material (ESI) for RSC Advances.

Supporting Information

for

Allylation of isatin-derived N-Boc-hydrazones followed by Pd-catalyzed carboamination reaction: an entry to 3-spiro-pyrazolidyl-oxindoles

Stefano Gazzotti, Marco Manenti, Leonardo Lo Presti and Alessandra Silvani*

Table of Contents

4a ^{1}H NMR (300 MHz, $CDCl_3$):

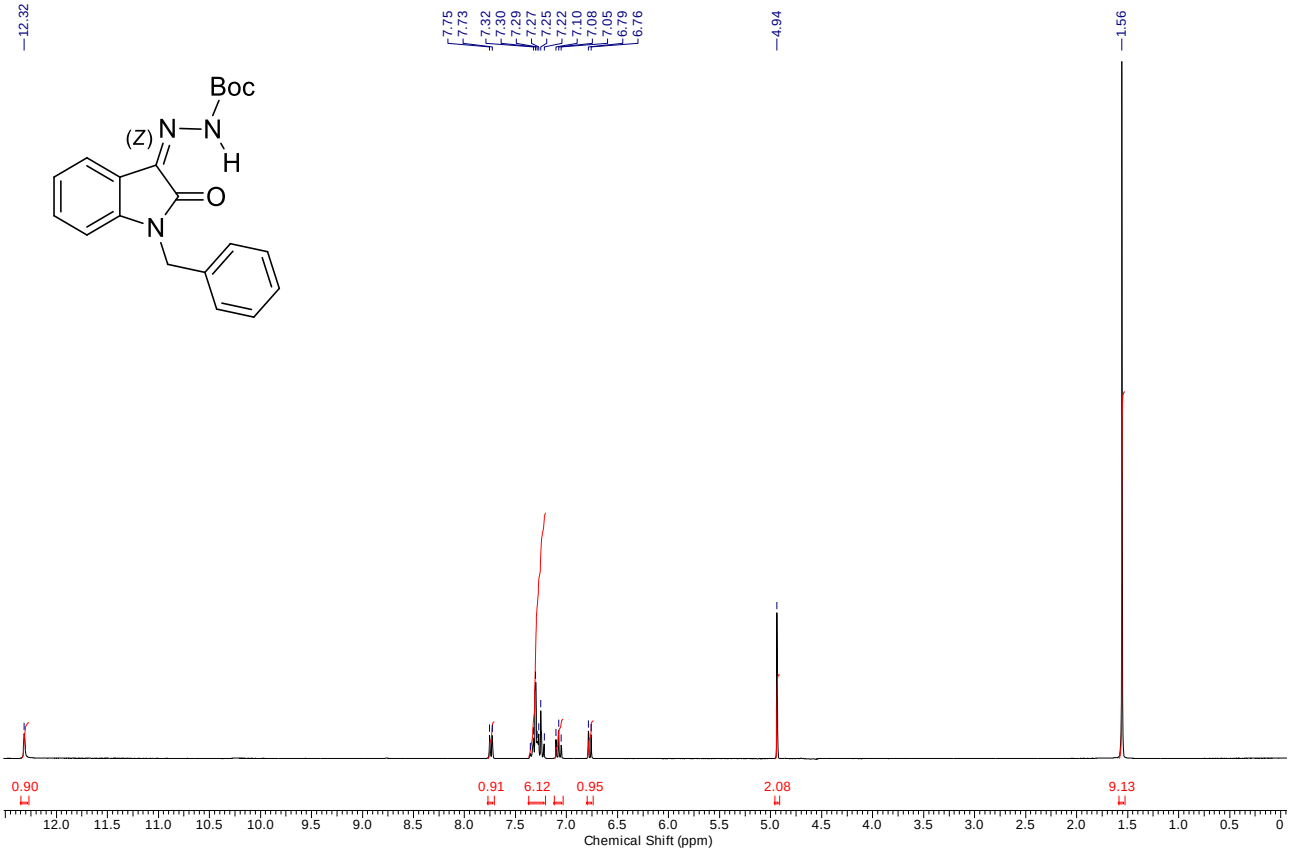

4a ^{13}C NMR (101 MHz, ATP, $CDCl_3$):

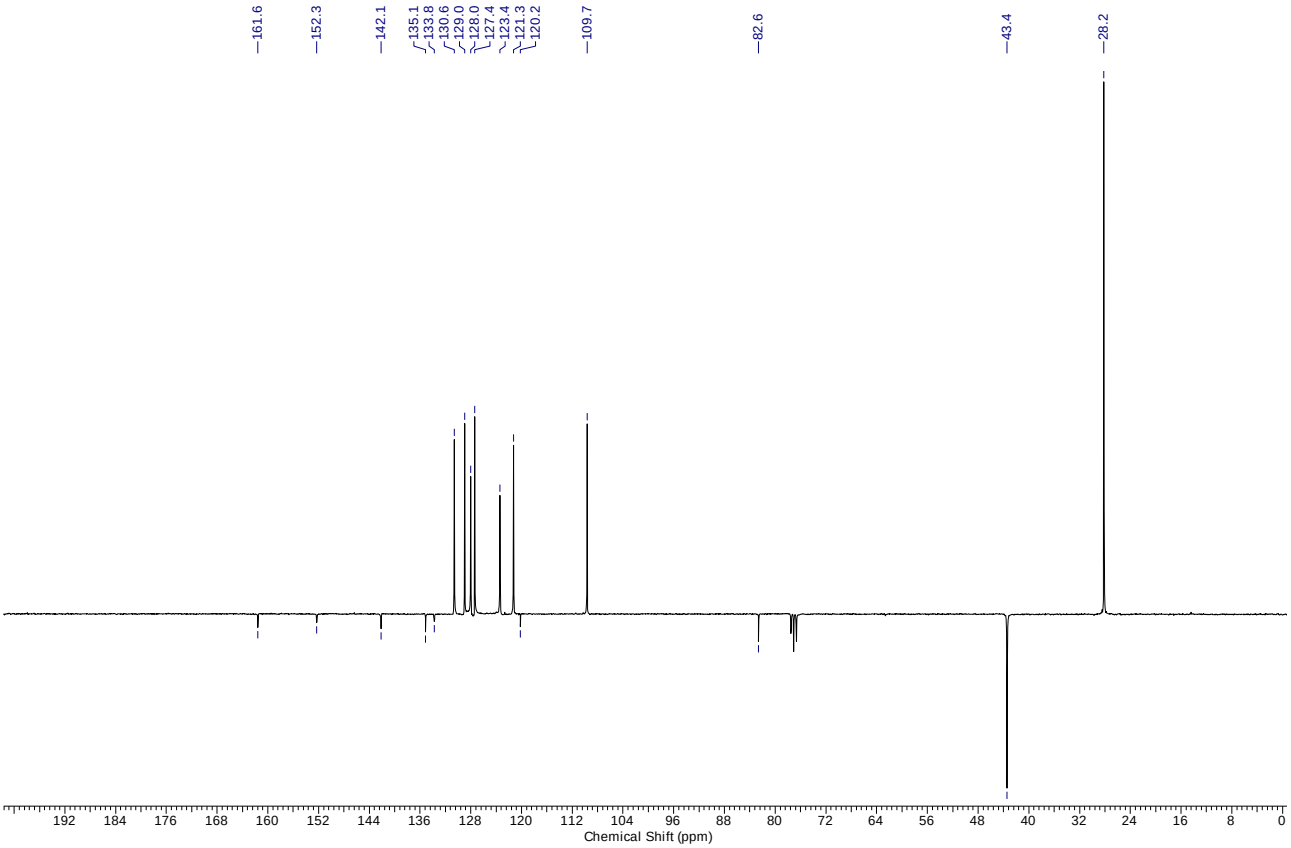

4b ^{1}H NMR (300 MHz, $CDCl_3$):

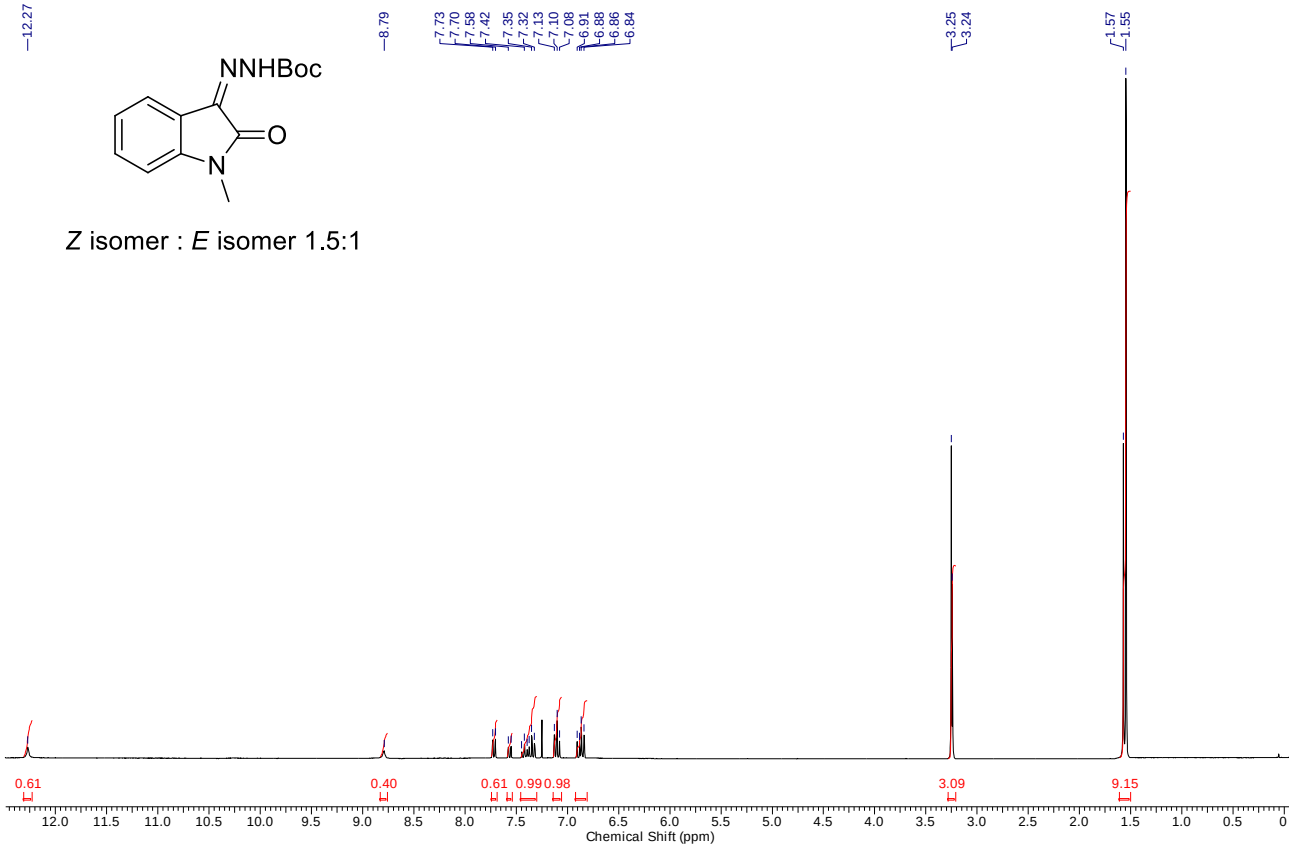

4b ^{13}C NMR (101 MHz, ATP, $CDCl_3$):

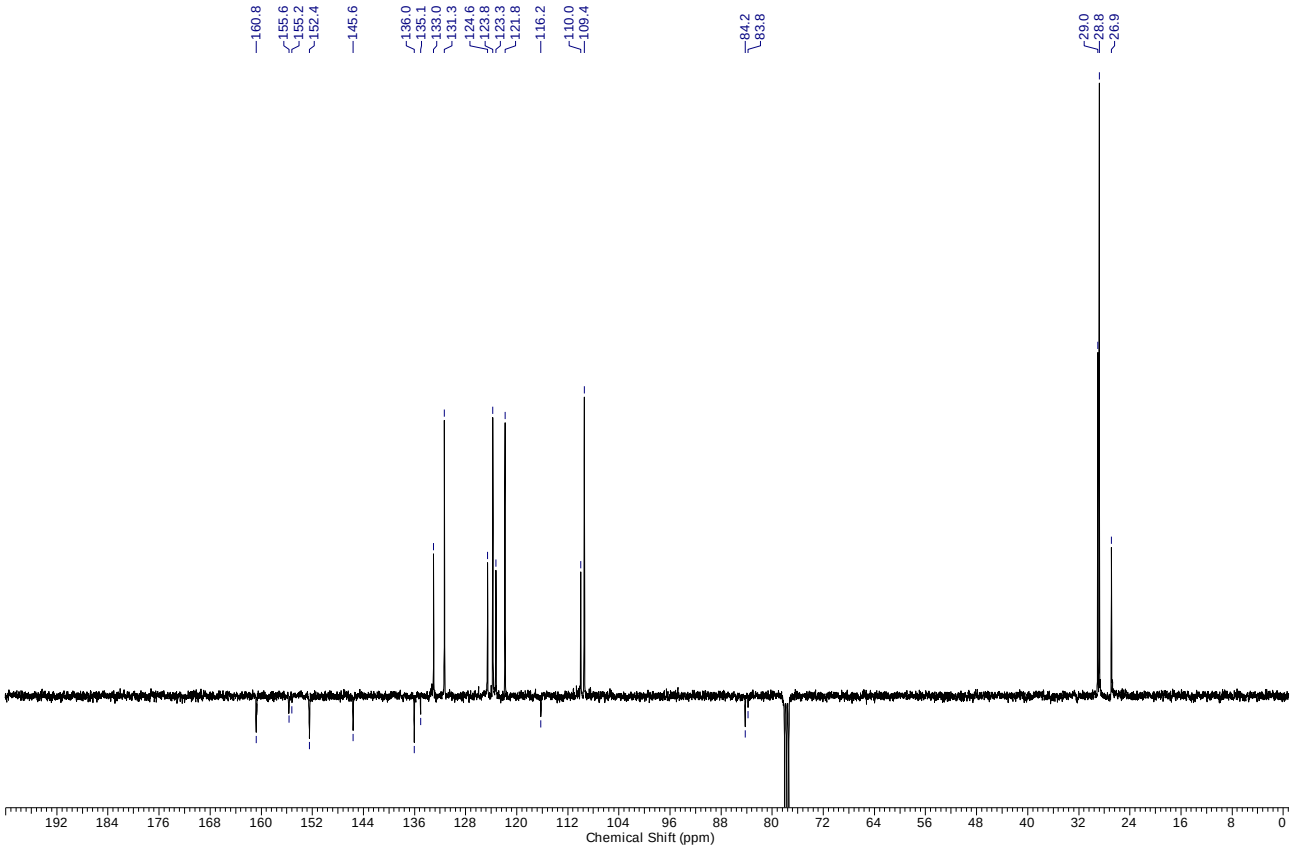

4c ^{1}H NMR (300 MHz, $CDCl_3$):

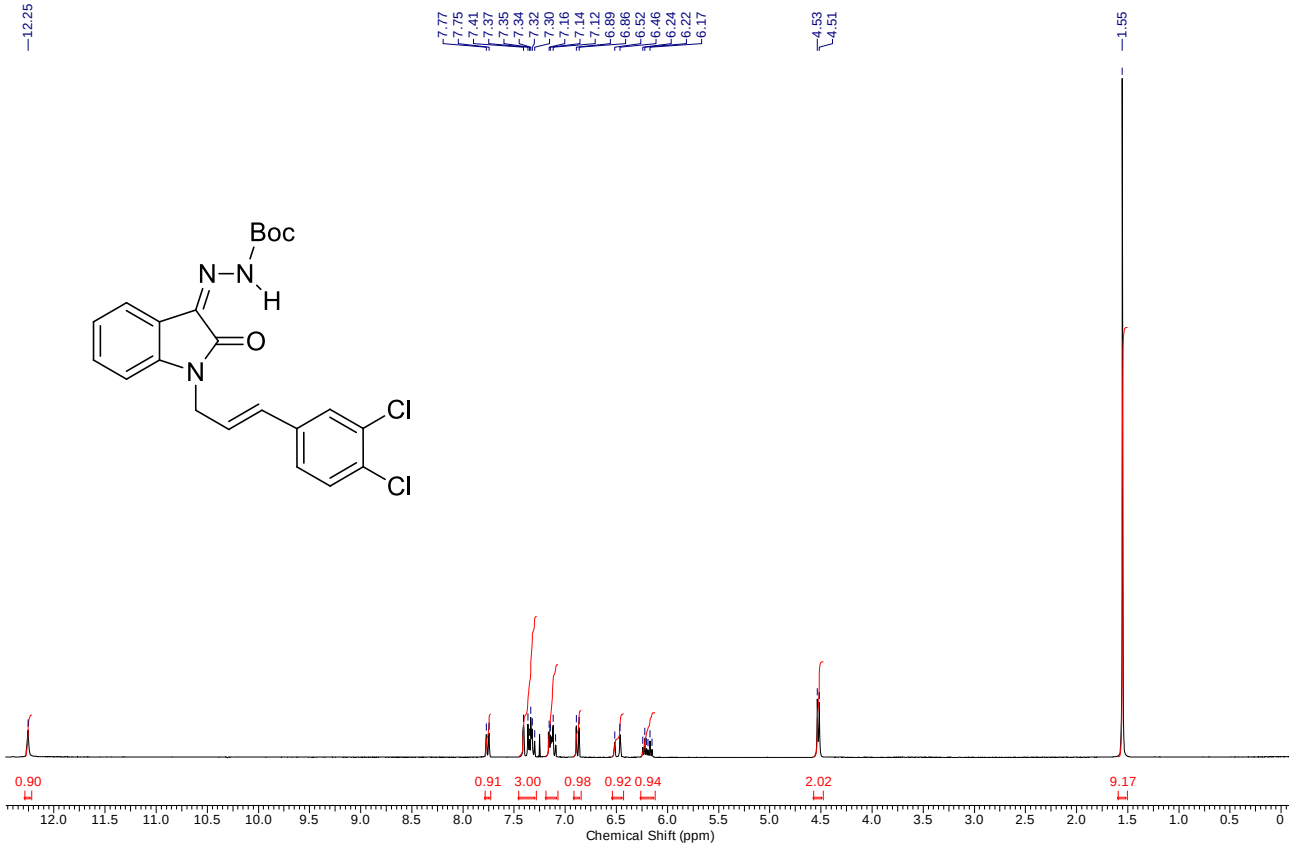

4c ^{13}C NMR (101 MHz, ATP, $CDCl_3$):

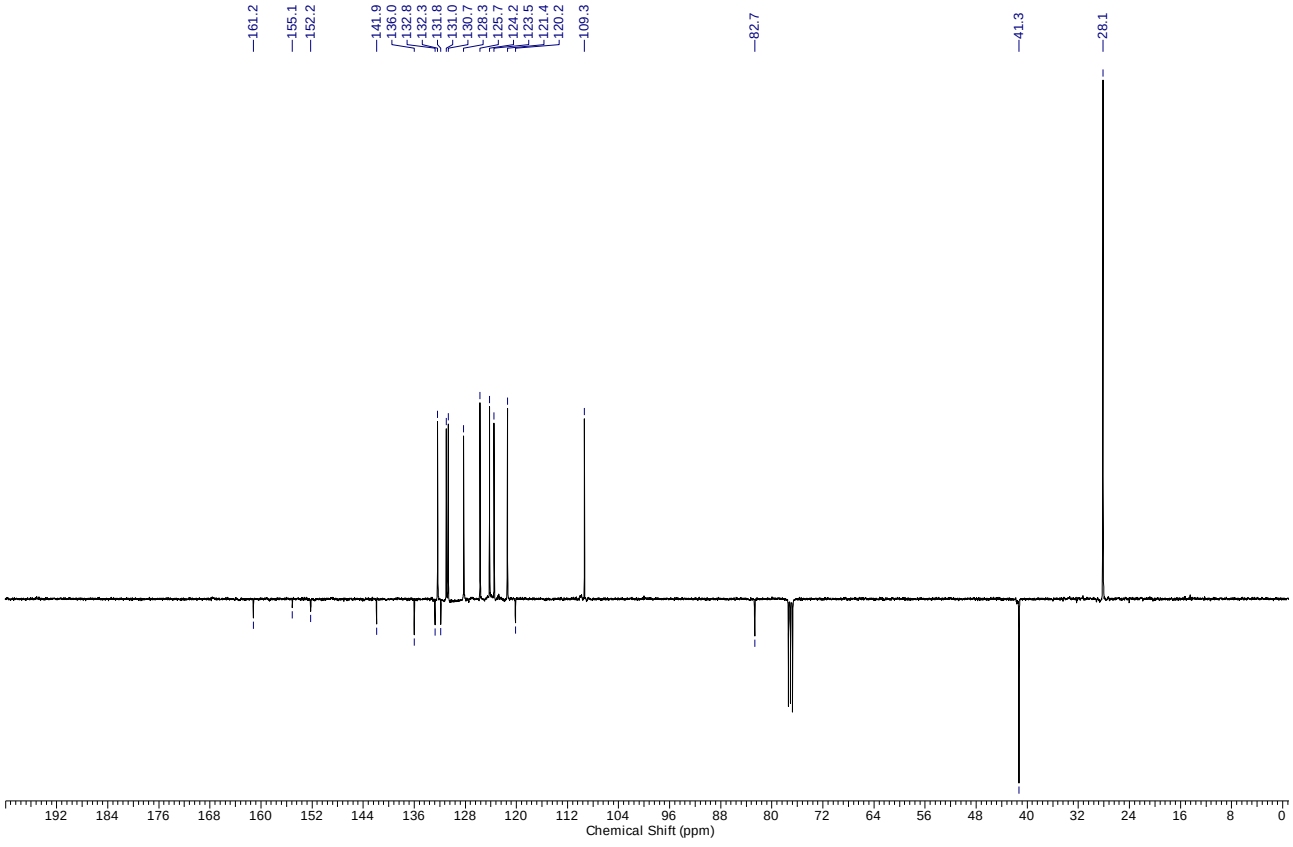

4d ^{1}H NMR (300 MHz, $CDCl_3$):

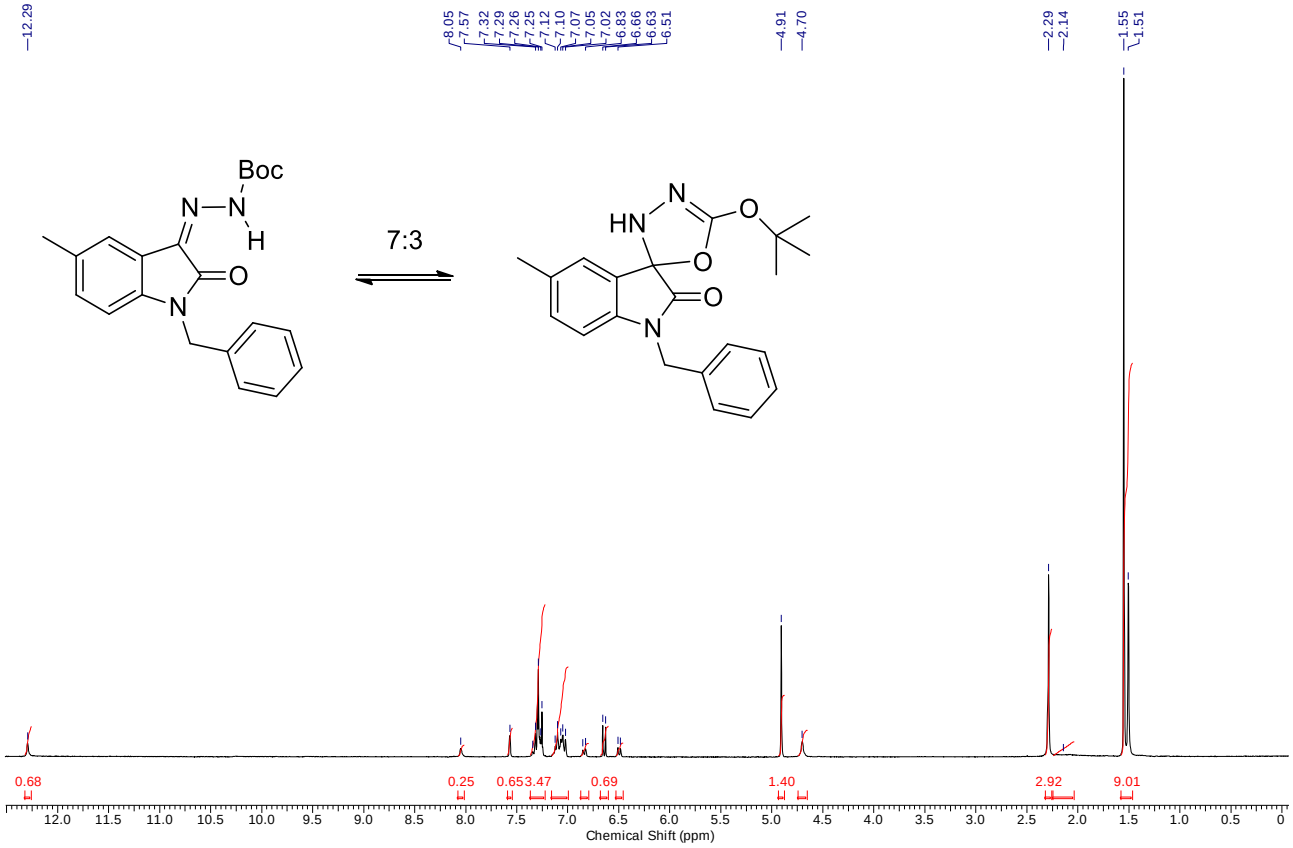

4d ^{13}C NMR (101 MHz, ATP, $CDCl_3$):

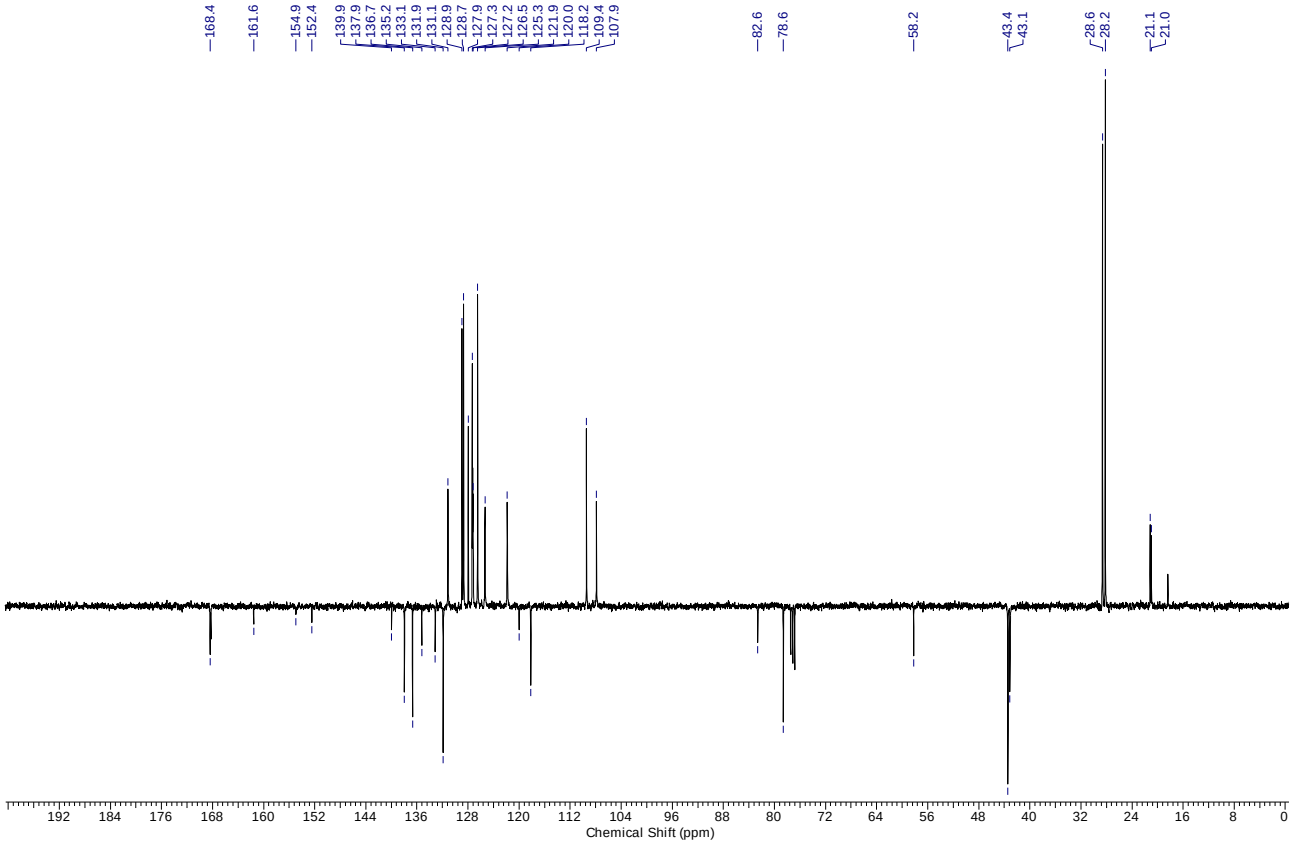

4e ^{1}H NMR (300 MHz, $CDCl_3$):

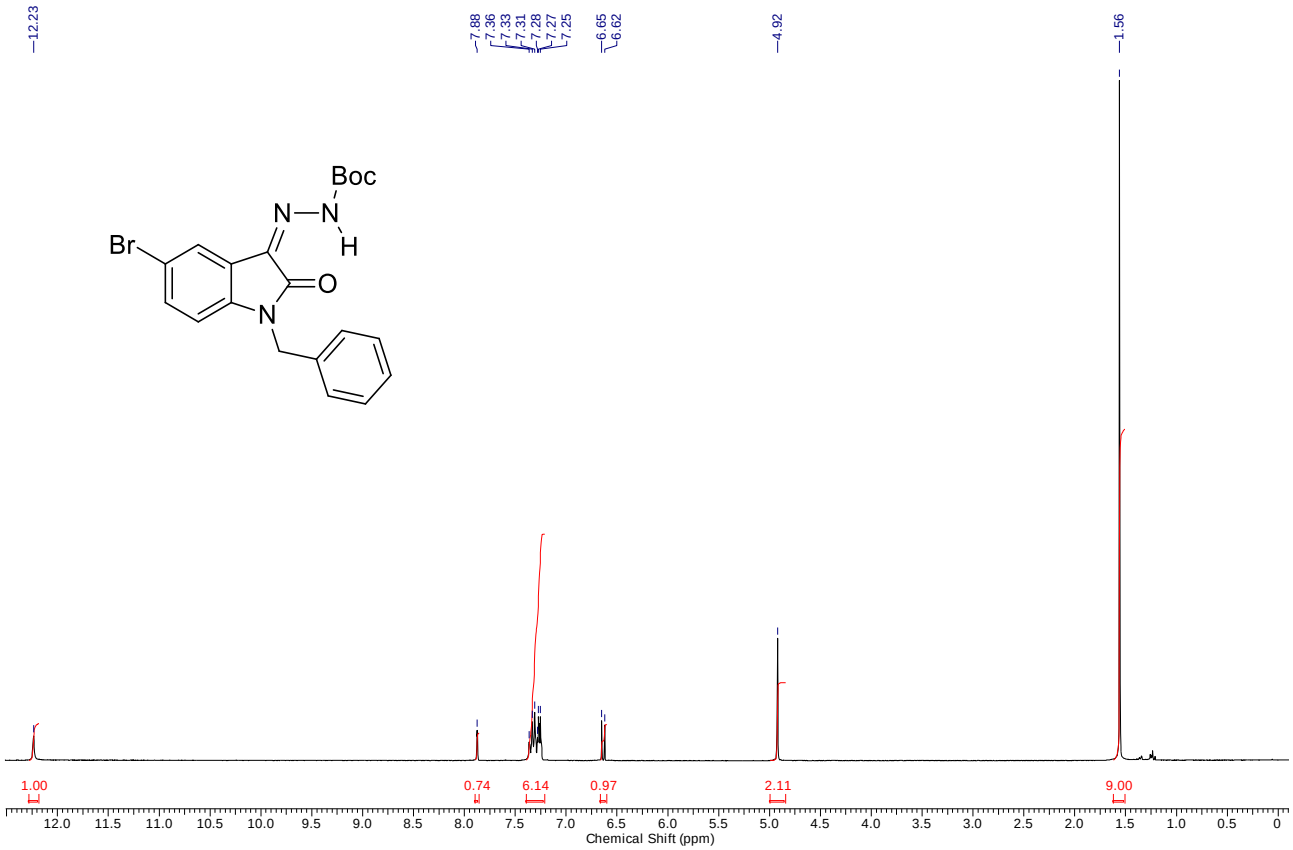

4e ^{13}C NMR (101 MHz, ATP, $CDCl_3$):

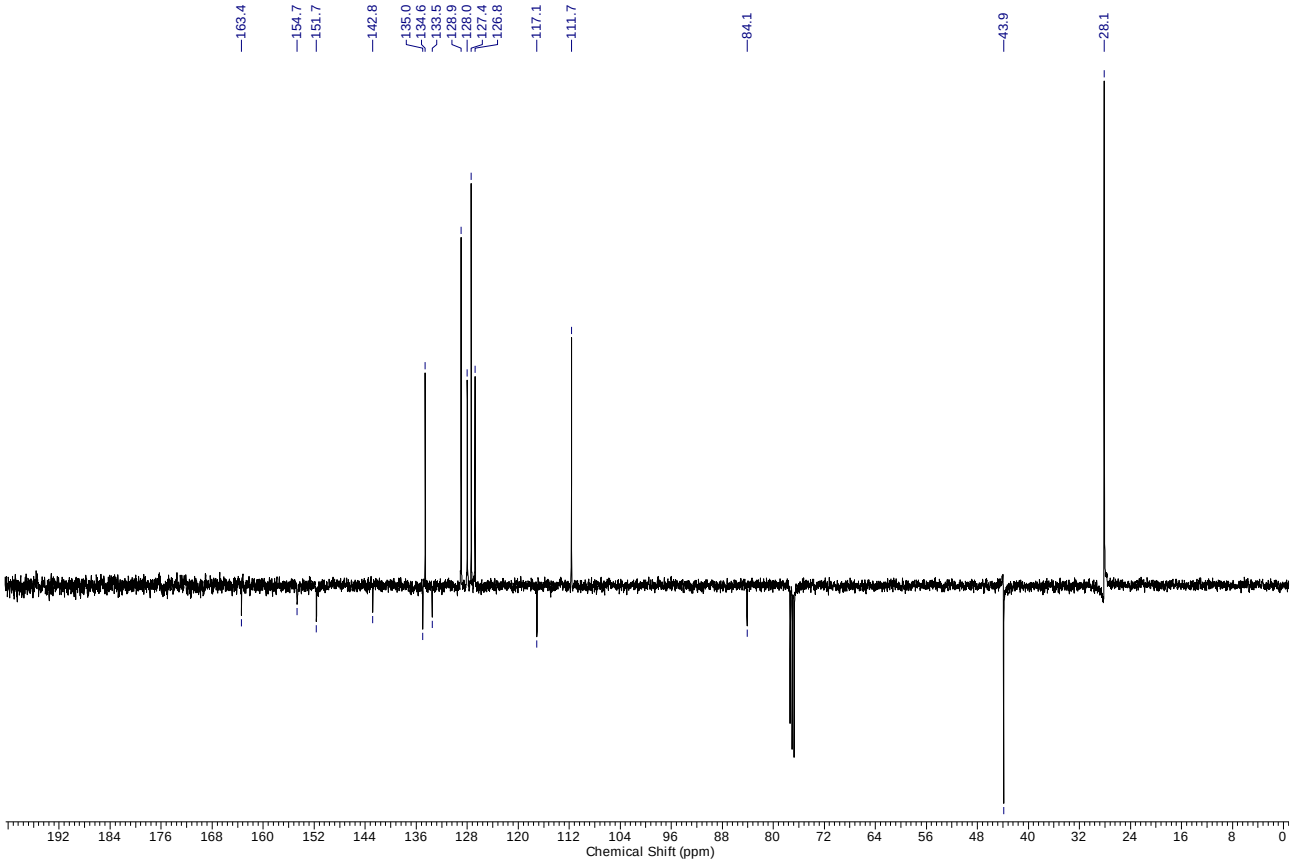

4f ^{1}H NMR (400 MHz, $CDCl_3$):

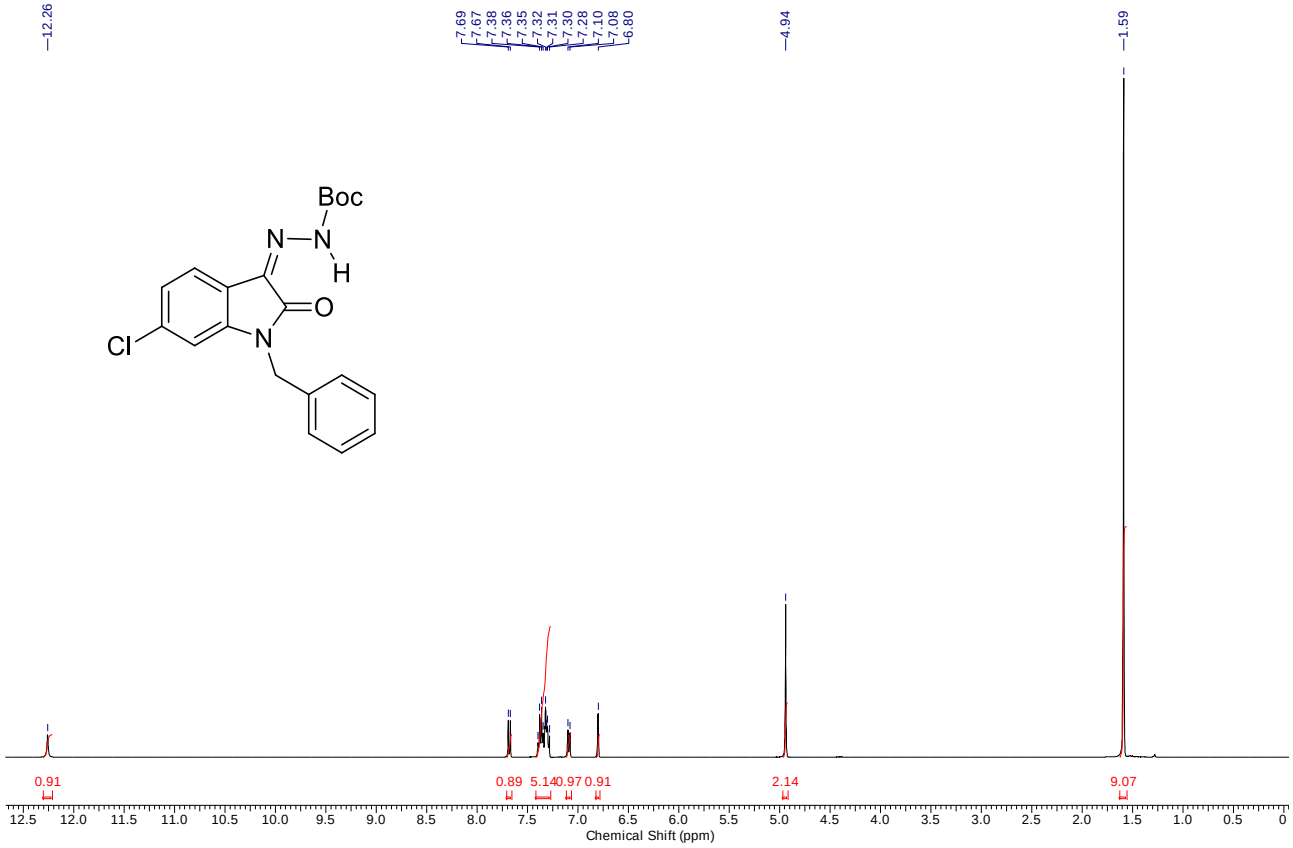

4f ^{13}C NMR (101 MHz, ATP, $CDCl_3$):

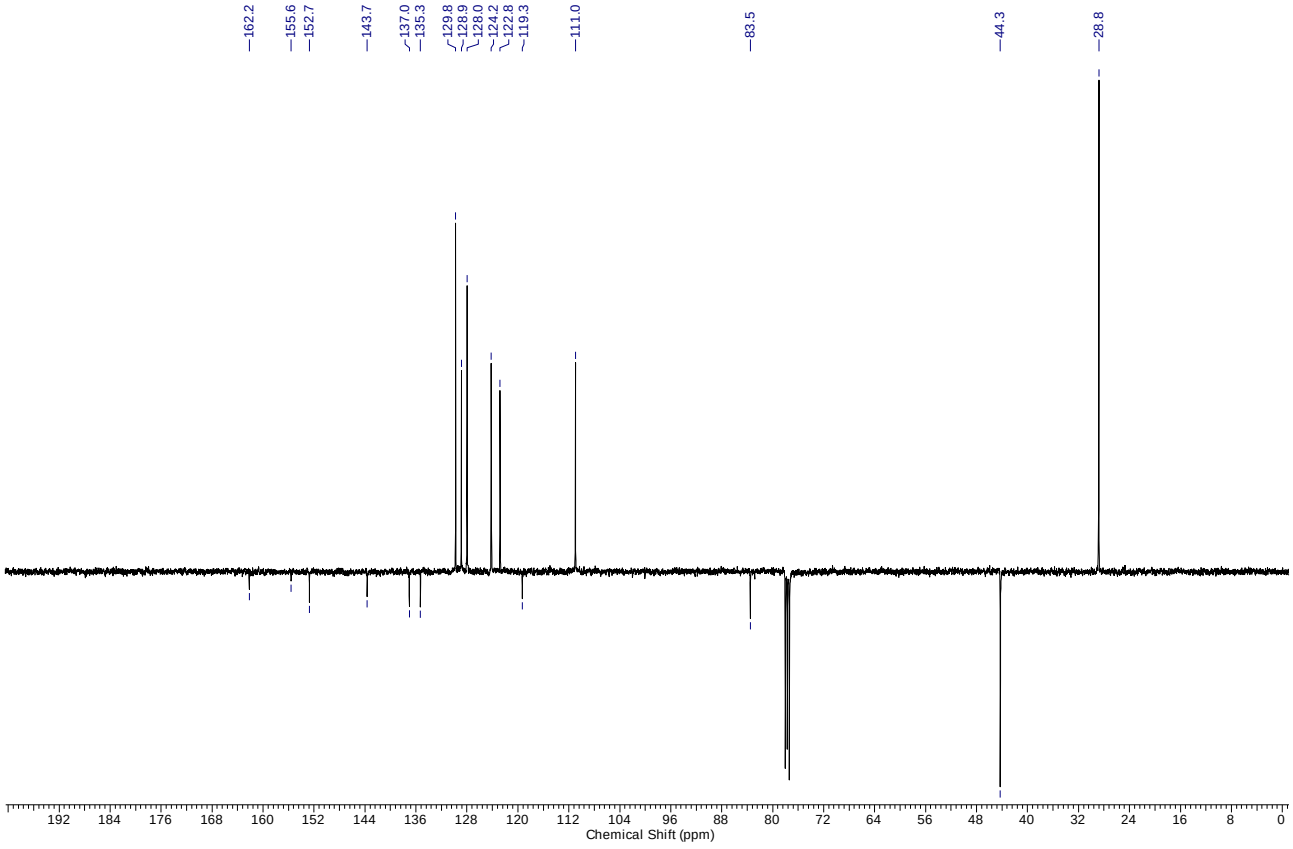

4g ^{1}H NMR (300 MHz, $CDCl_3$):

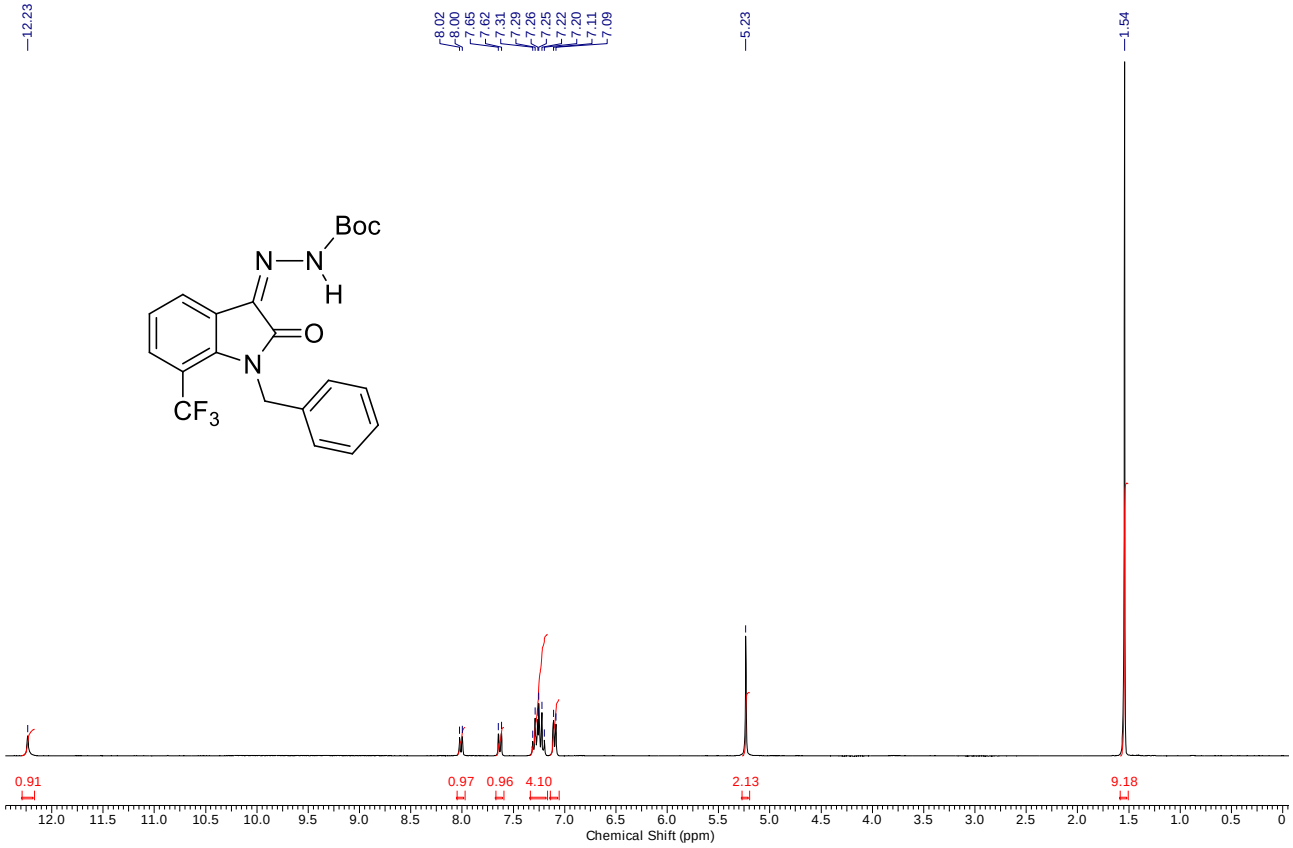

4g ^{13}C NMR (101 MHz, ATP, $CDCl_3$):

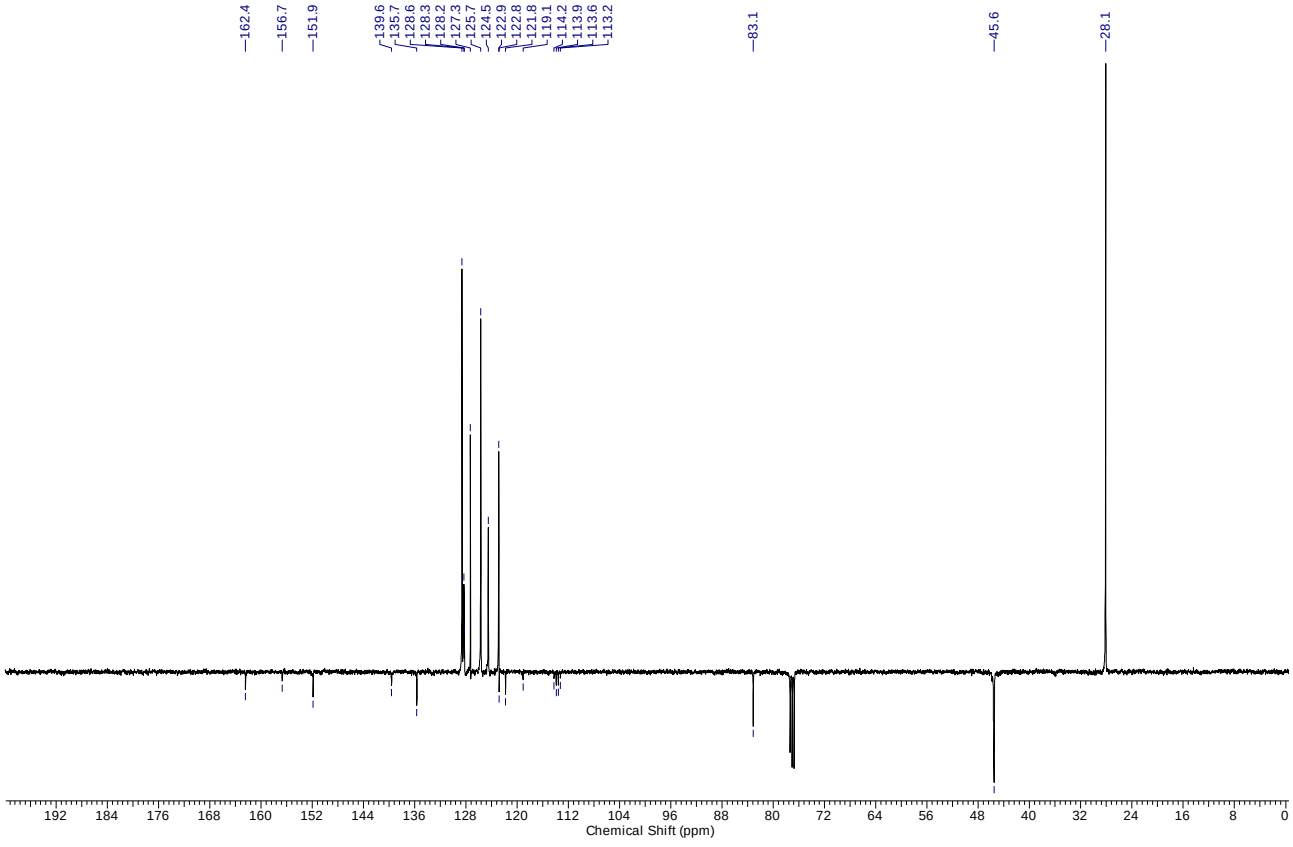

4h^{1}H NMR (400 MHz, $CDCl_3$):

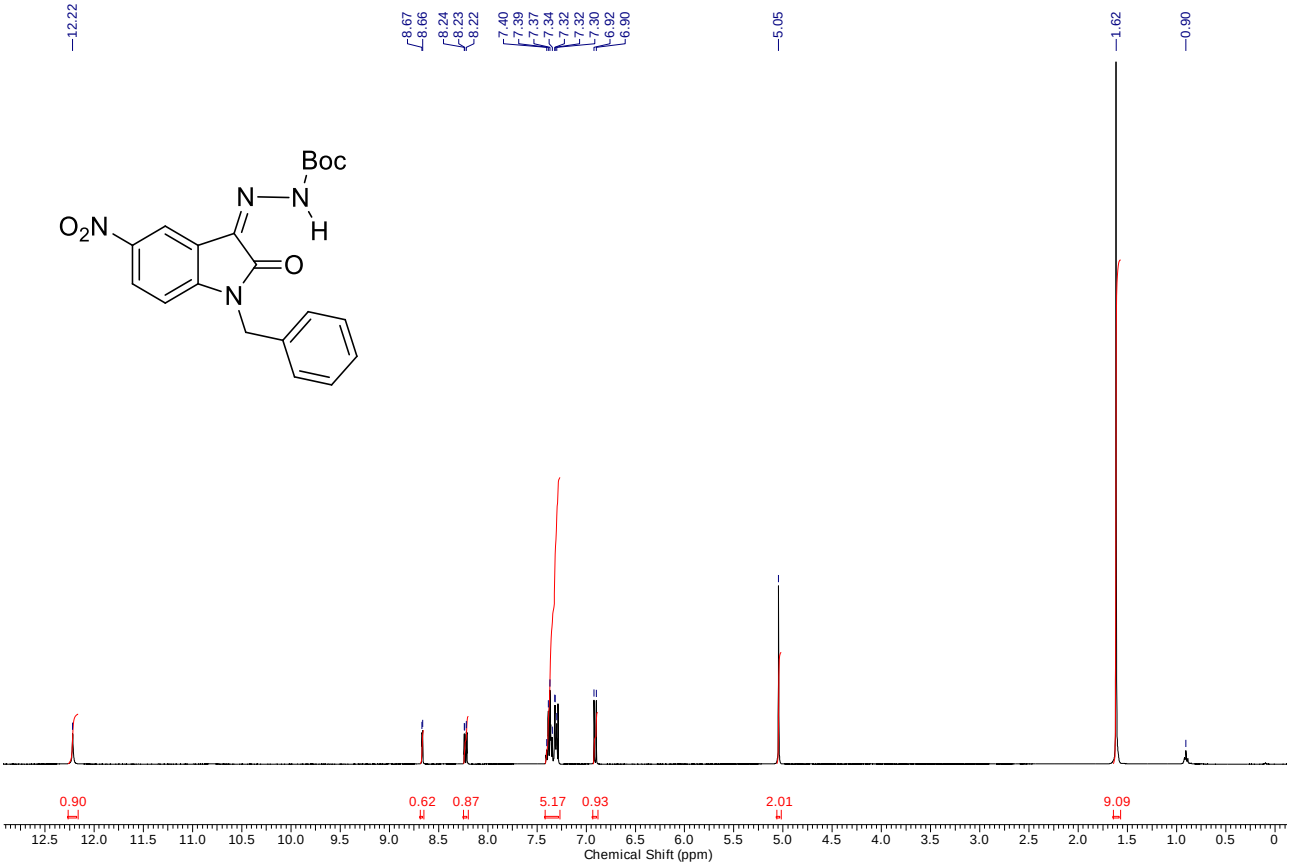

4h ^{13}C NMR (101 MHz, APT, $CDCl_3$):

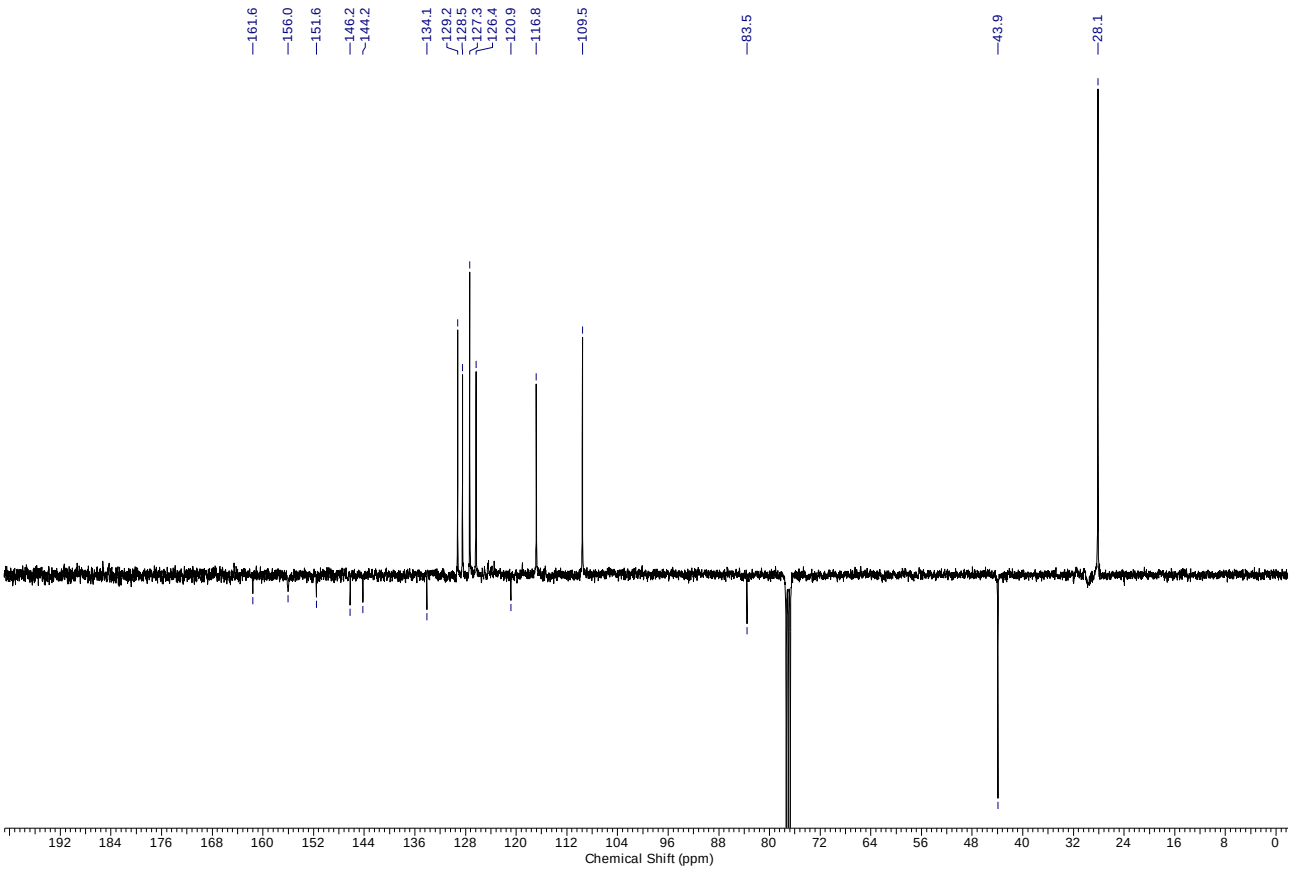

4i ^{1}H NMR (300 MHz, $CDCl_3$):

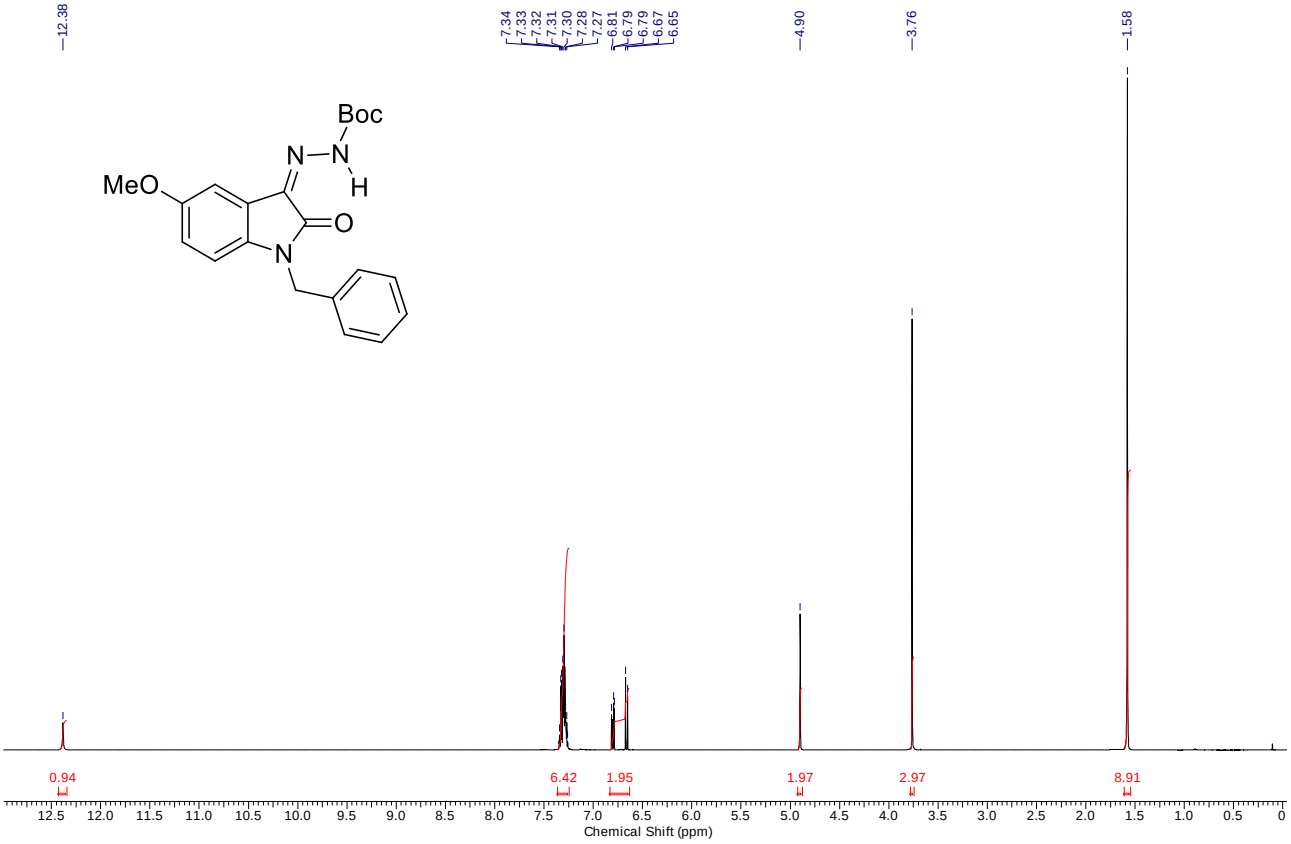

4i ^{13}C NMR (75 MHz, APT, $CDCl_3$):

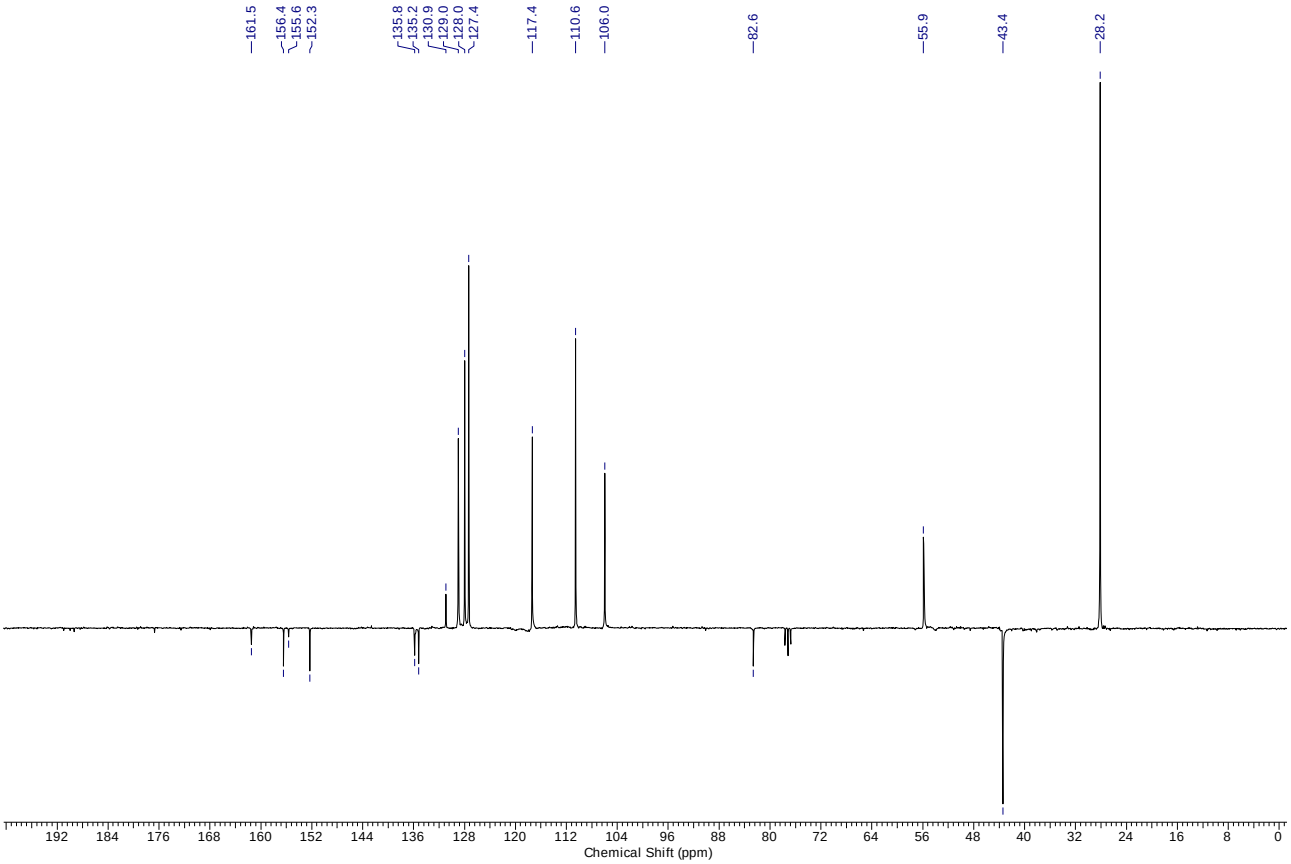

4j ^{1}H NMR (400 MHz, $CDCl_3$):

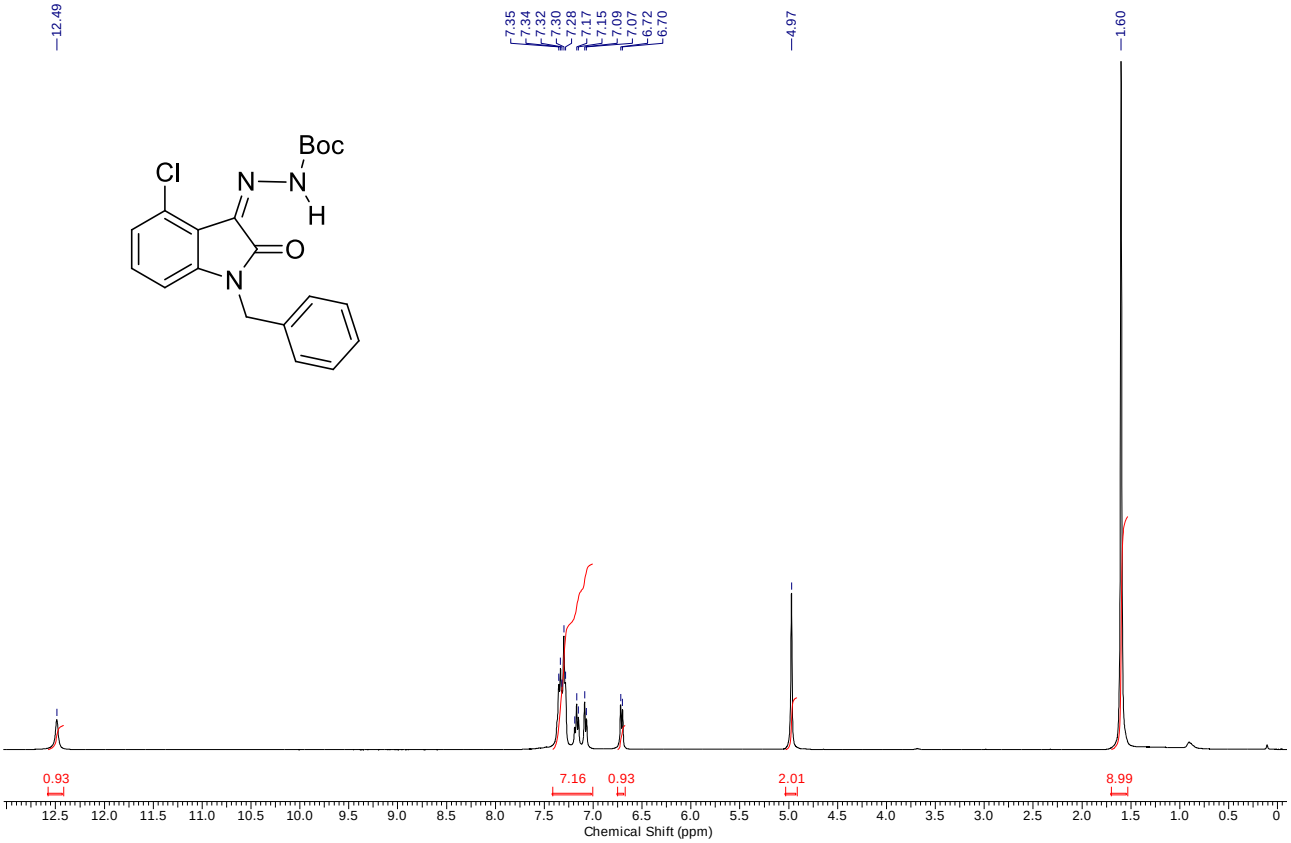

4j ^{13}C NMR (101 MHz, ATP, $CDCl_3$):

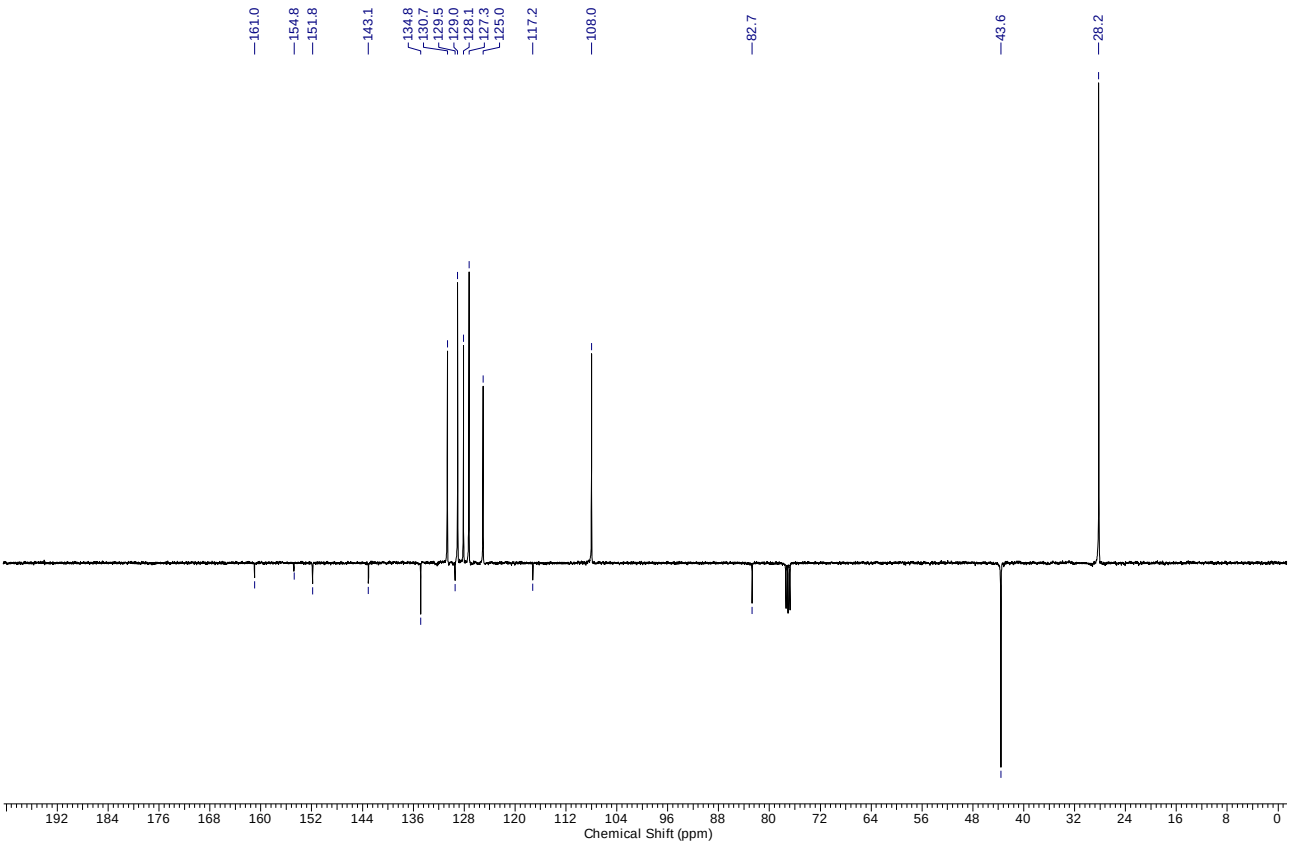

5a ^{1}H NMR (400 MHz, $CDCl_3$):

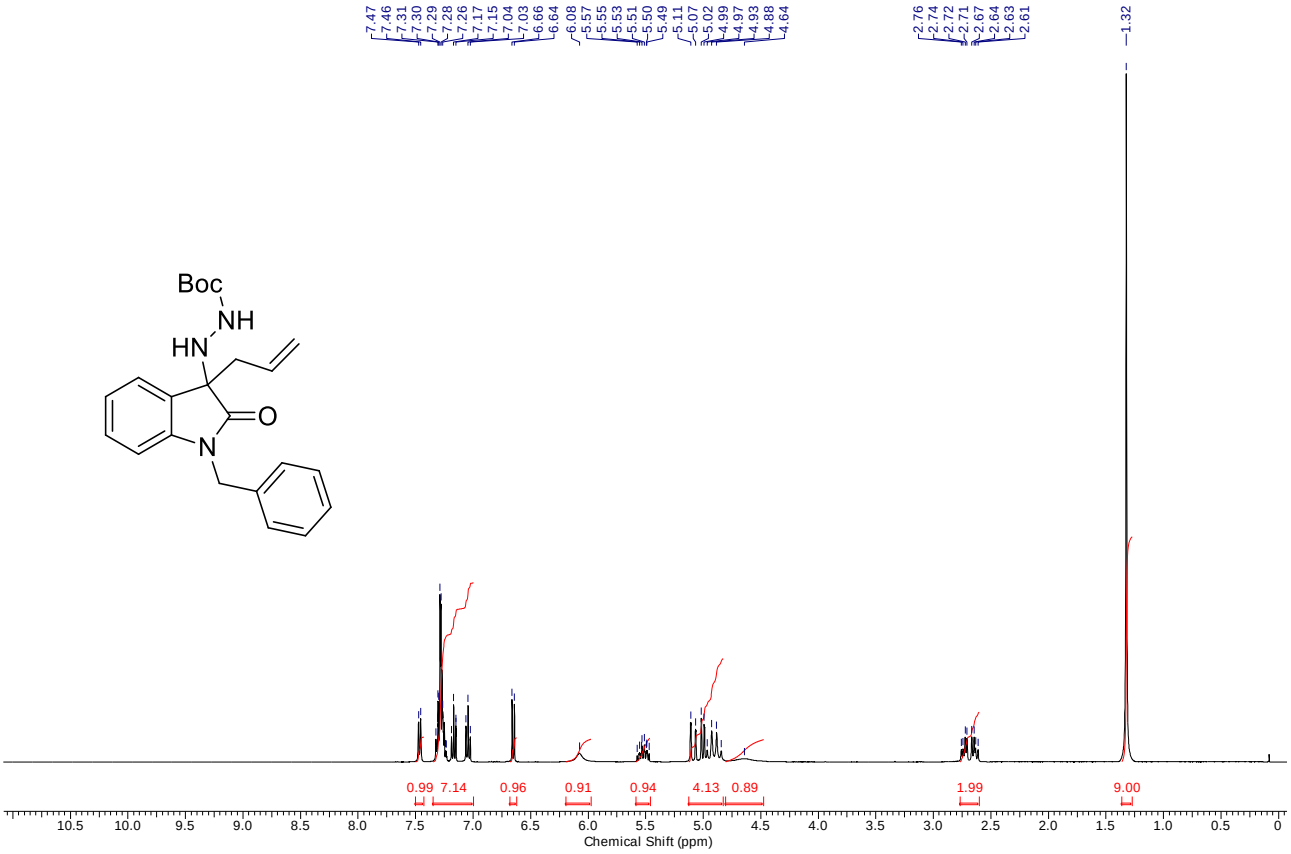

5a ^{13}C NMR (101 MHz, ATP, $CDCl_3$):

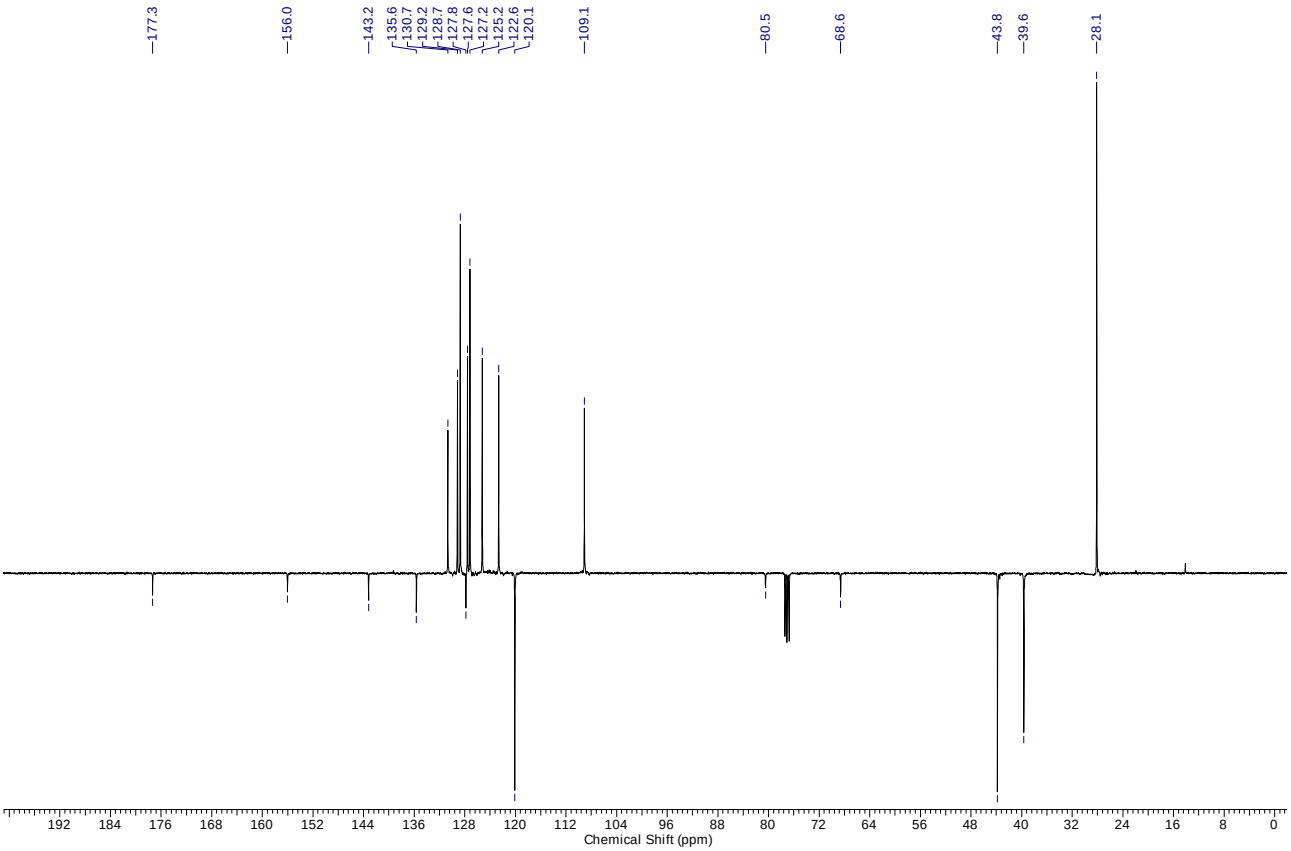

5b ^{1}H NMR (300 MHz, $CDCl_3$):

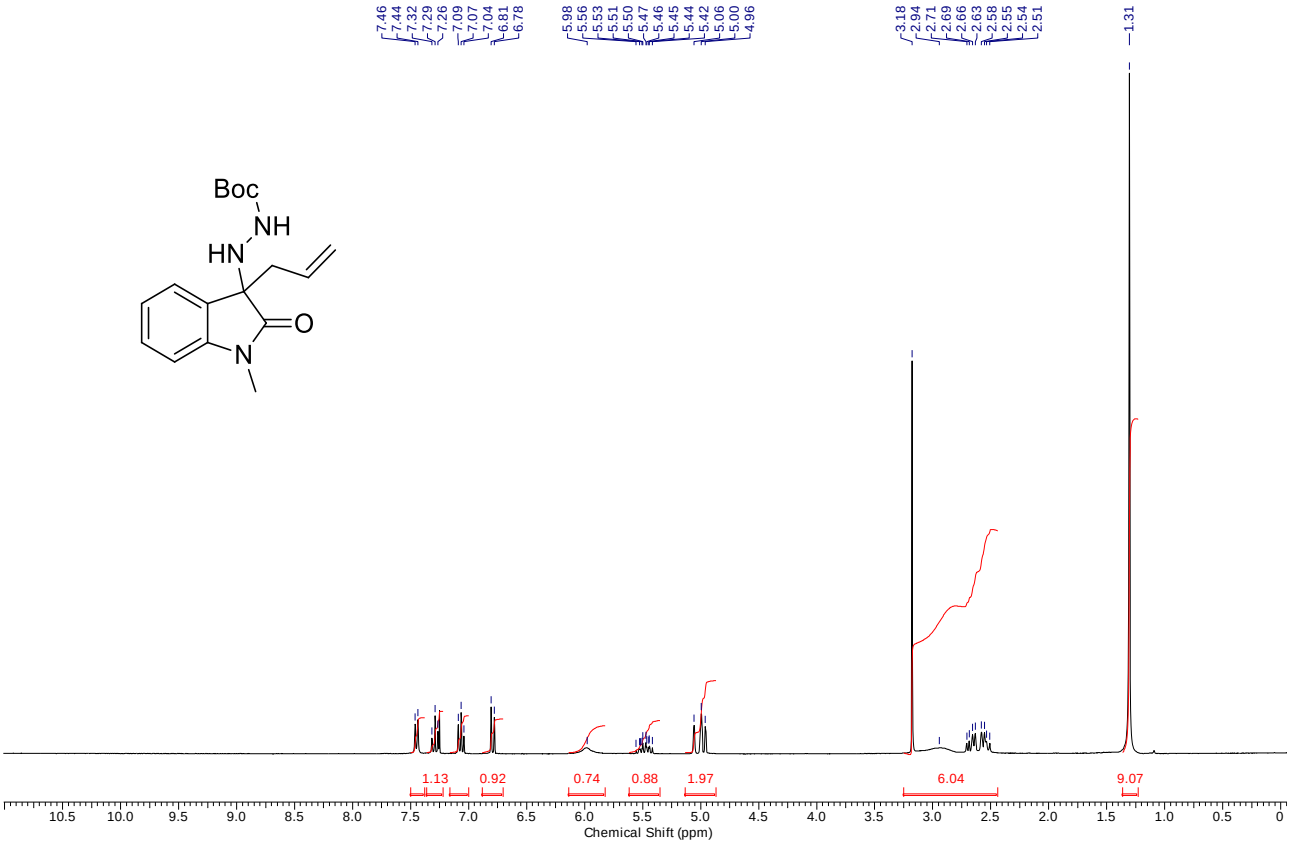

5b ^{13}C NMR (101 MHz, ATP, $CDCl_3$):

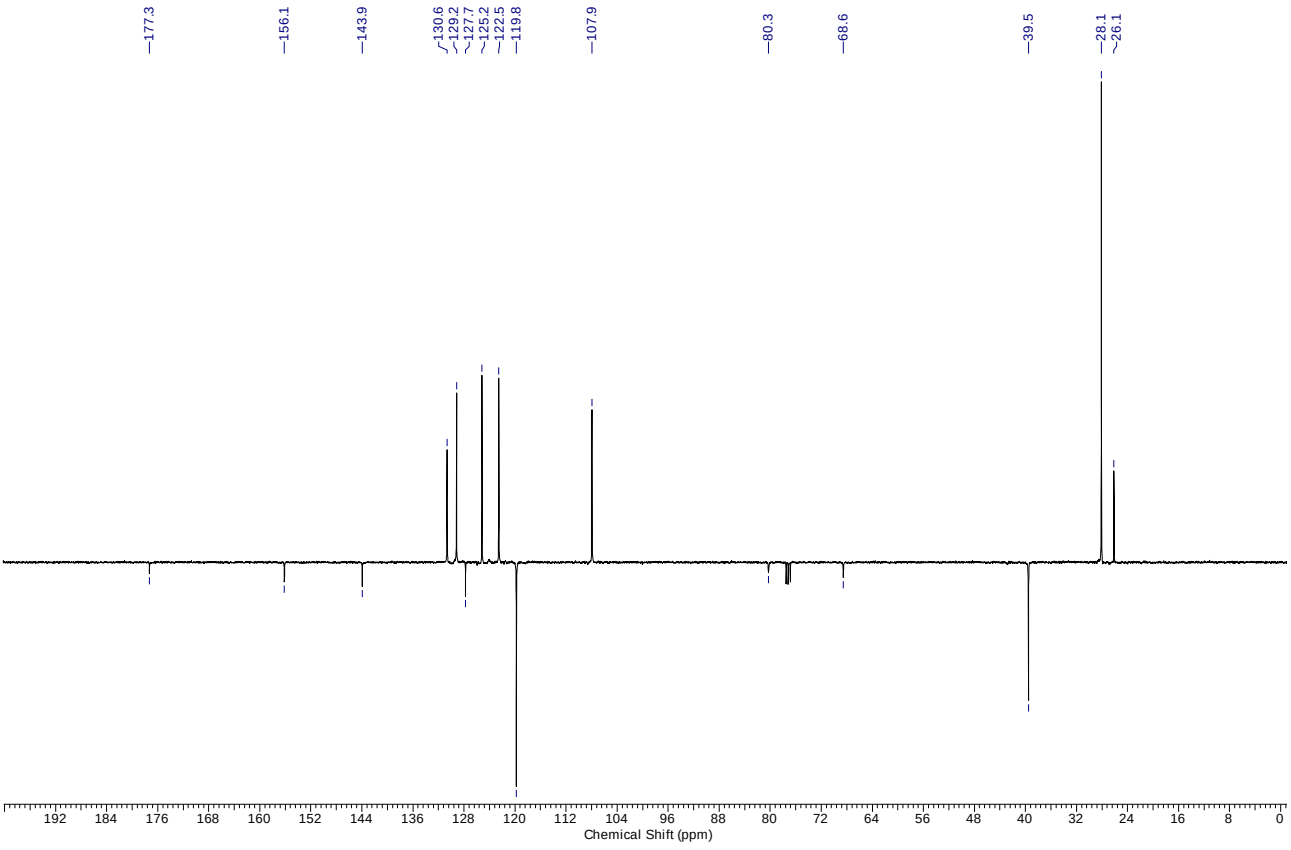

5c ^{1}H NMR (300 MHz, $CDCl_3$):

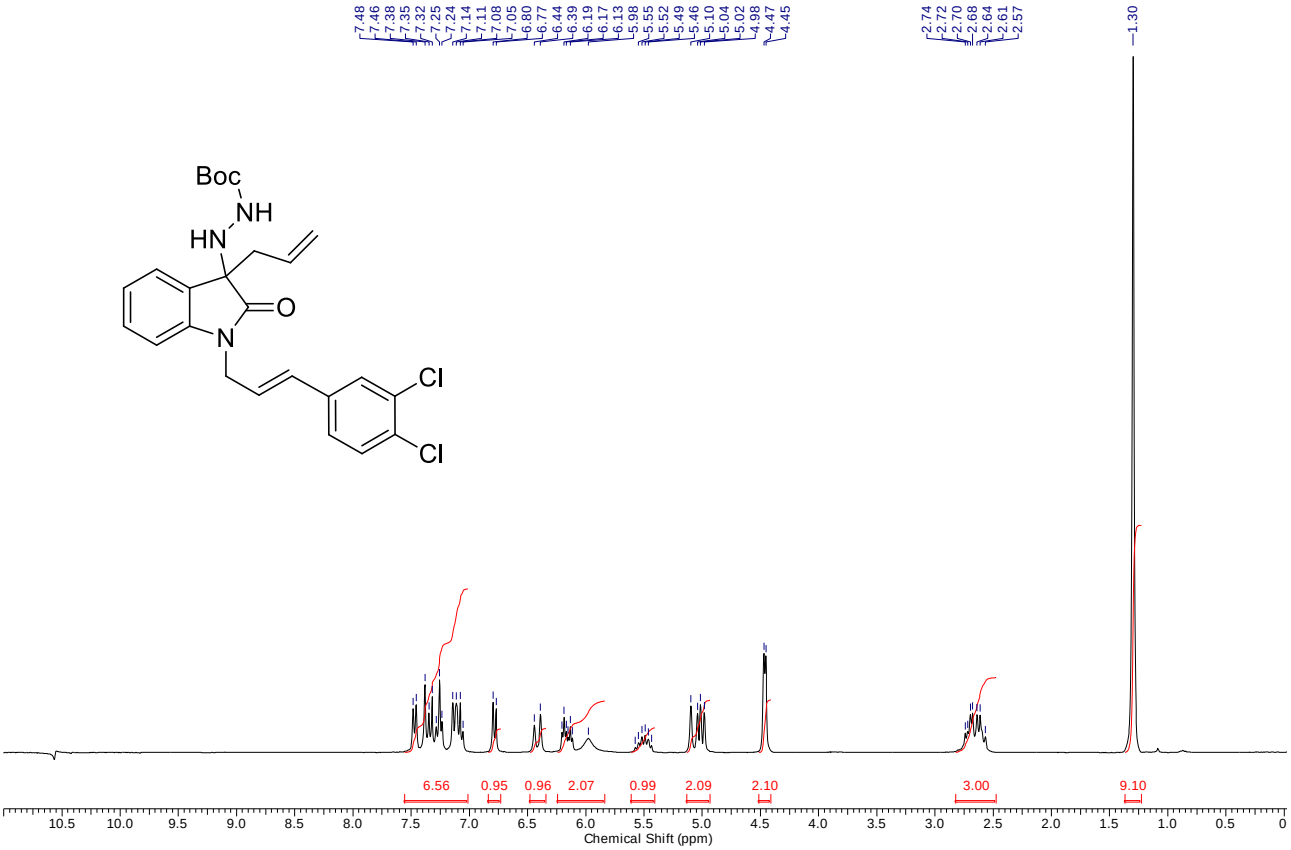

5c ^{13}C NMR (101 MHz, ATP, $CDCl_3$):

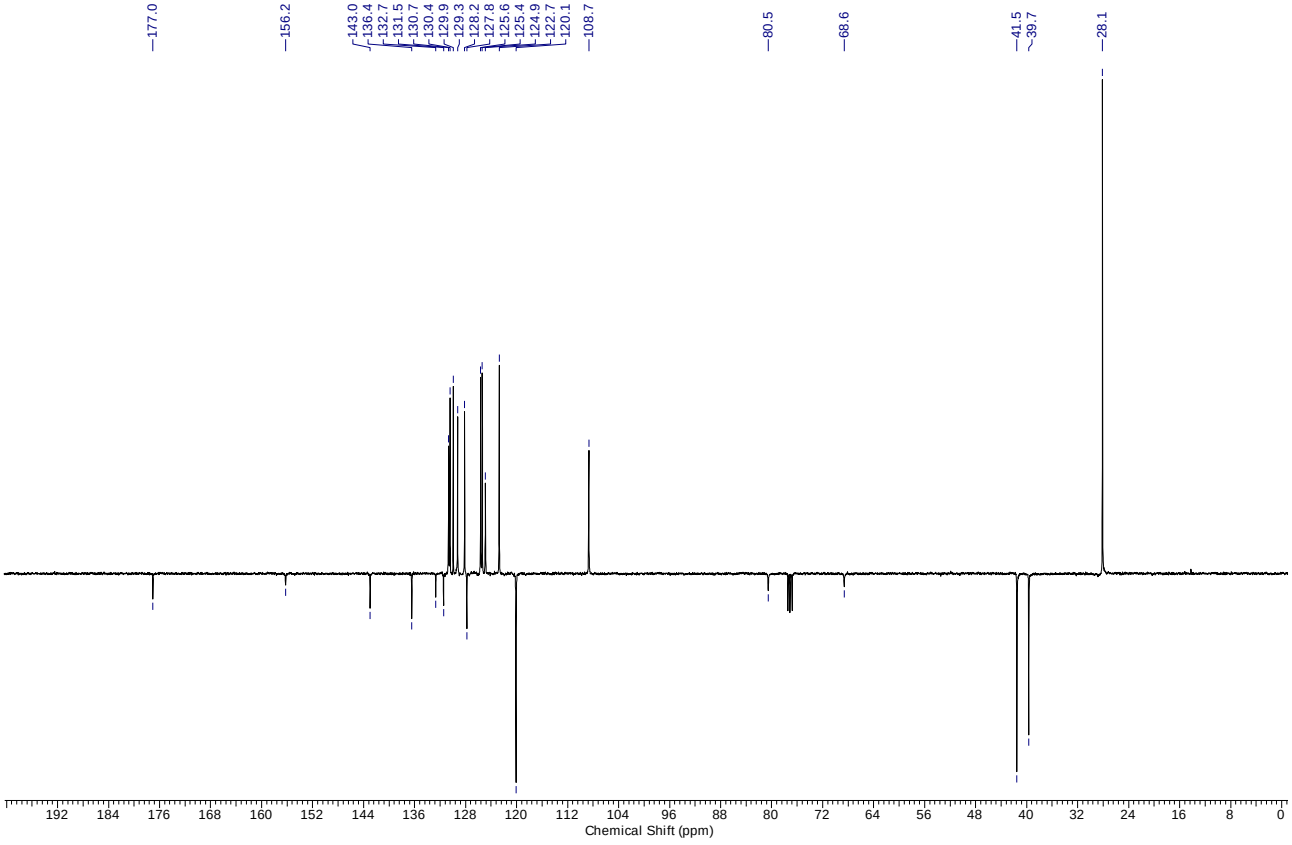

5d ^{1}H NMR (300 MHz, $CDCl_3$):

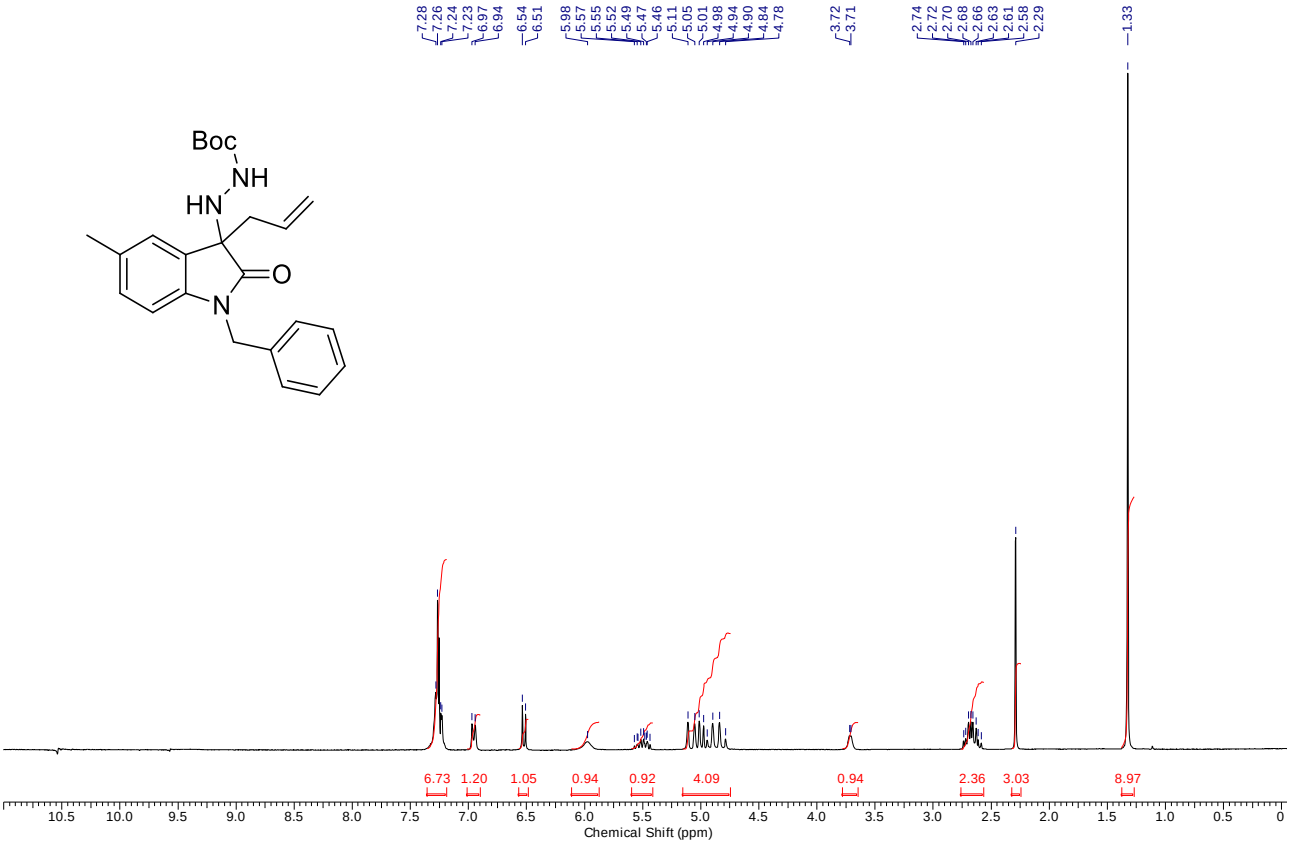

5d ^{13}C NMR (101 MHz, ATP, $CDCl_3$):

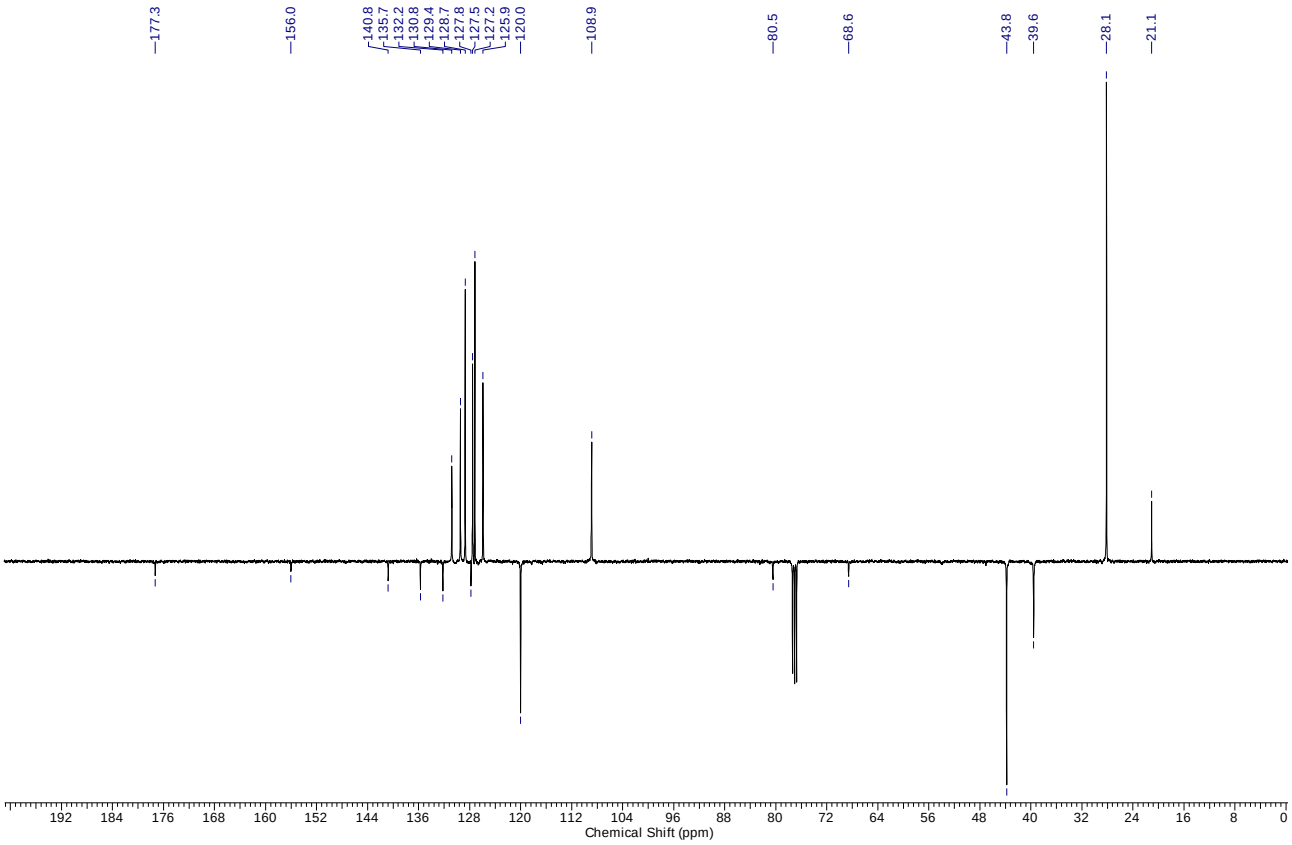

5e ^{1}H NMR (300 MHz, $CDCl_3$):

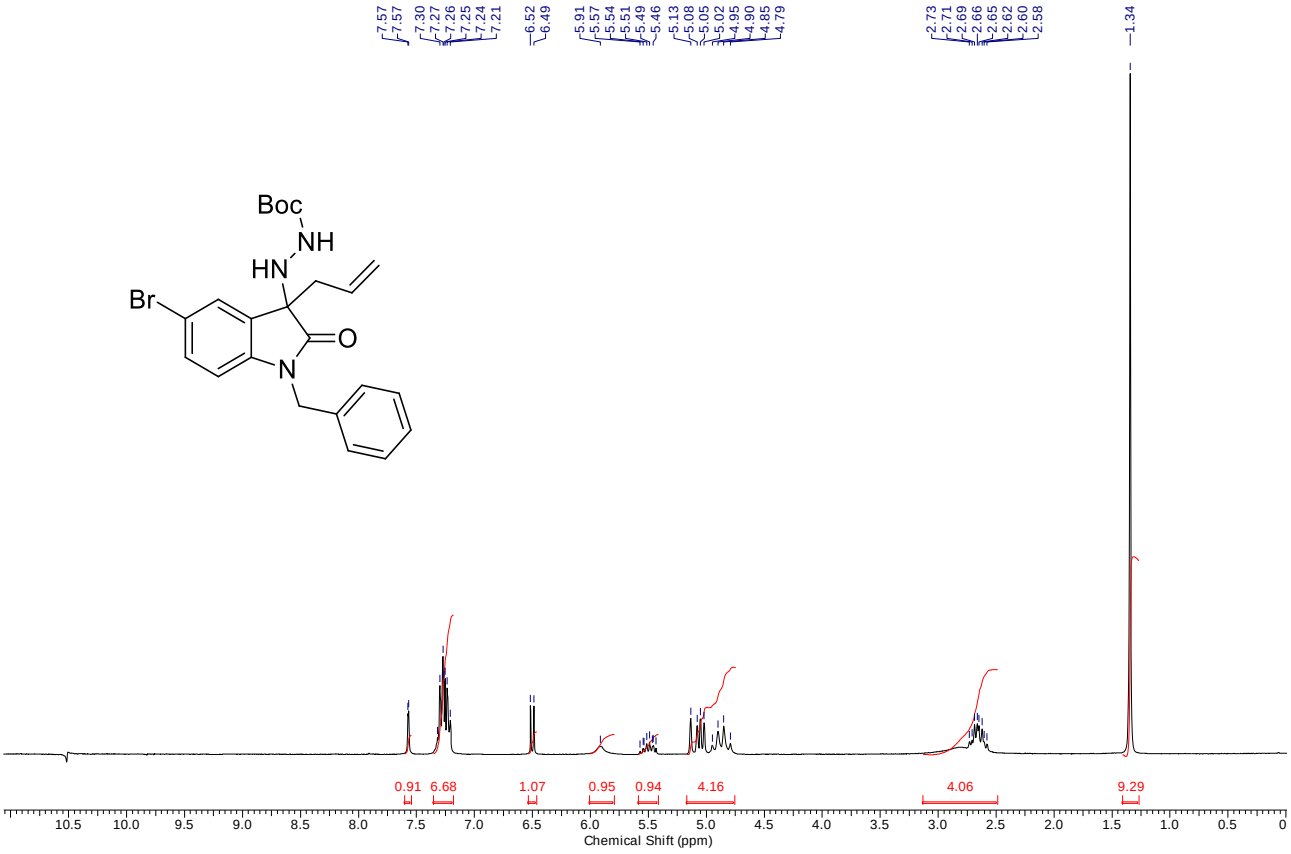

5e ^{13}C NMR (101 MHz, ATP, $CDCl_3$):

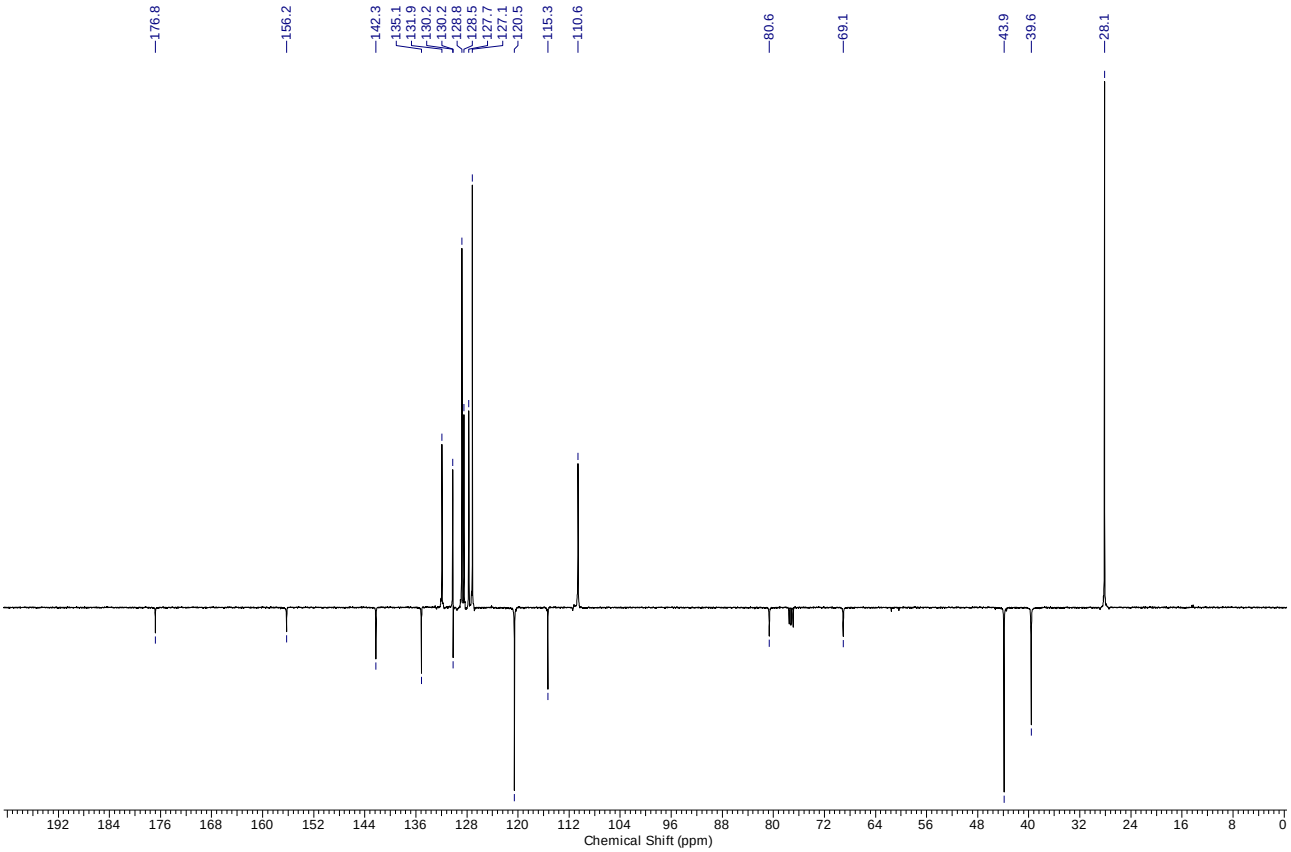

5f ^{1}H NMR (300 MHz, $CDCl_3$):

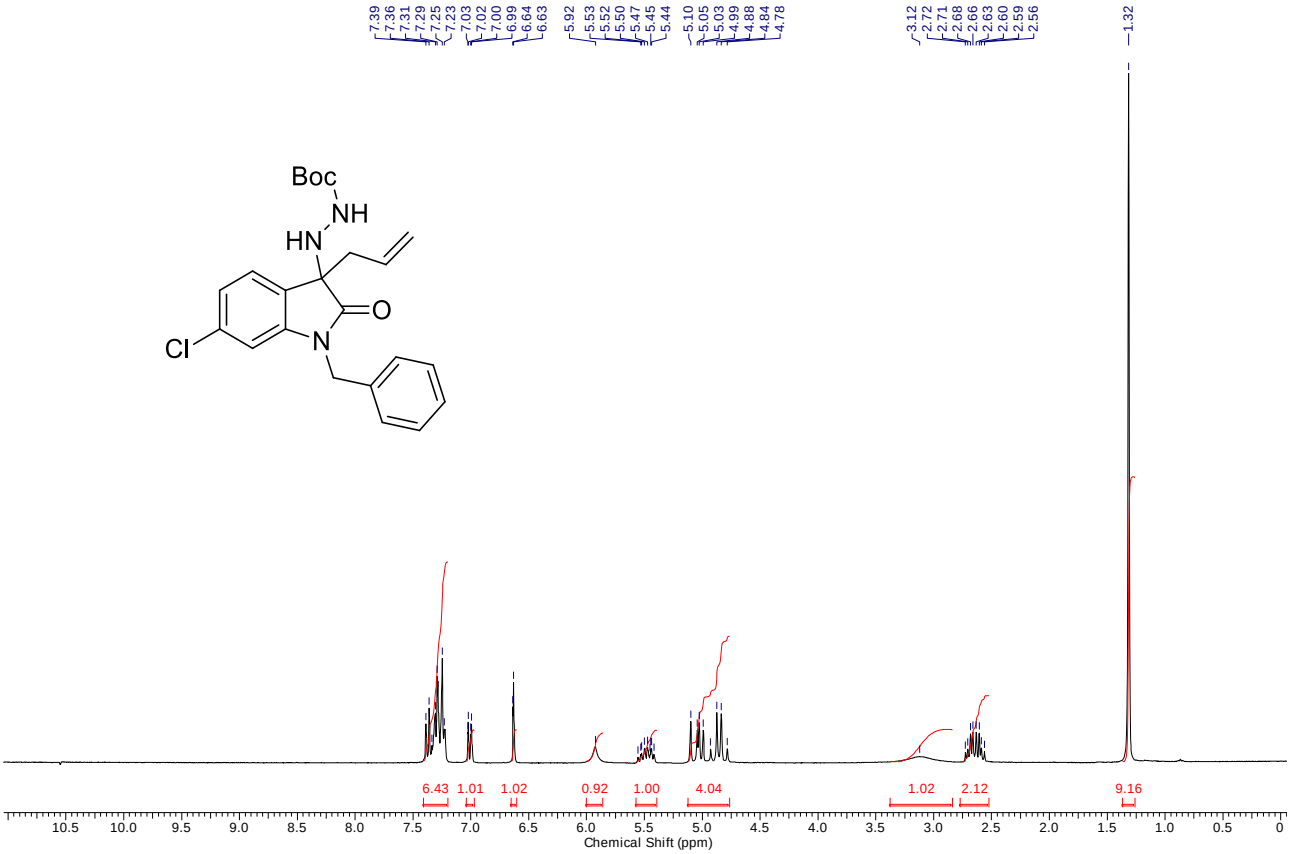

5f ^{13}C NMR (101 MHz, ATP, $CDCl_3$):

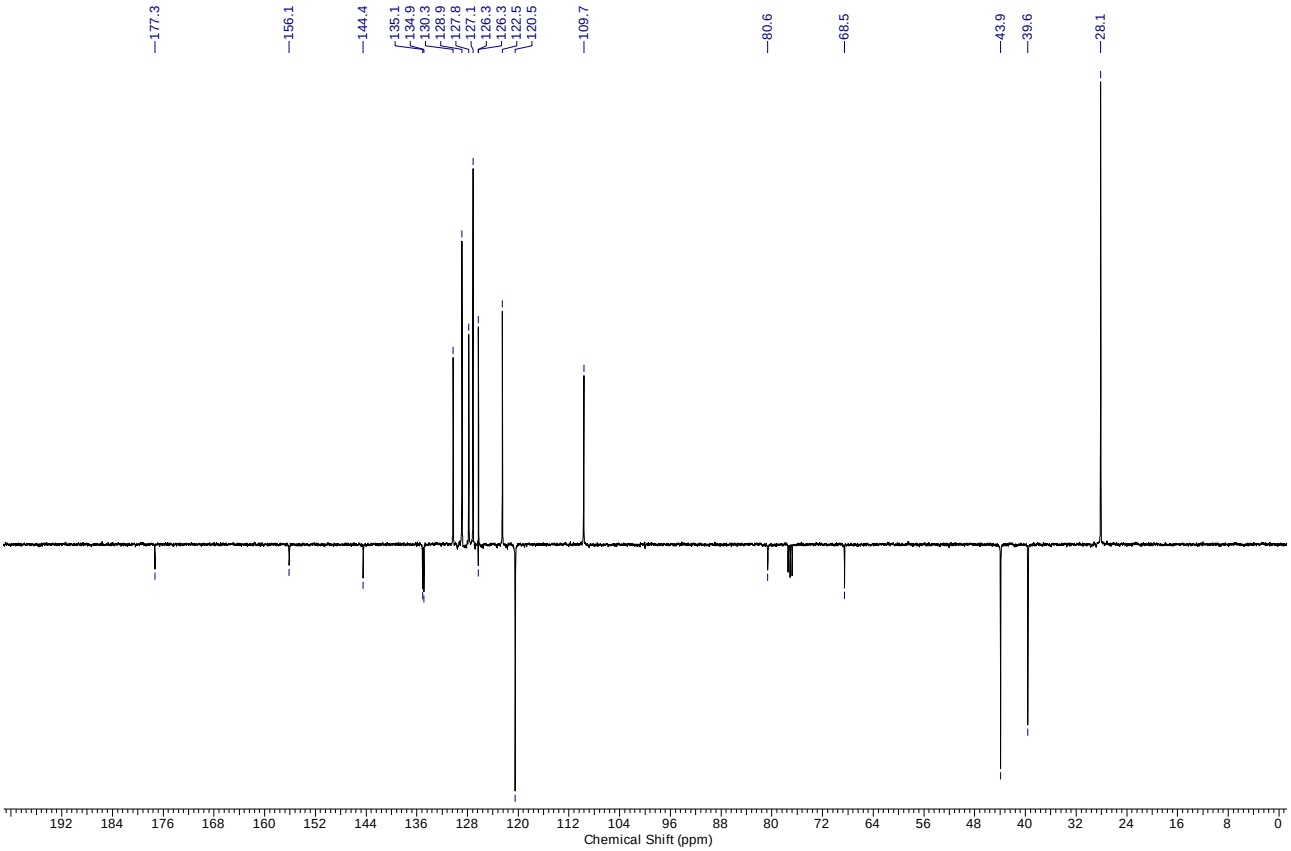

5g ^{1}H NMR (300 MHz, $CDCl_3$):

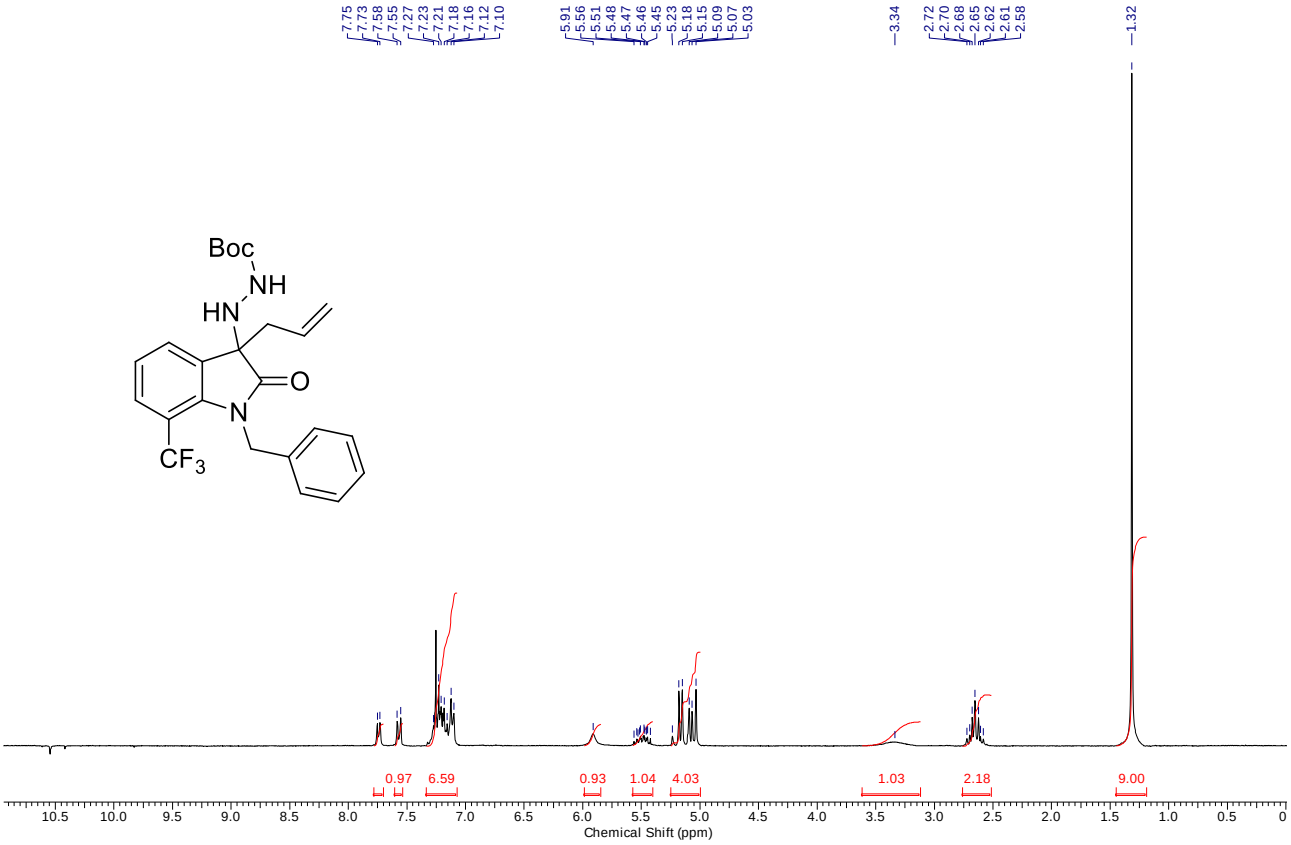

5g ^{13}C NMR (101 MHz, ATP, $CDCl_3$):

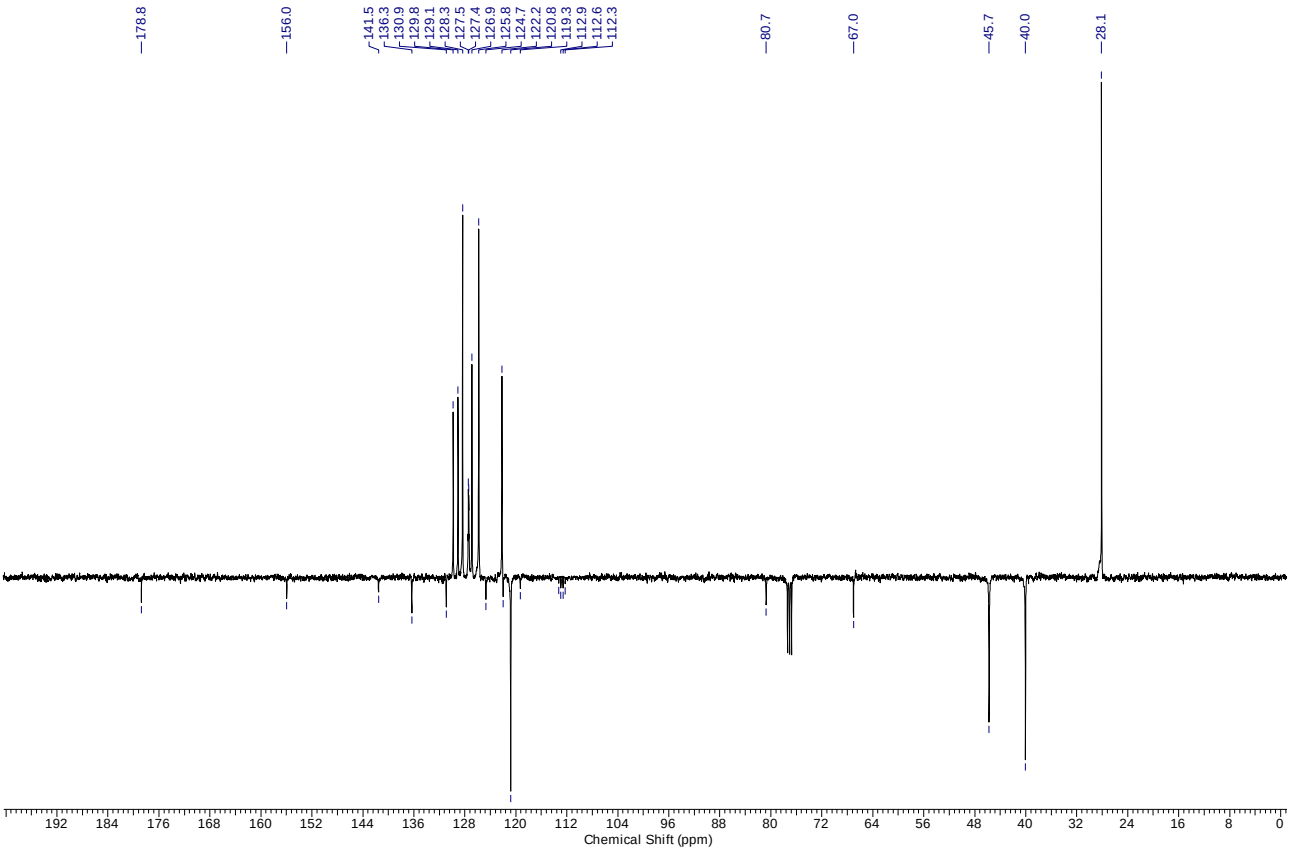

5h ^{1}H NMR (300 MHz, $CDCl_3$):

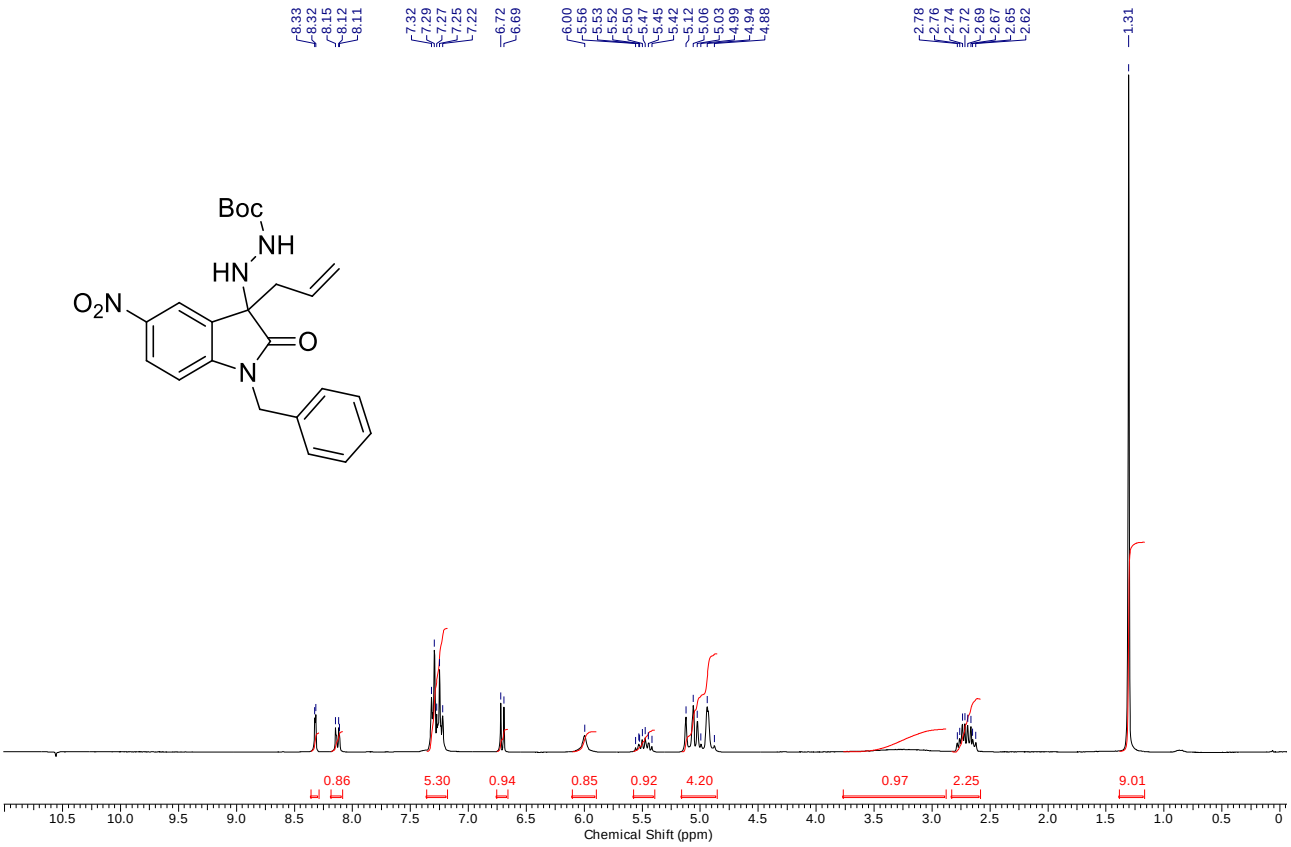

5h ^{13}C NMR (101 MHz, ATP, $CDCl_3$):

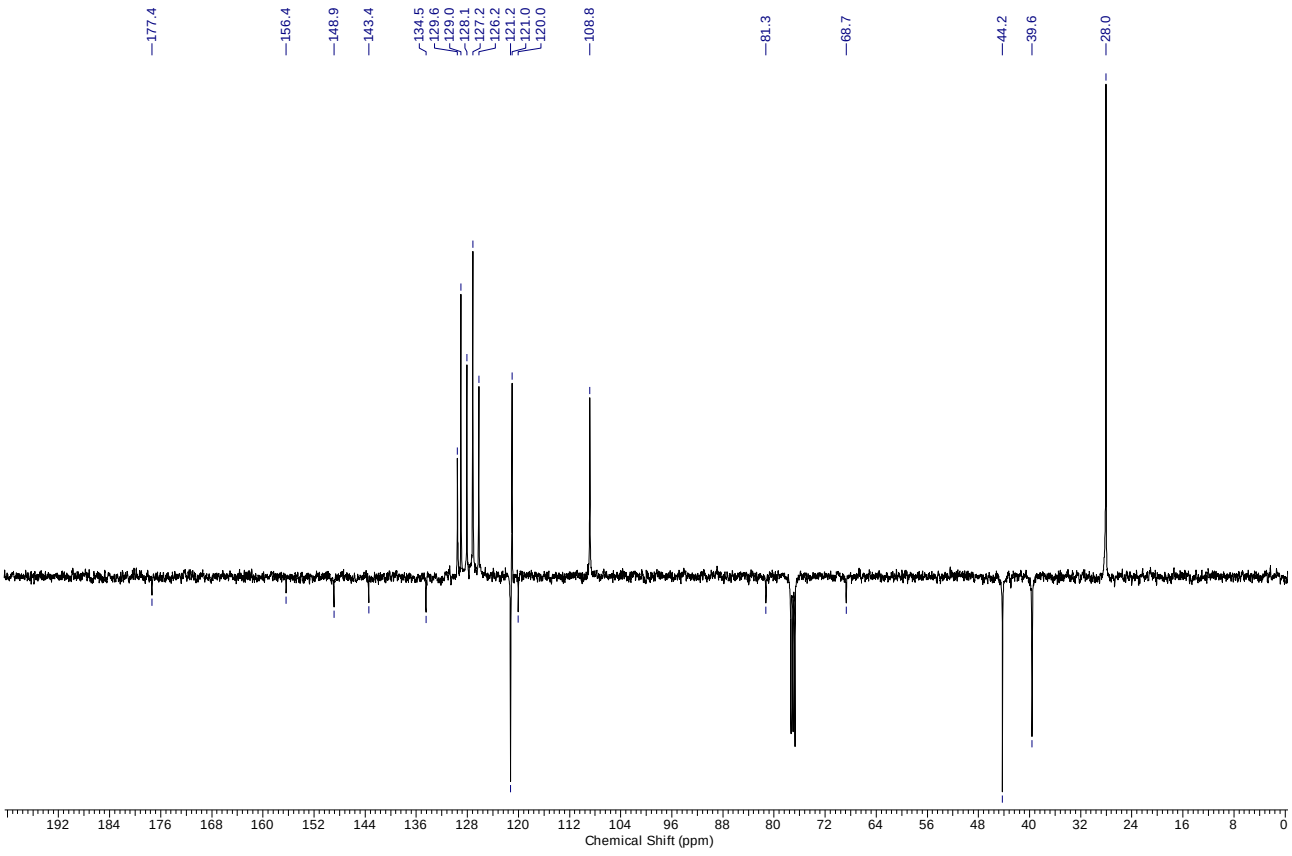

5i ^{1}H NMR (300 MHz, $CDCl_3$):

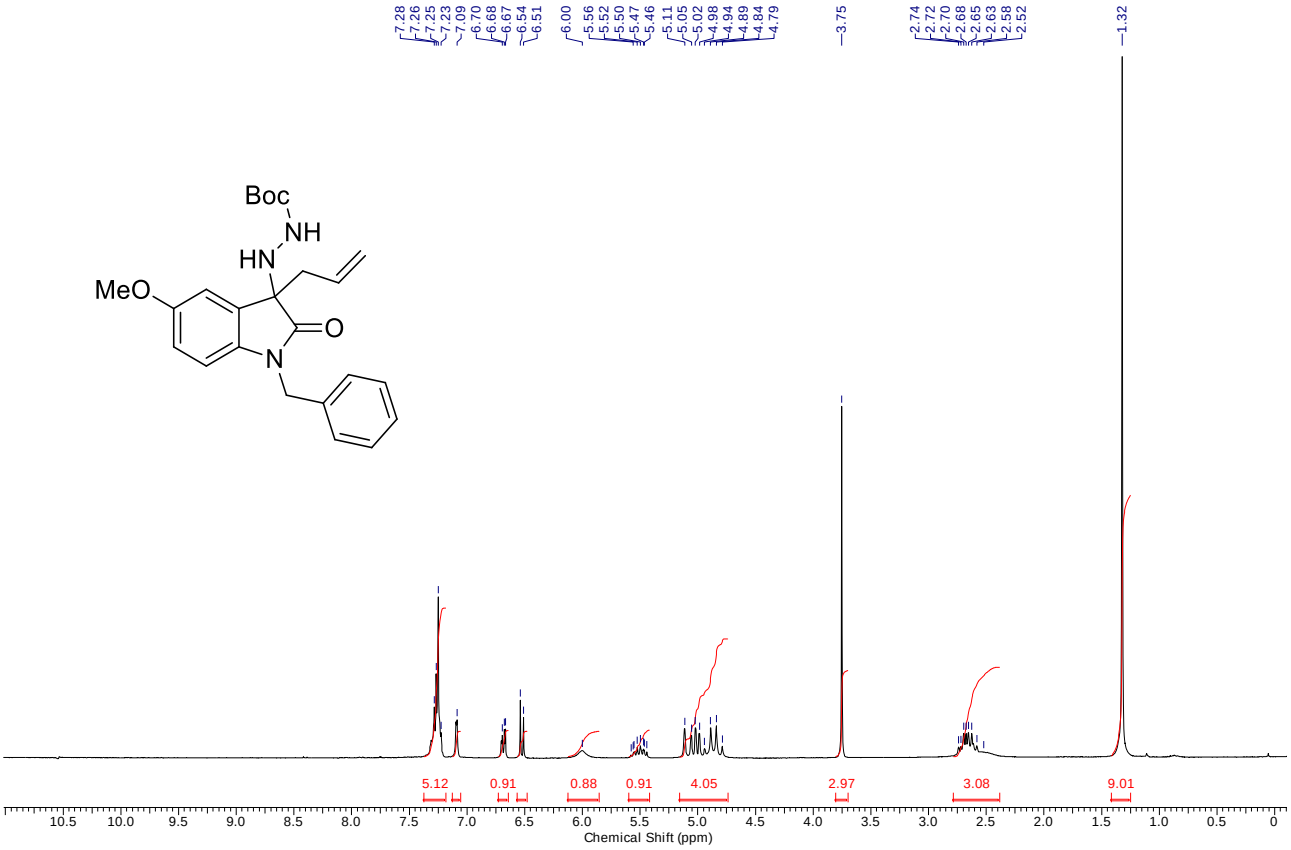

5i ^{13}C NMR (101 MHz, ATP, $CDCl_3$):

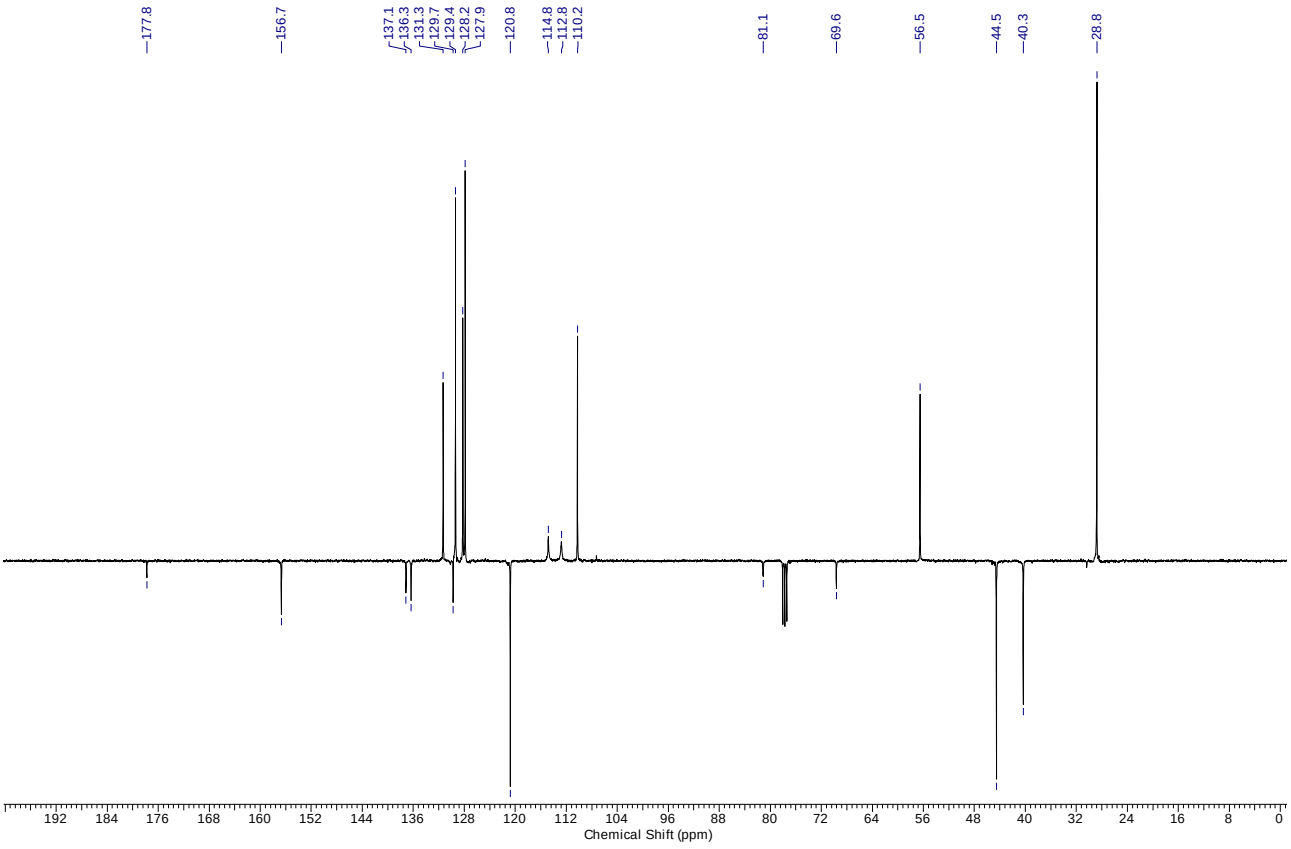

5j ^{1}H NMR (300 MHz, $CDCl_3$):

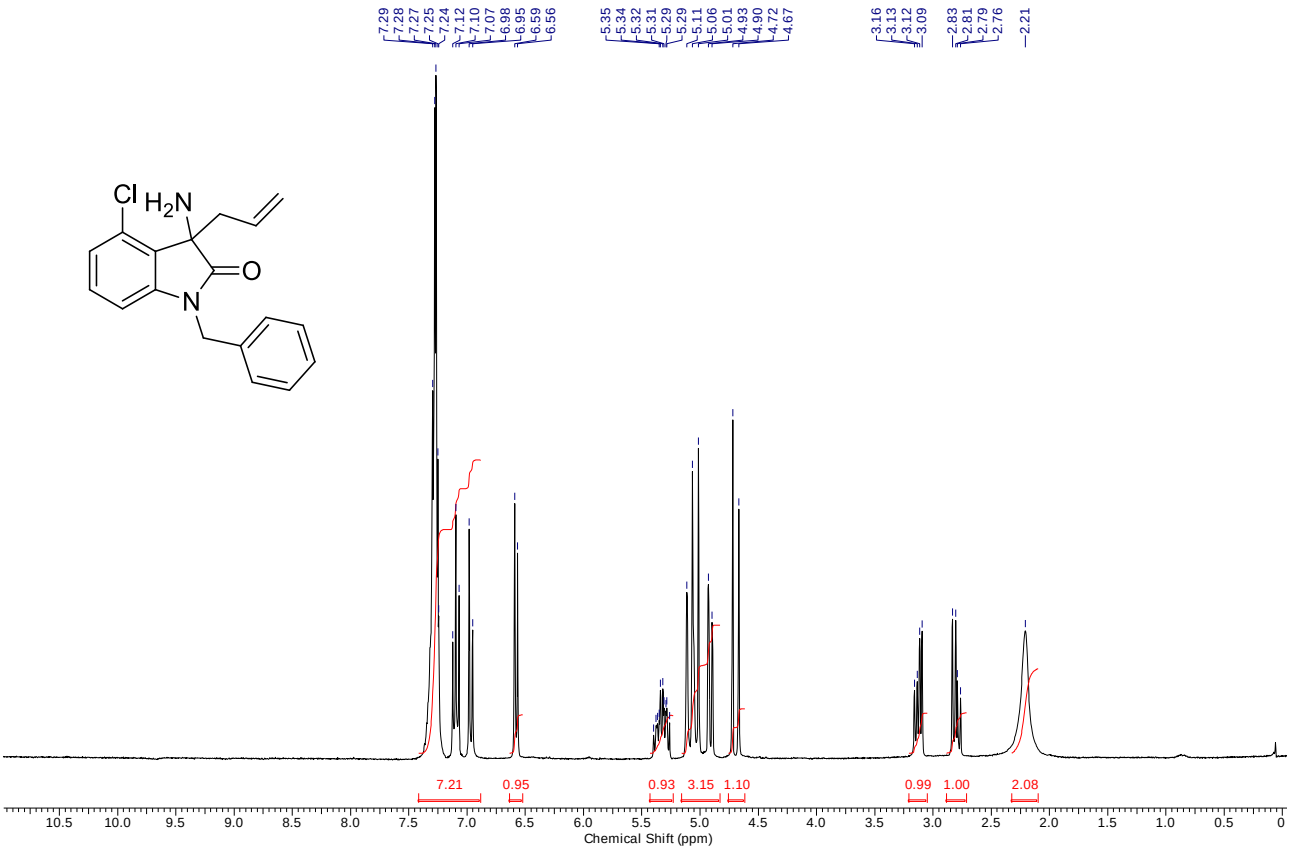

5j ^{13}C NMR (101 MHz, ATP, $CDCl_3$):

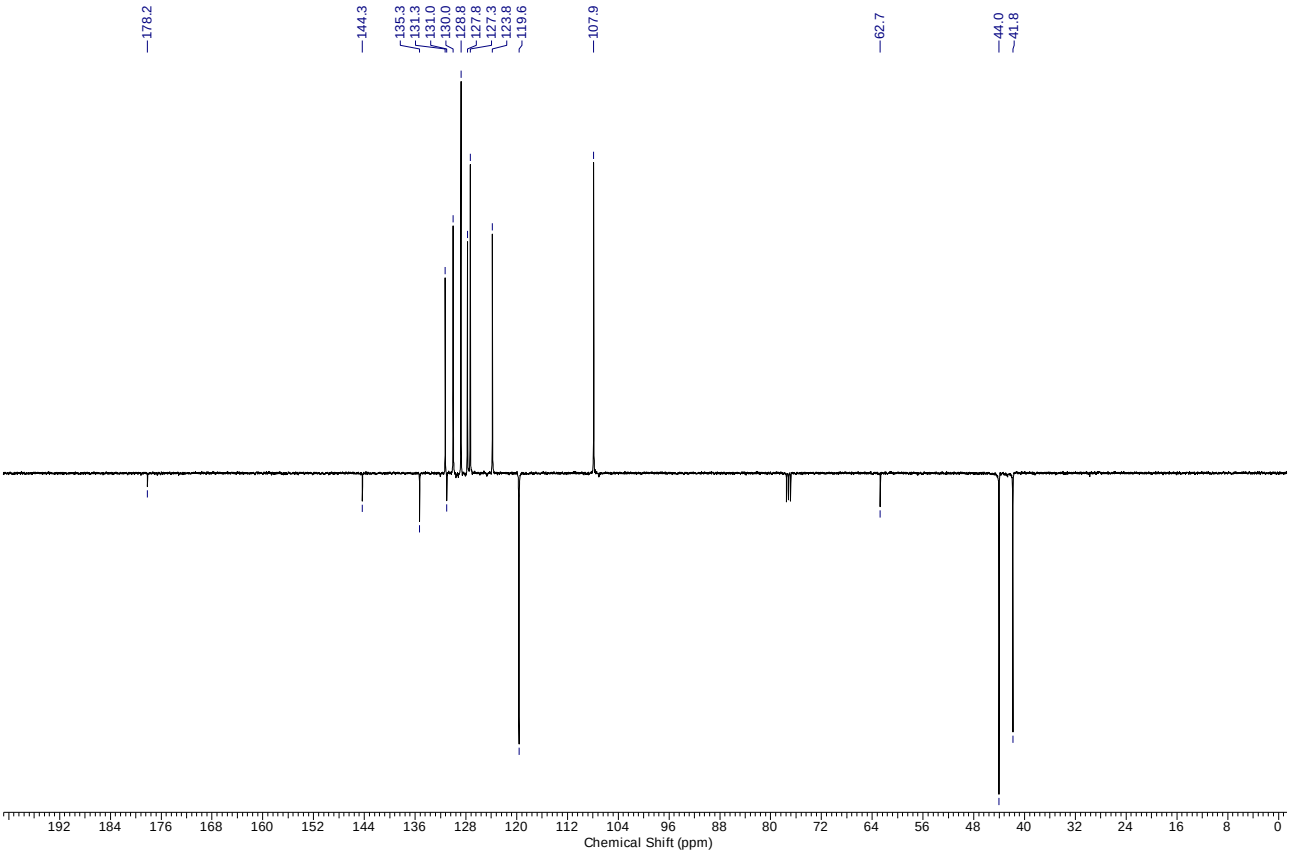

6a ^{1}H NMR (400 MHz, $CDCl_3$):

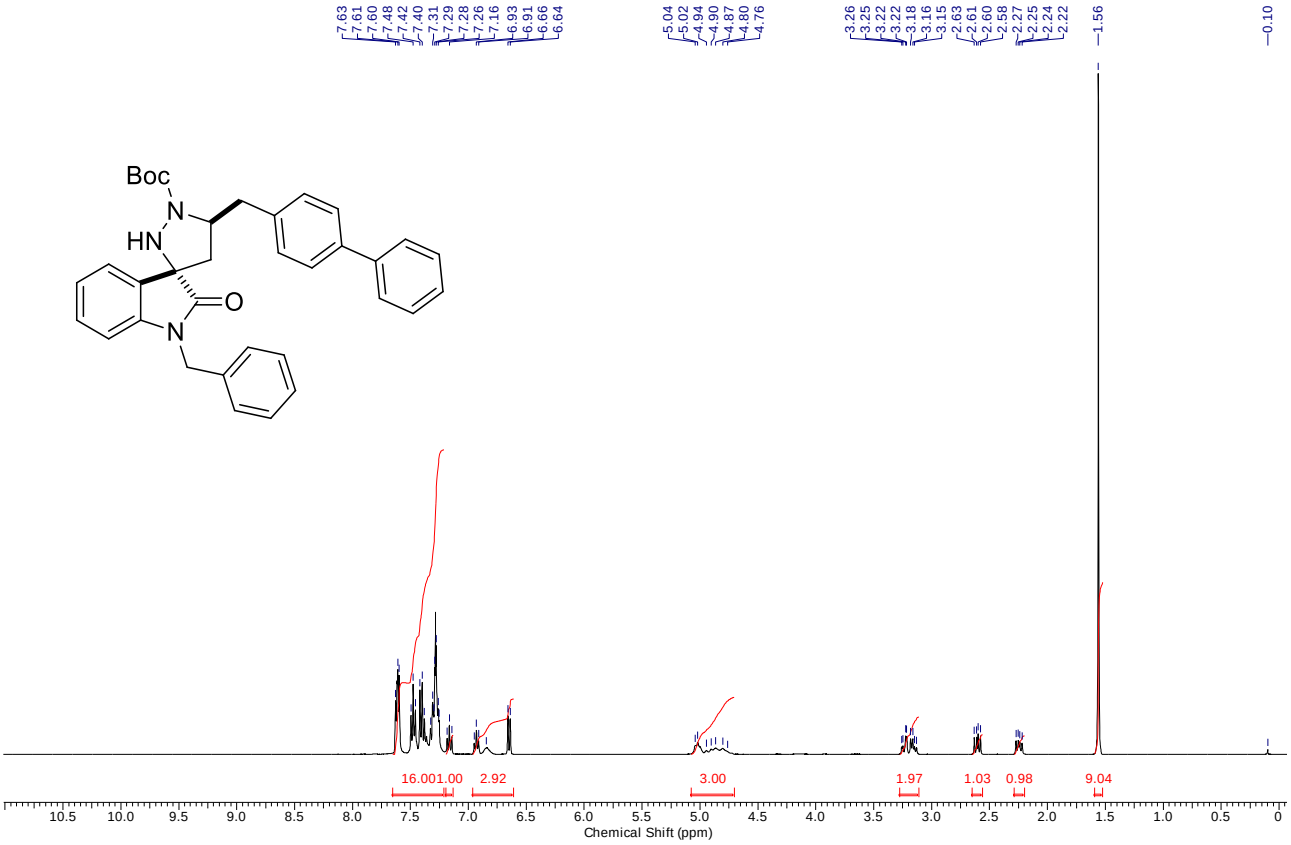

6a ^{13}C NMR (101 MHz, ATP, $CDCl_3$):

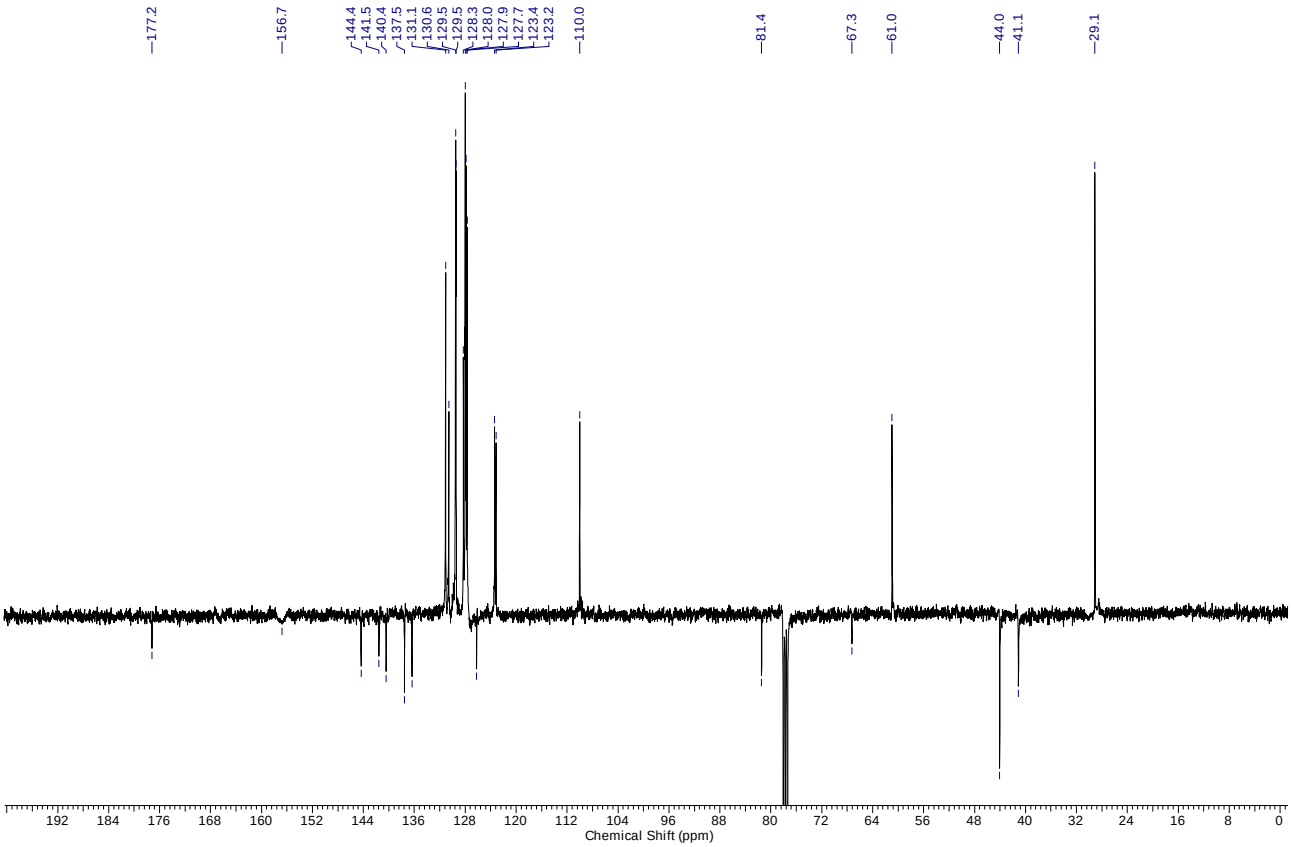

6a' ^{1}H NMR (400 MHz, $CDCl_3$):

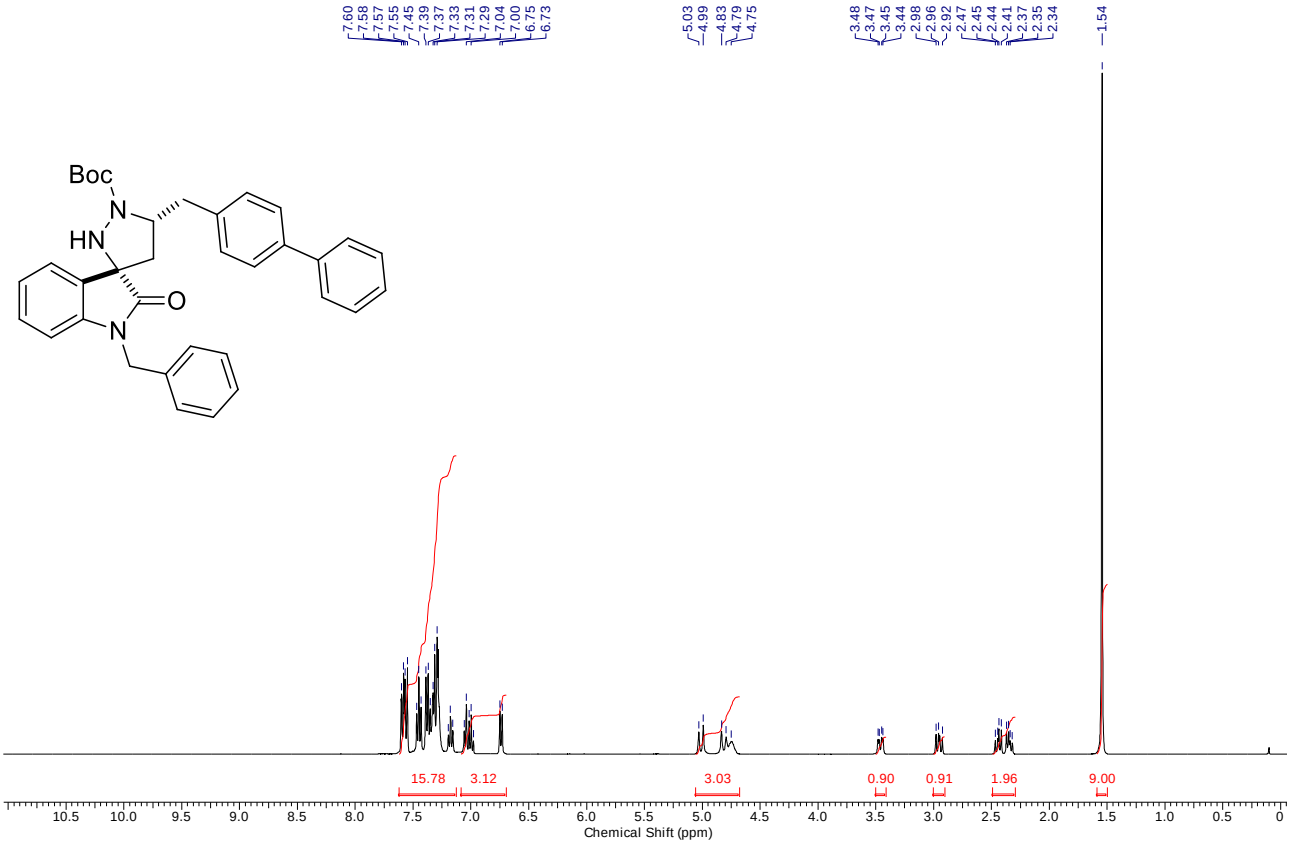

6a' ^{13}C NMR (101 MHz, ATP, $CDCl_3$):

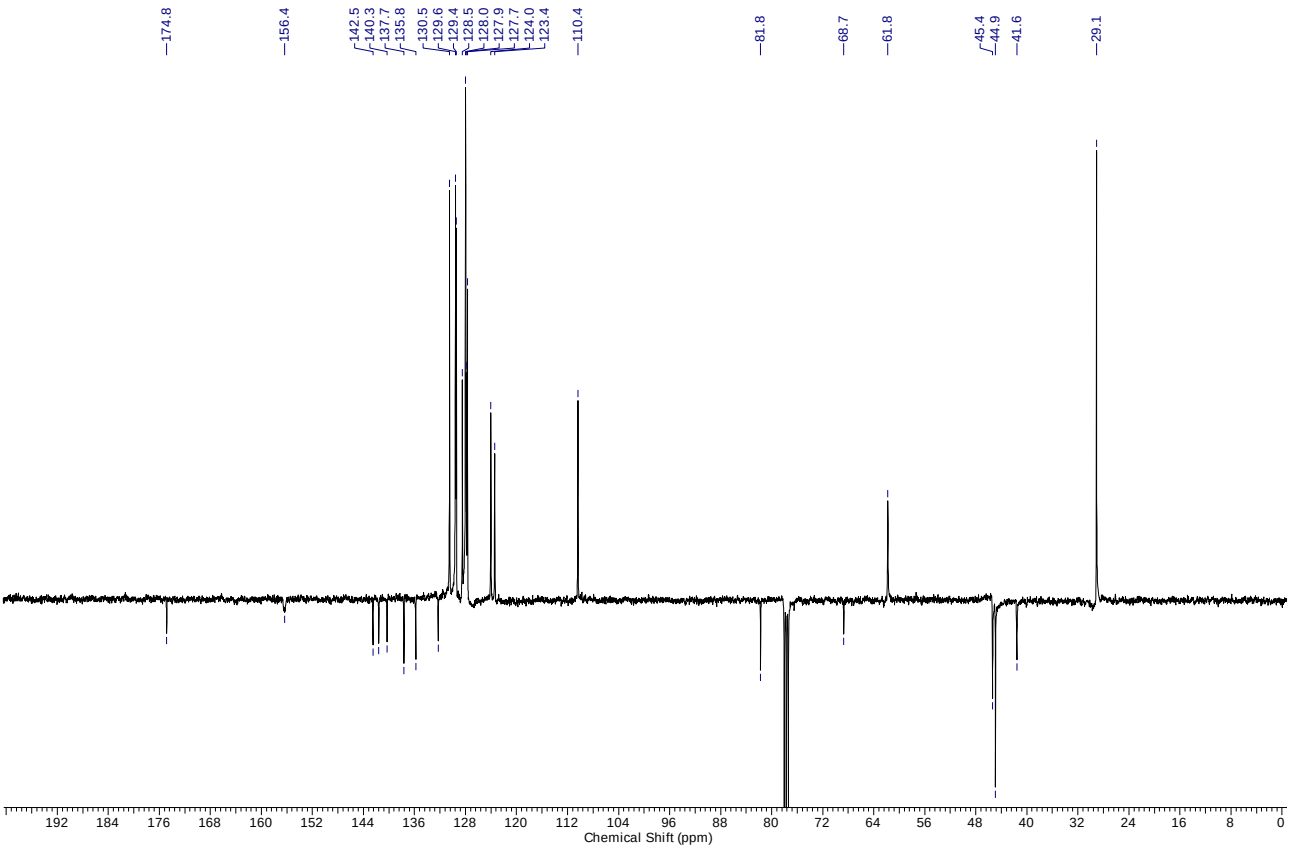

6b ^{1}H NMR (300 MHz, $CDCl_3$):

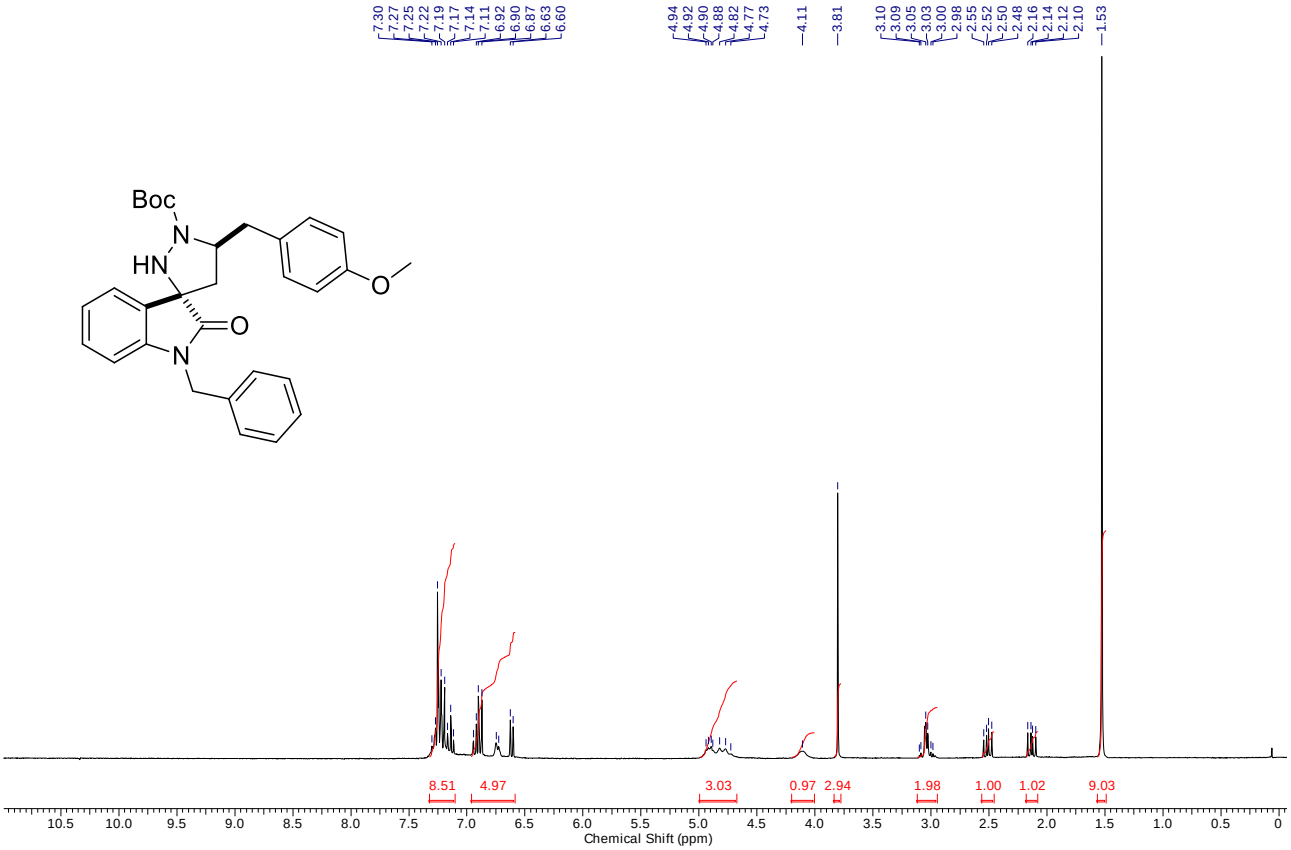

6b ^{13}C NMR (101 MHz, ATP, $CDCl_3$):

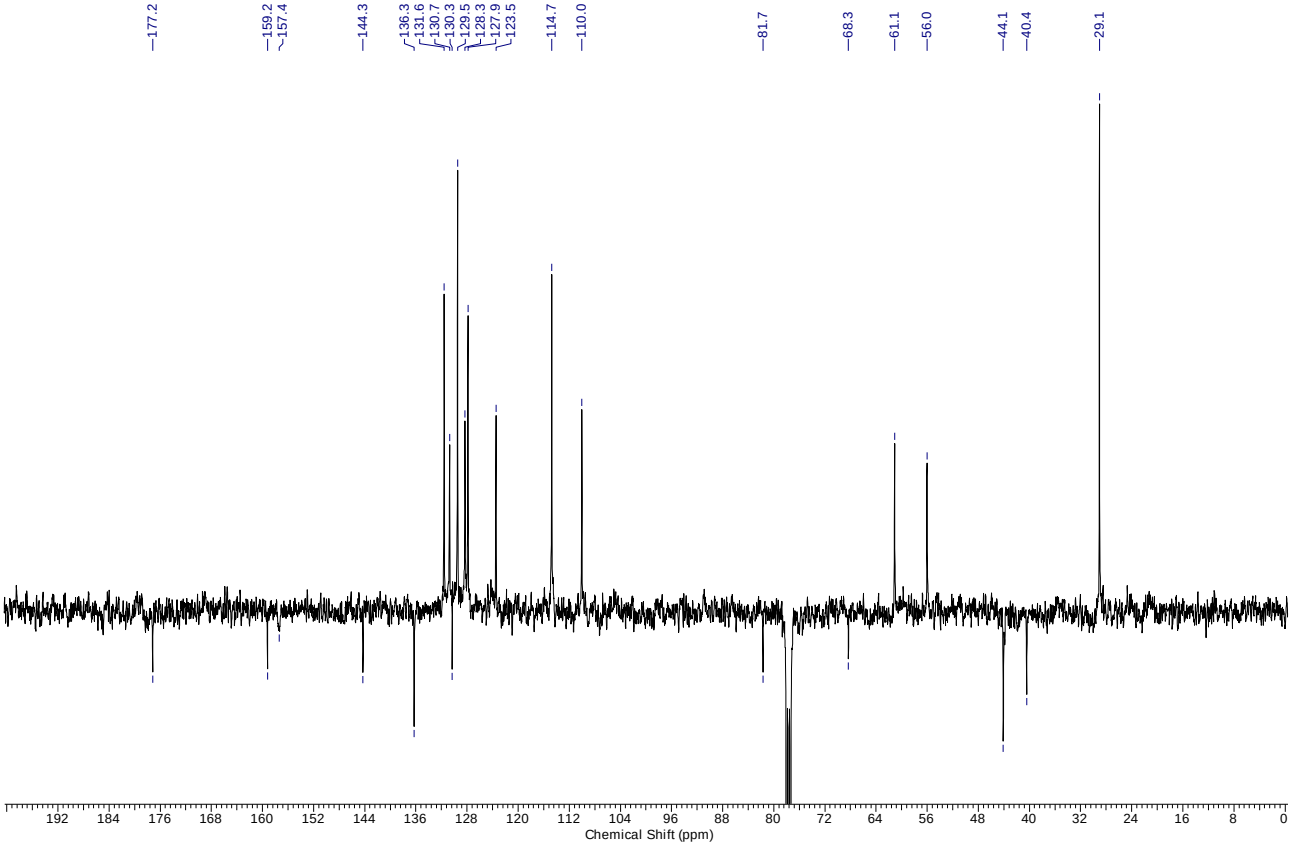

6b' ^{1}H NMR (300 MHz, $CDCl_3$):

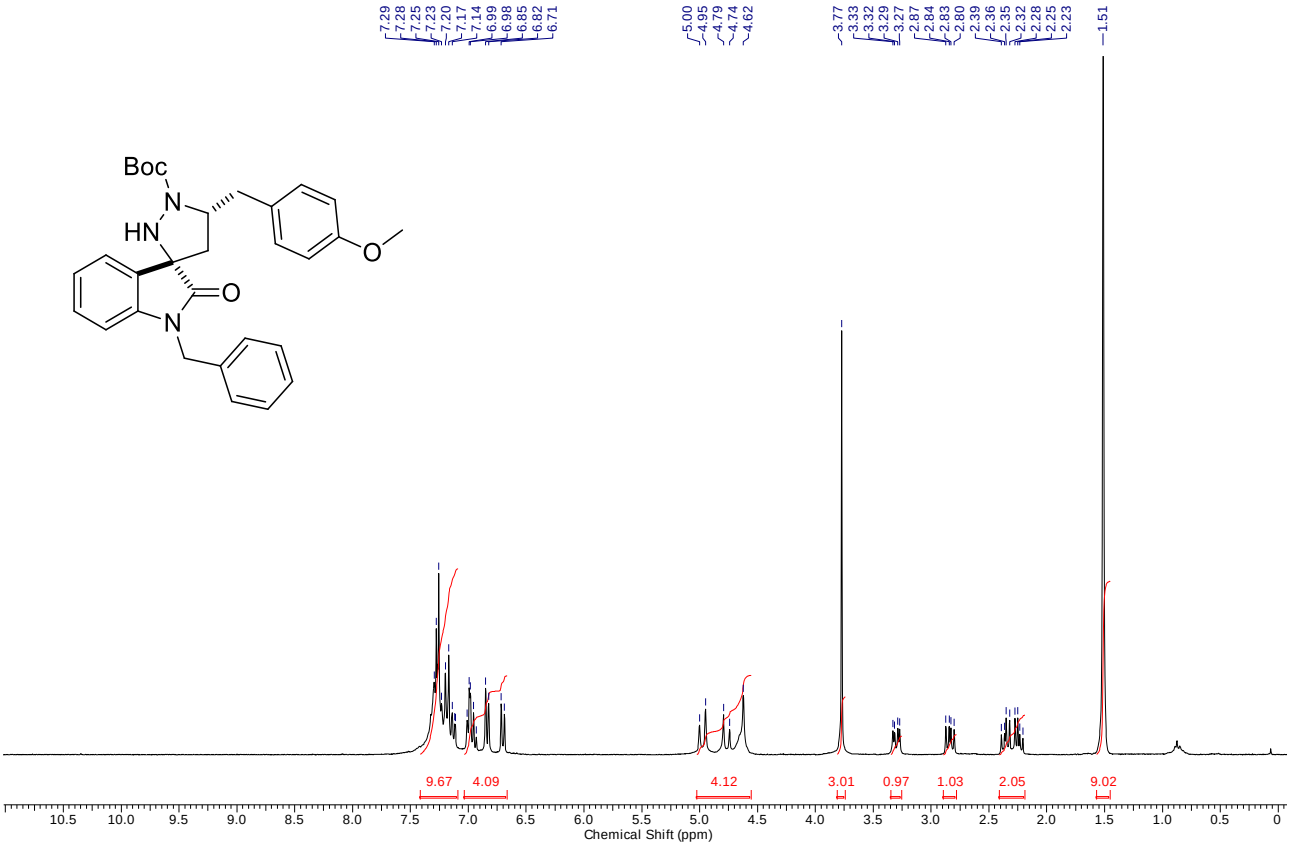

6b' ^{13}C NMR (101 MHz, ATP, $CDCl_3$):

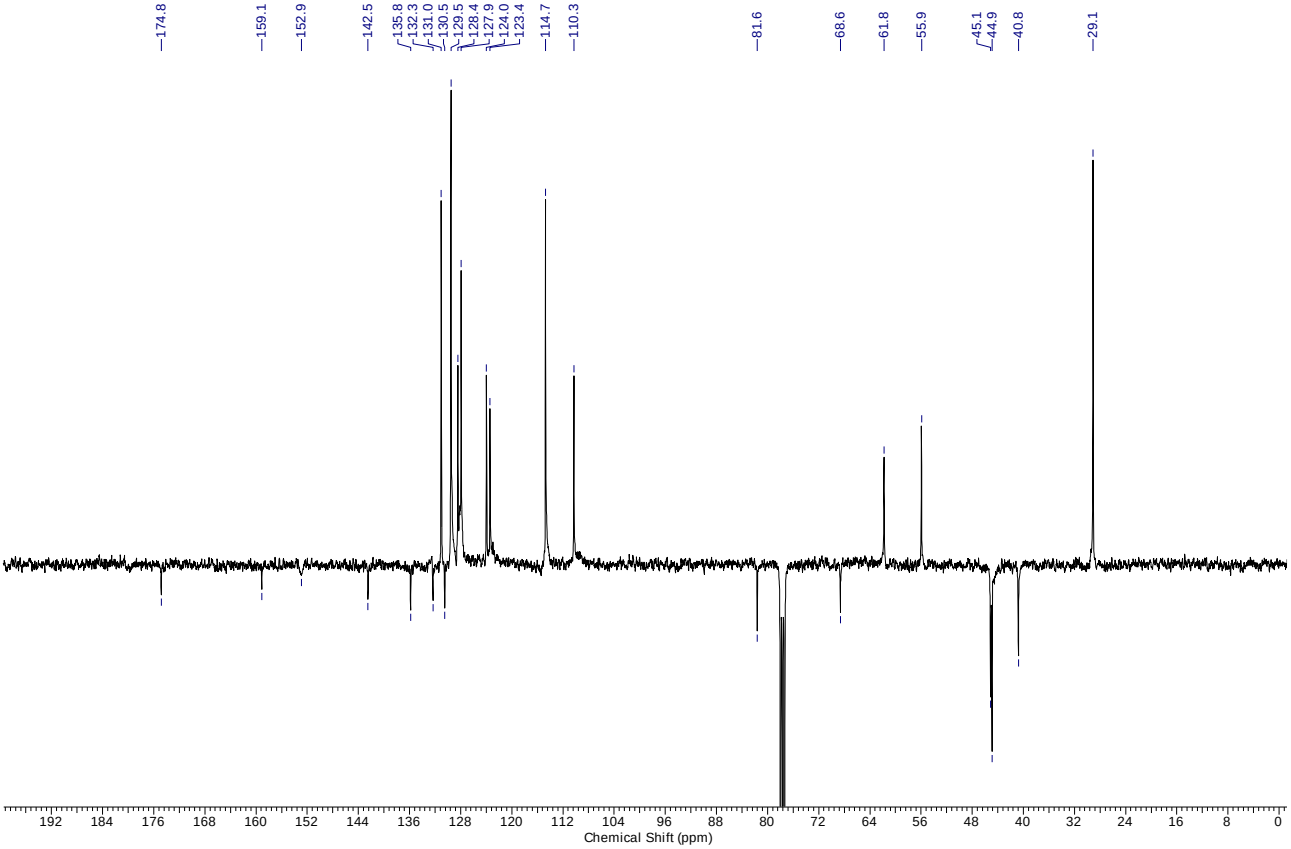

6c ^{1}H NMR (300 MHz, $CDCl_3$):

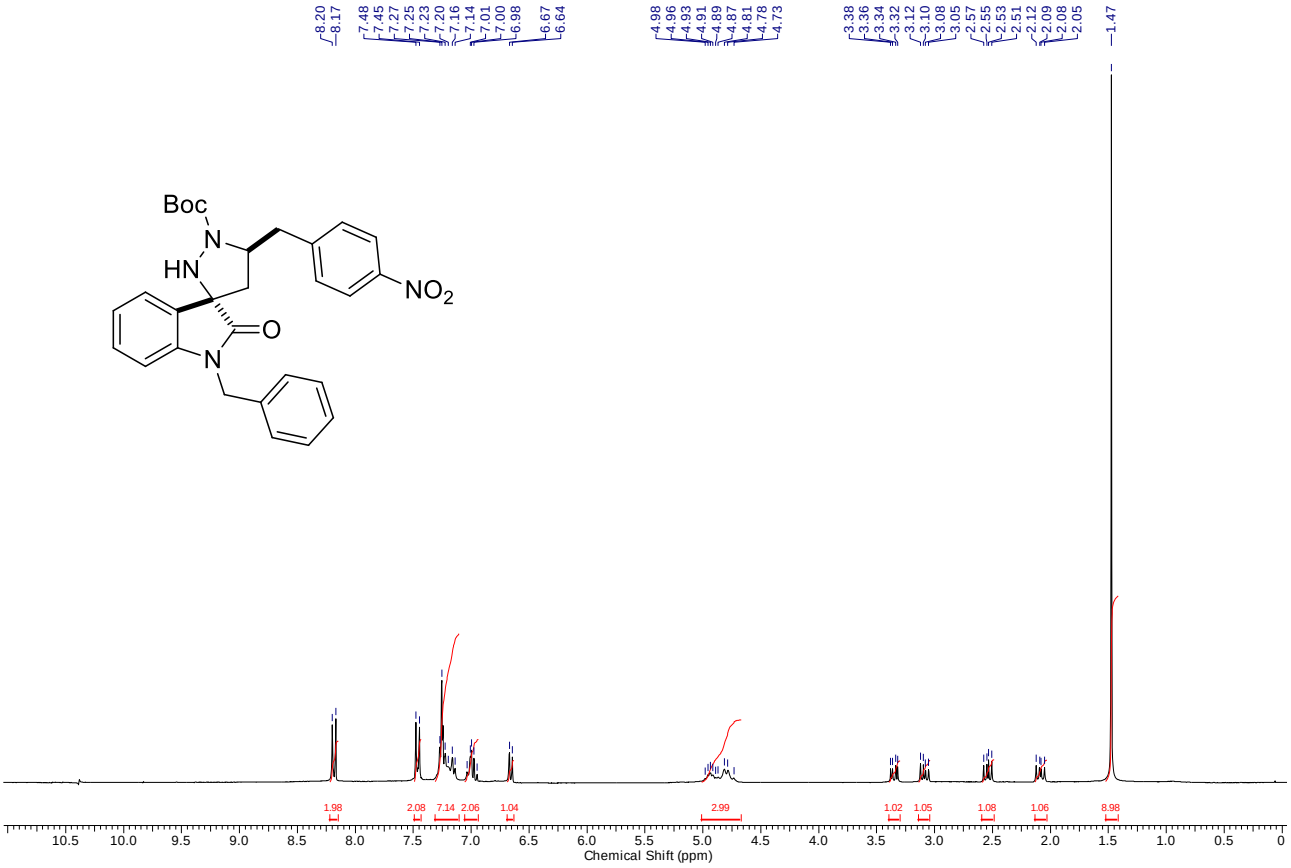

6c ^{13}C NMR (75 MHz, ATP, $CDCl_3$):

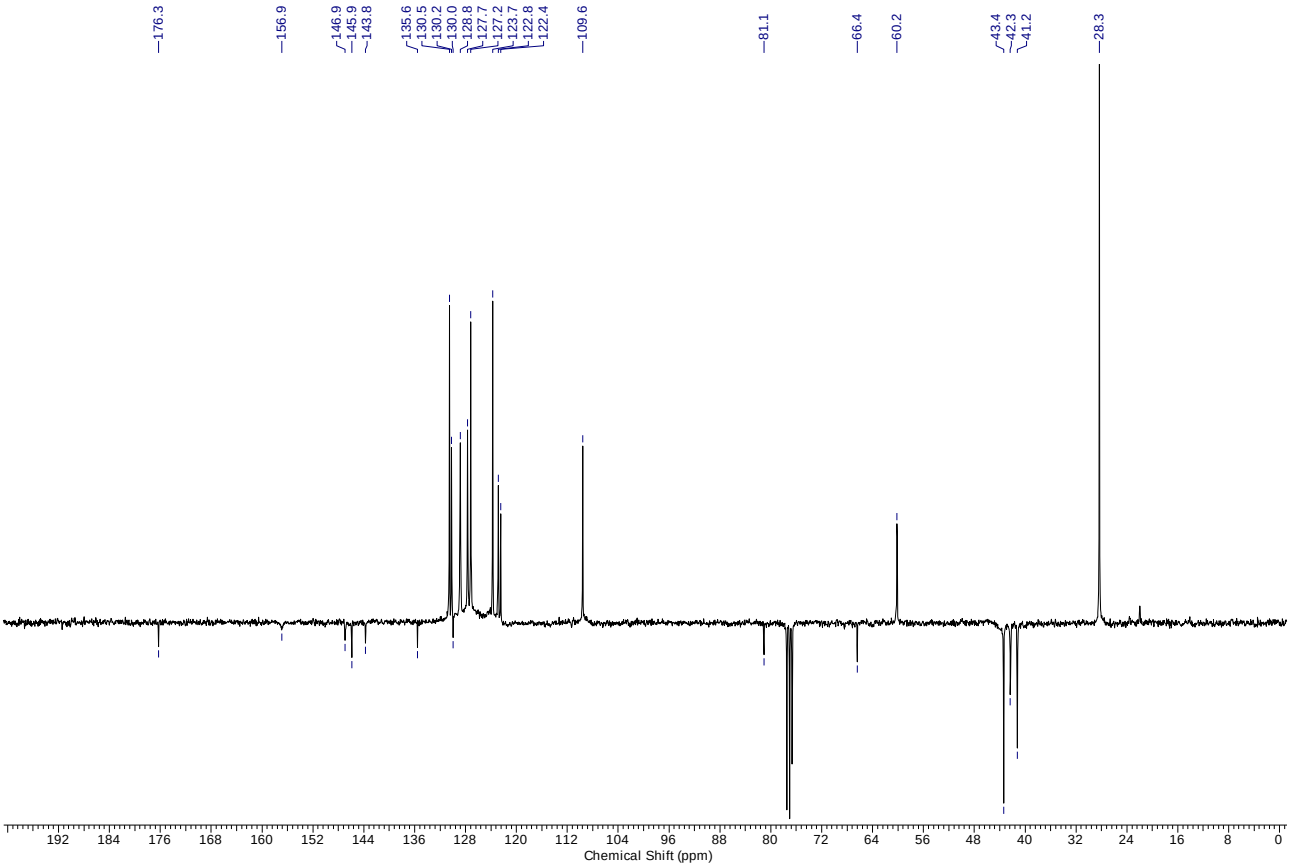

6c' ^{1}H NMR (400 MHz, $CDCl_3$):

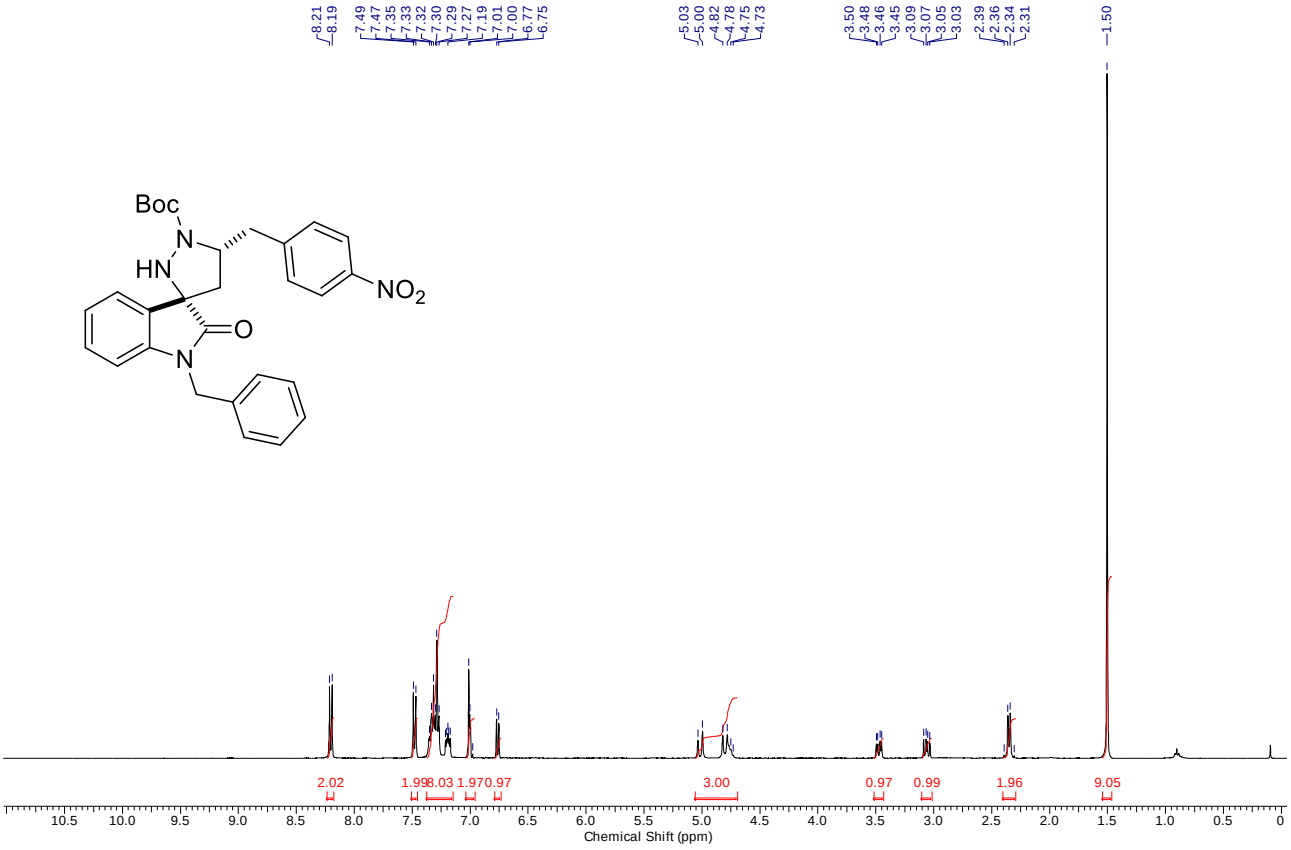

6c' ^{13}C NMR (101 MHz, ATP, $CDCl_3$):

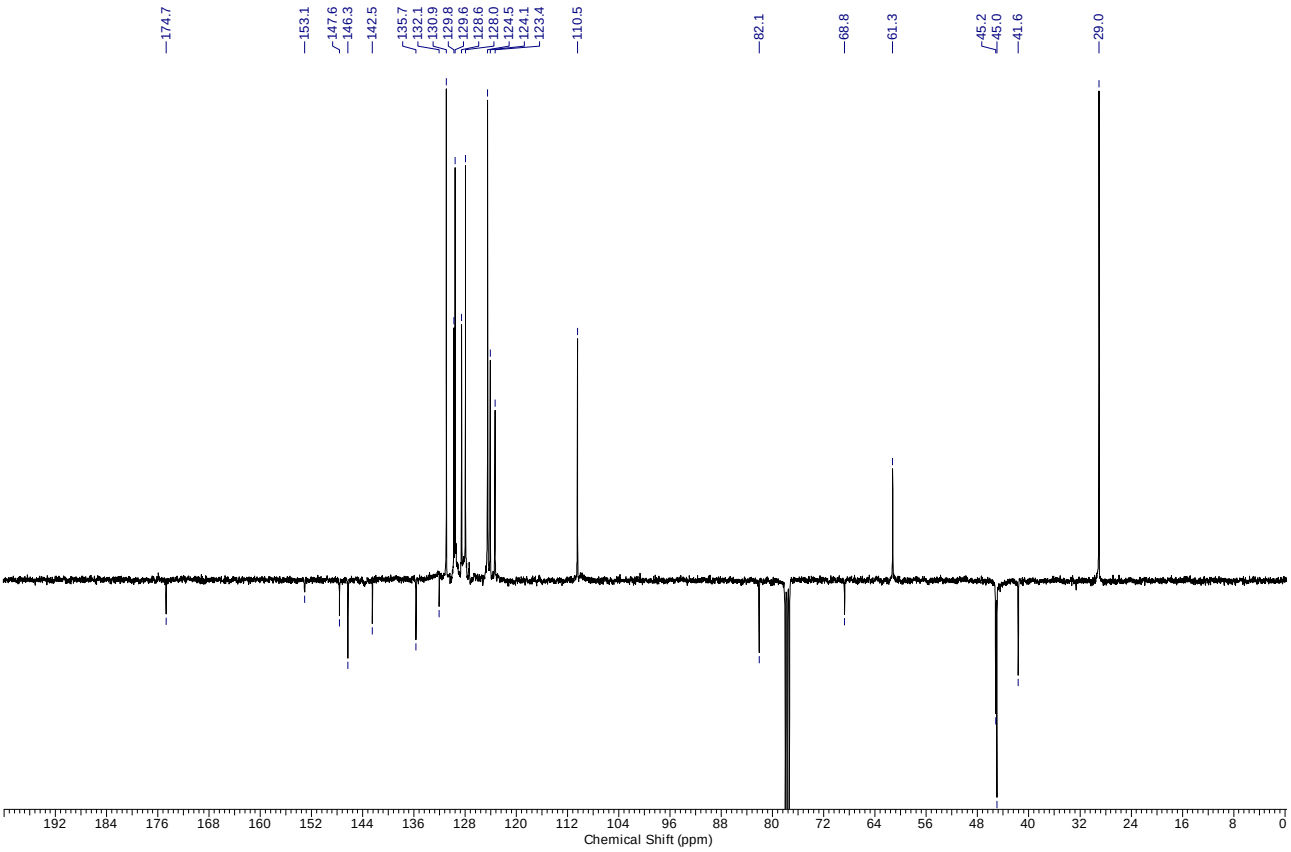

6d ^{1}H NMR (300 MHz, $CDCl_3$):

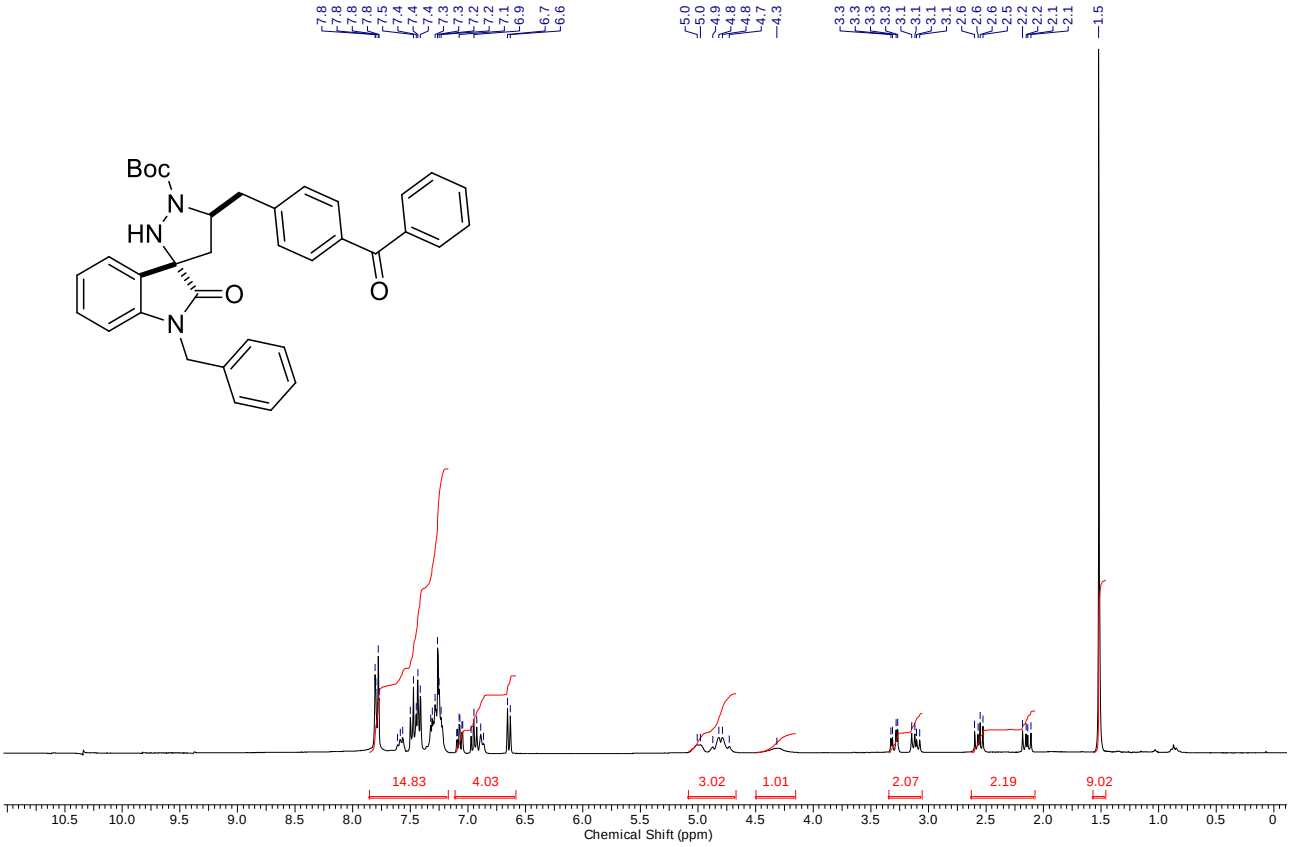

6d ^{13}C NMR (101 MHz, ATP, $CDCl_3$):

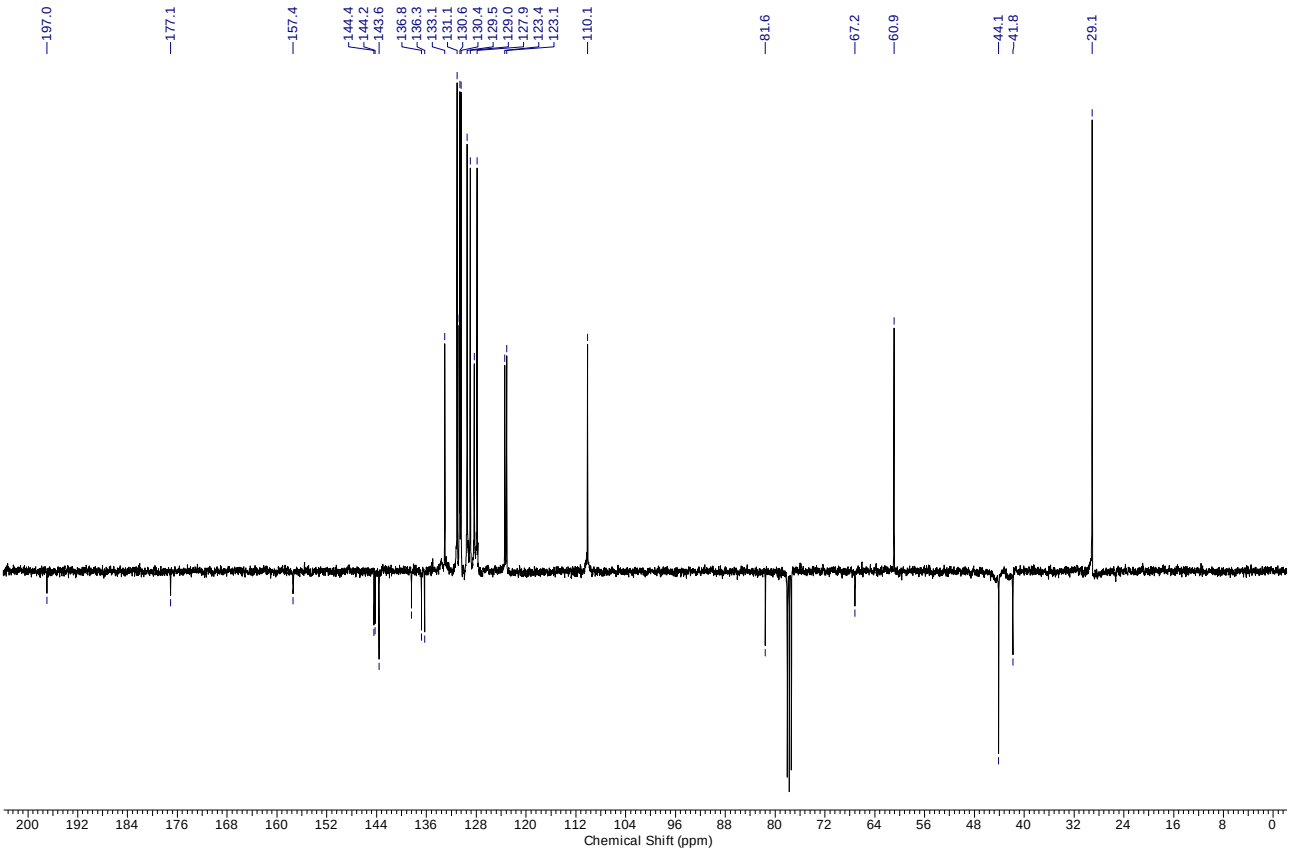

6d' ^{1}H NMR (300 MHz, $CDCl_3$):

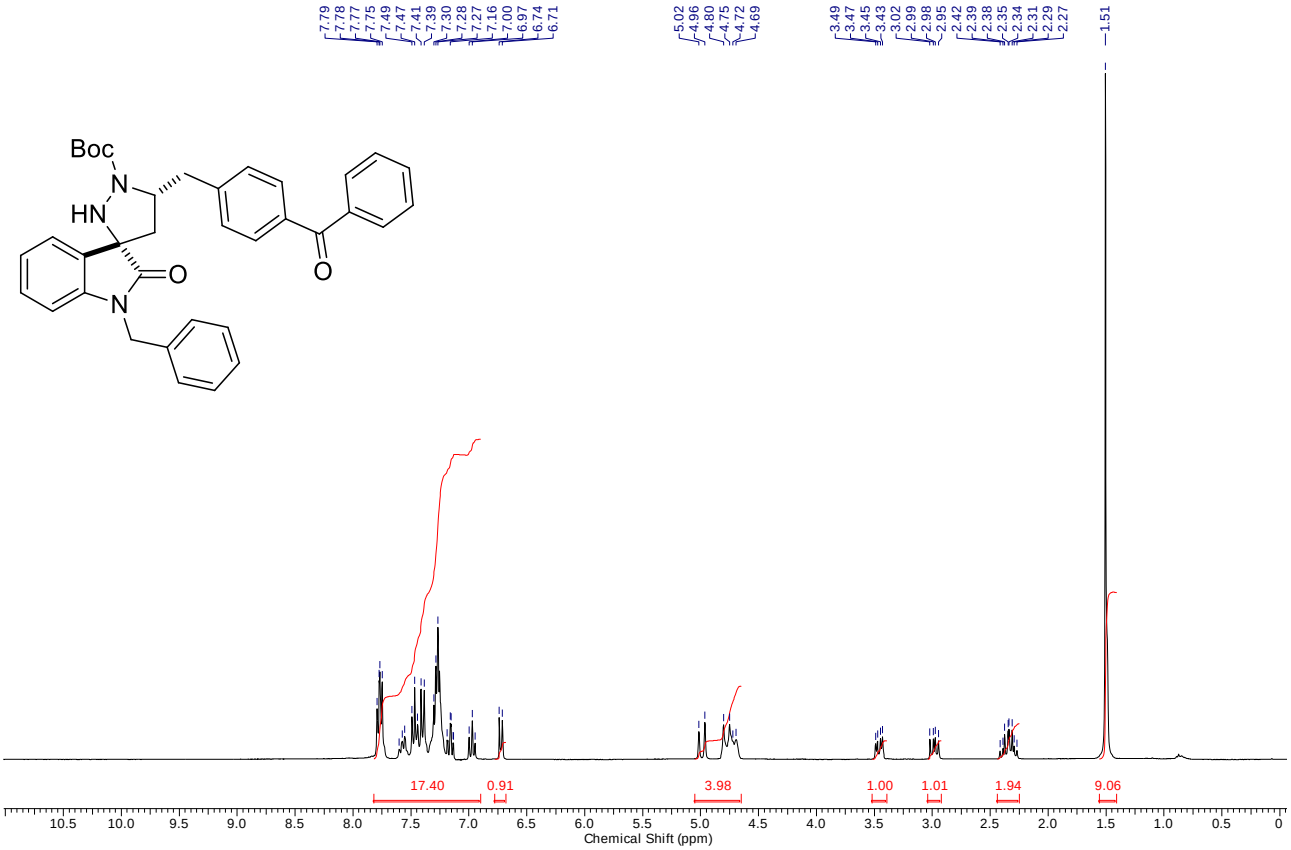

6d' ^{13}C NMR (101 MHz, ATP, $CDCl_3$):

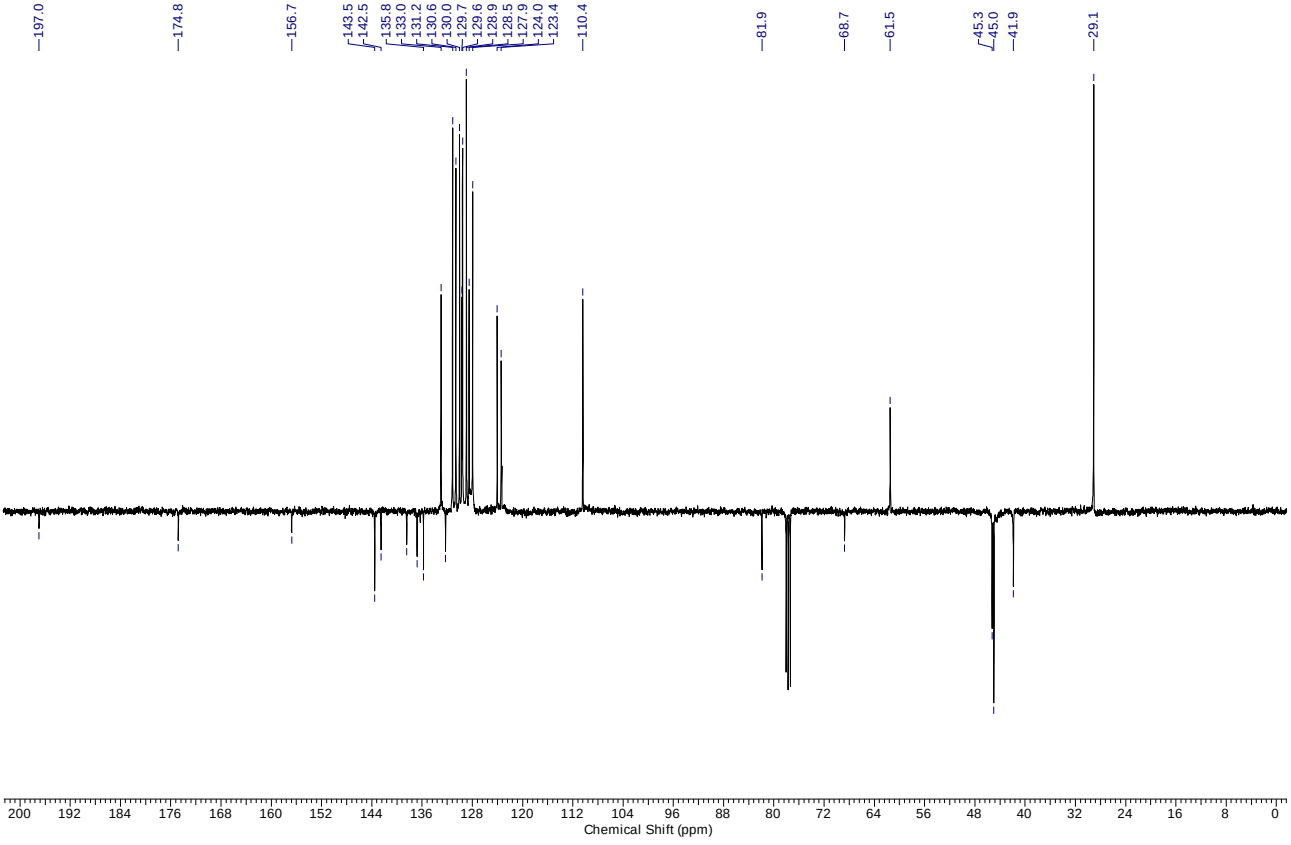

6e ^{1}H NMR (300 MHz, $CDCl_3$):

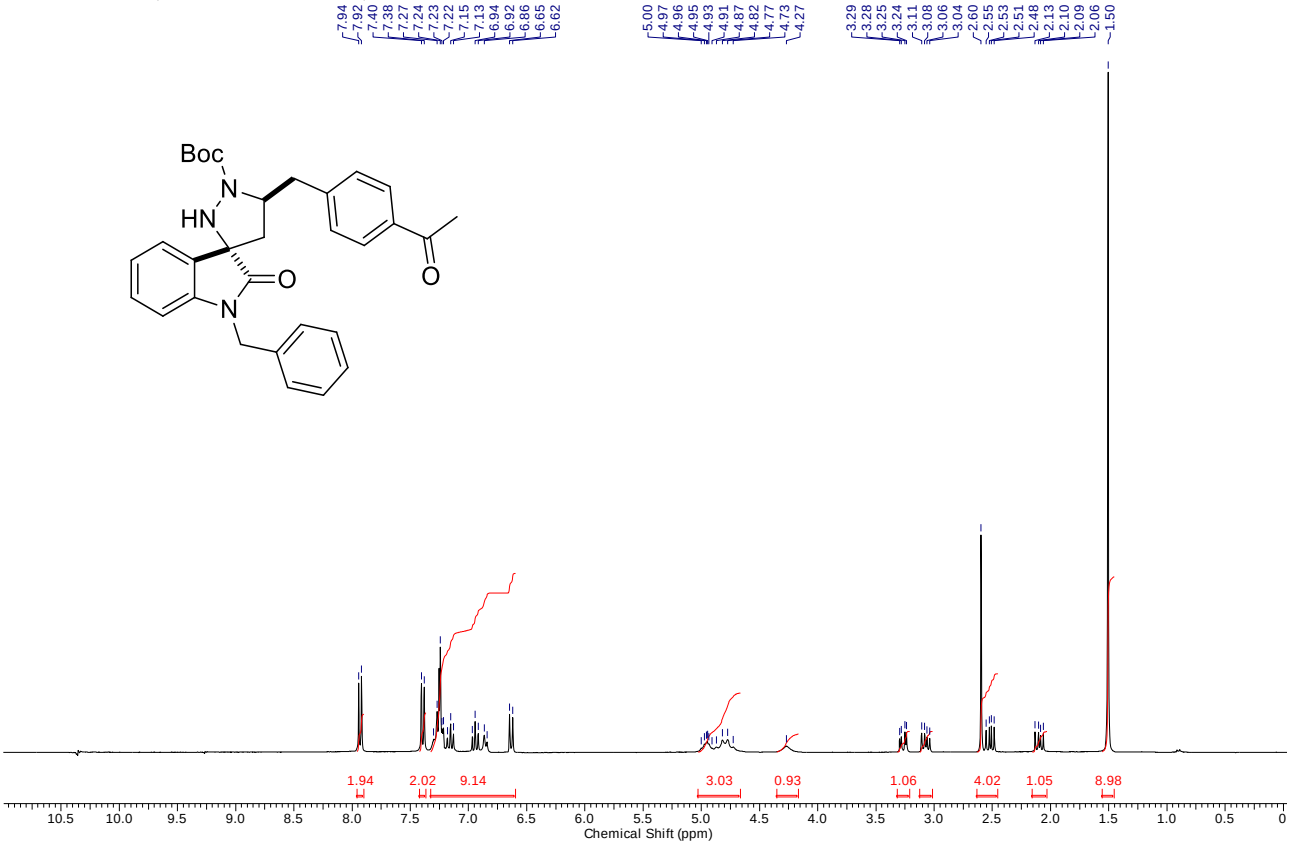

6e ^{13}C NMR (75 MHz, ATP, $CDCl_3$):

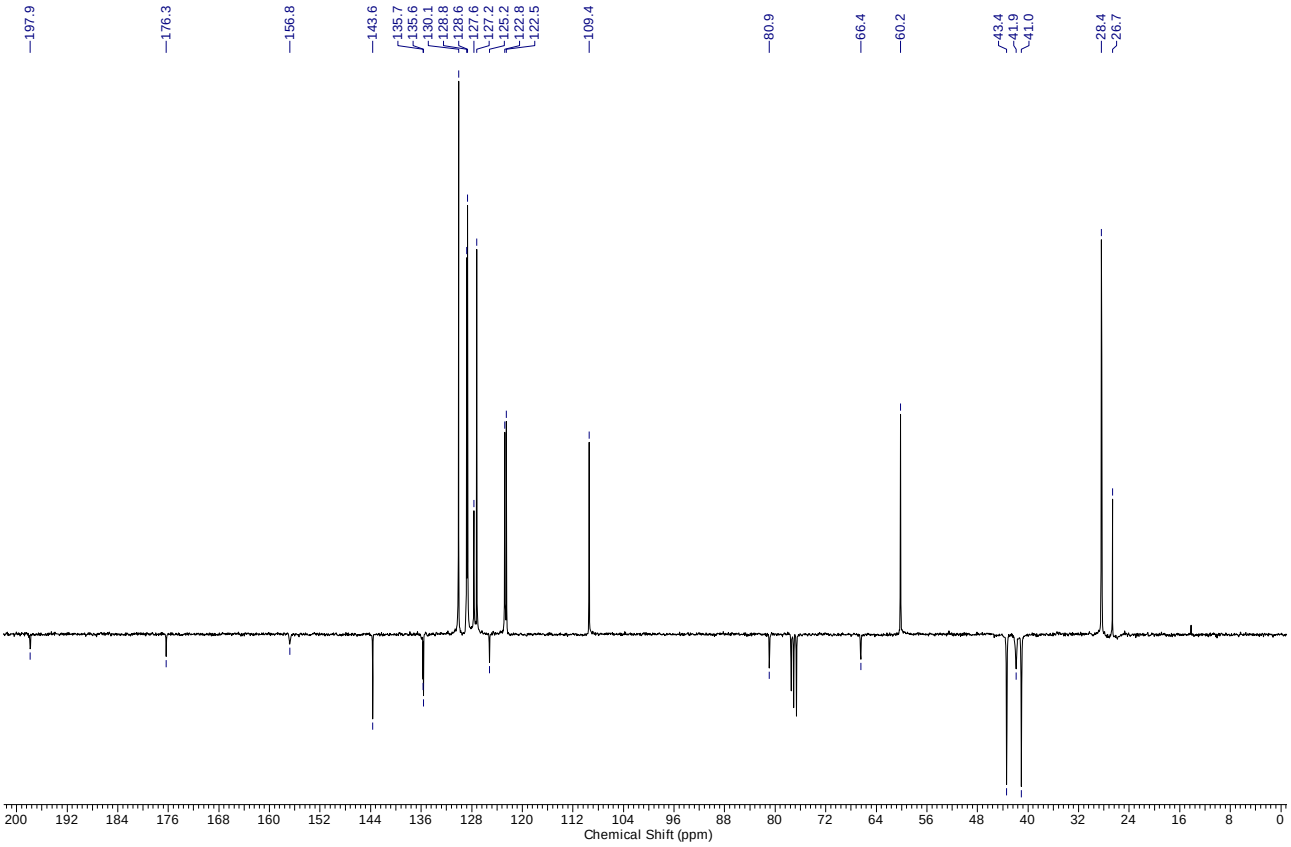

6e' ^{1}H NMR (300 MHz, $CDCl_3$):

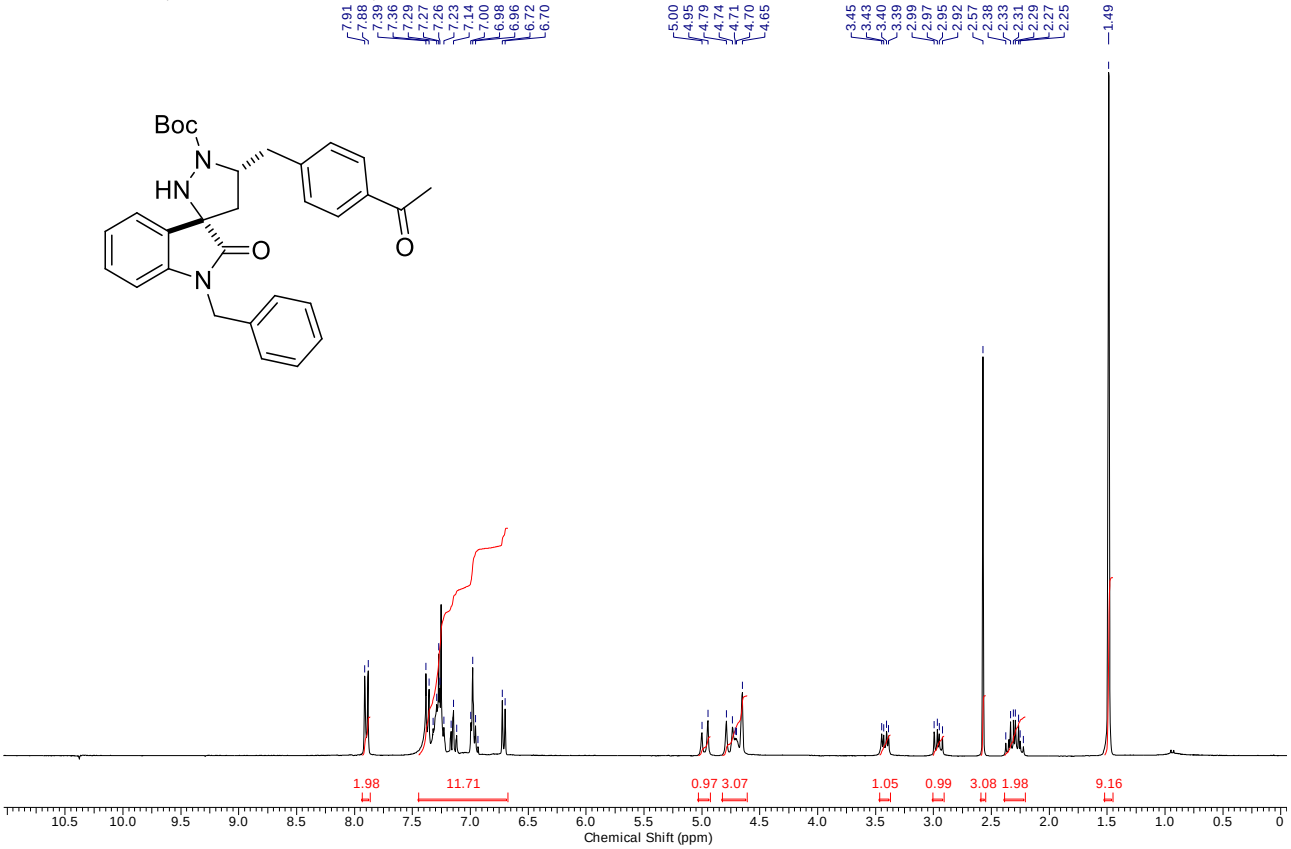

6e' ^{13}C NMR (75 MHz, ATP, $CDCl_3$):

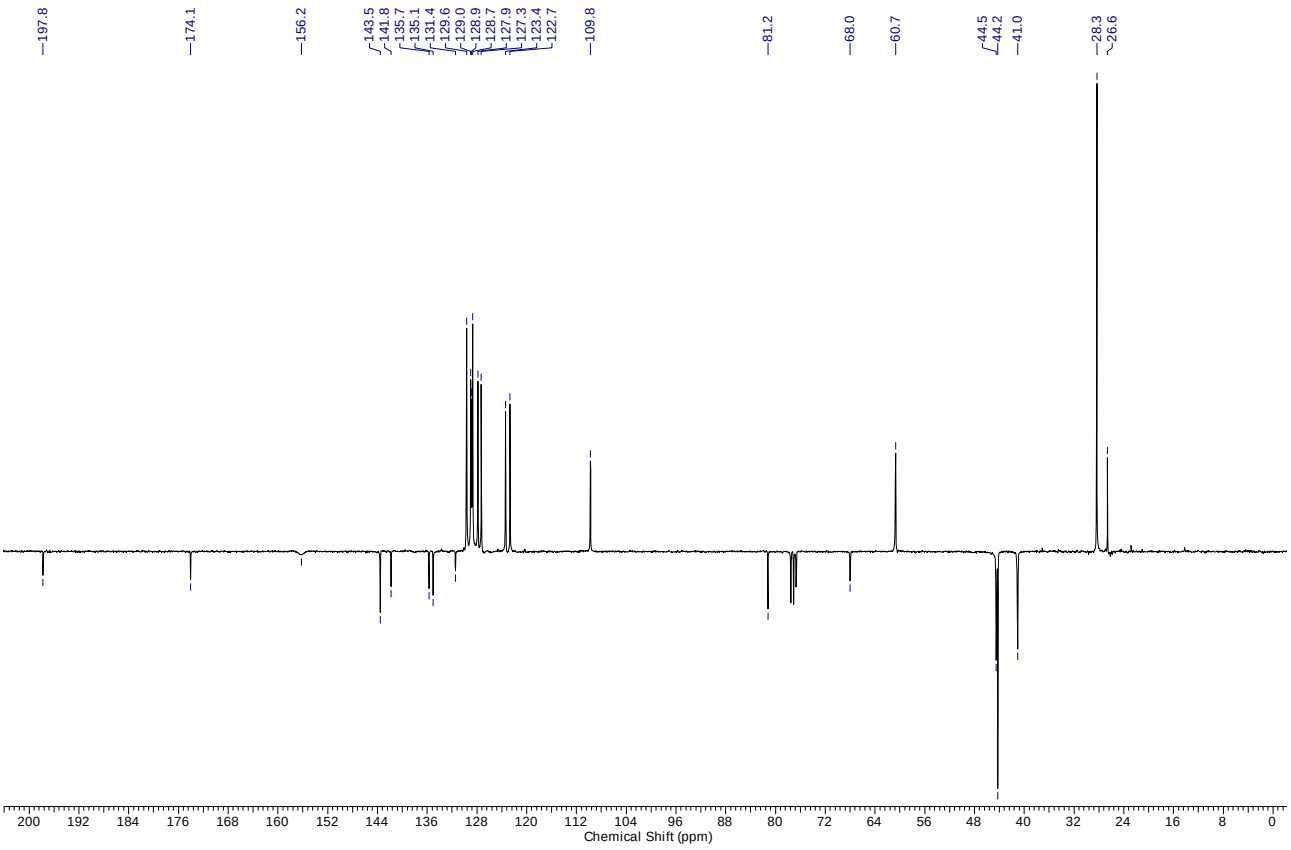

6f ^{1}H NMR (300 MHz, $CDCl_3$):

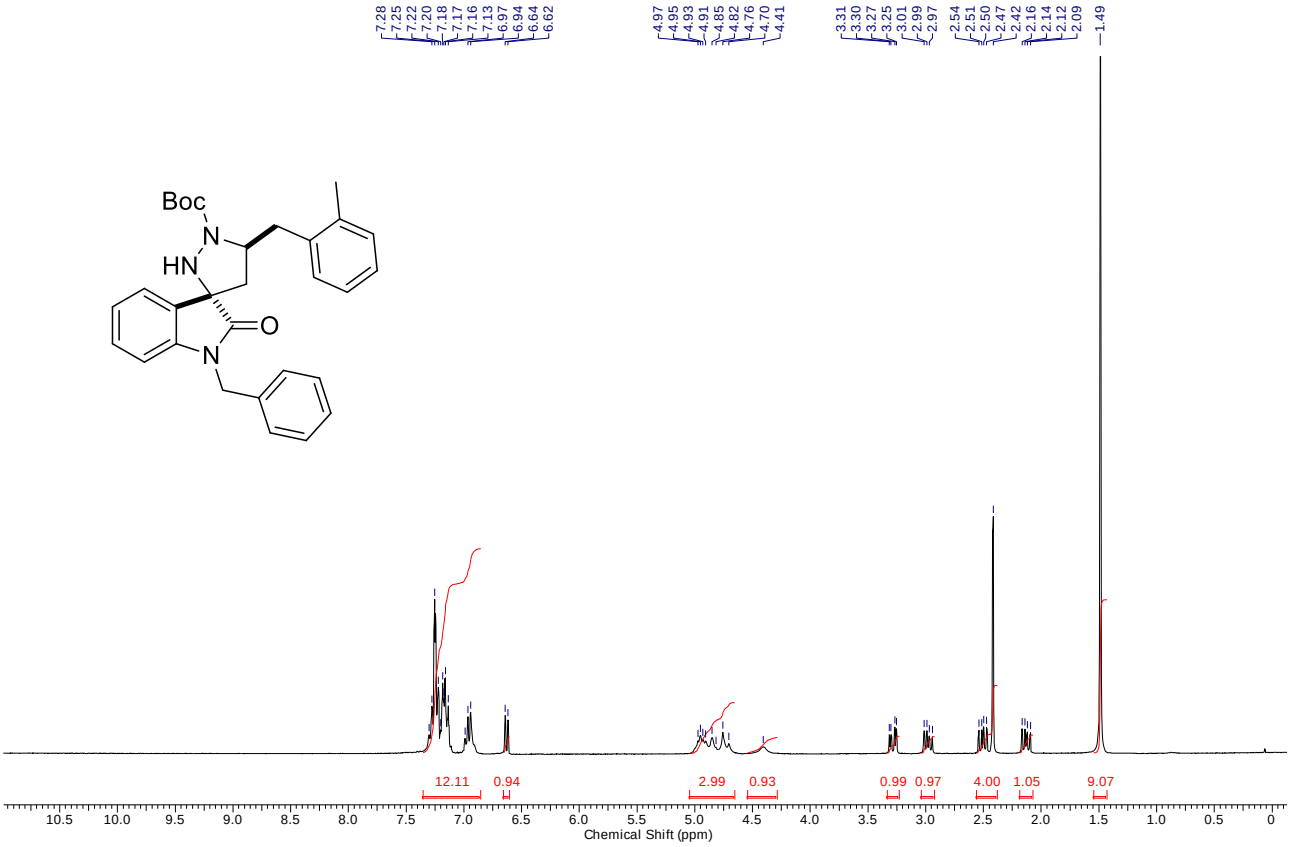

6f ^{13}C NMR (75 MHz, ATP, $CDCl_3$):

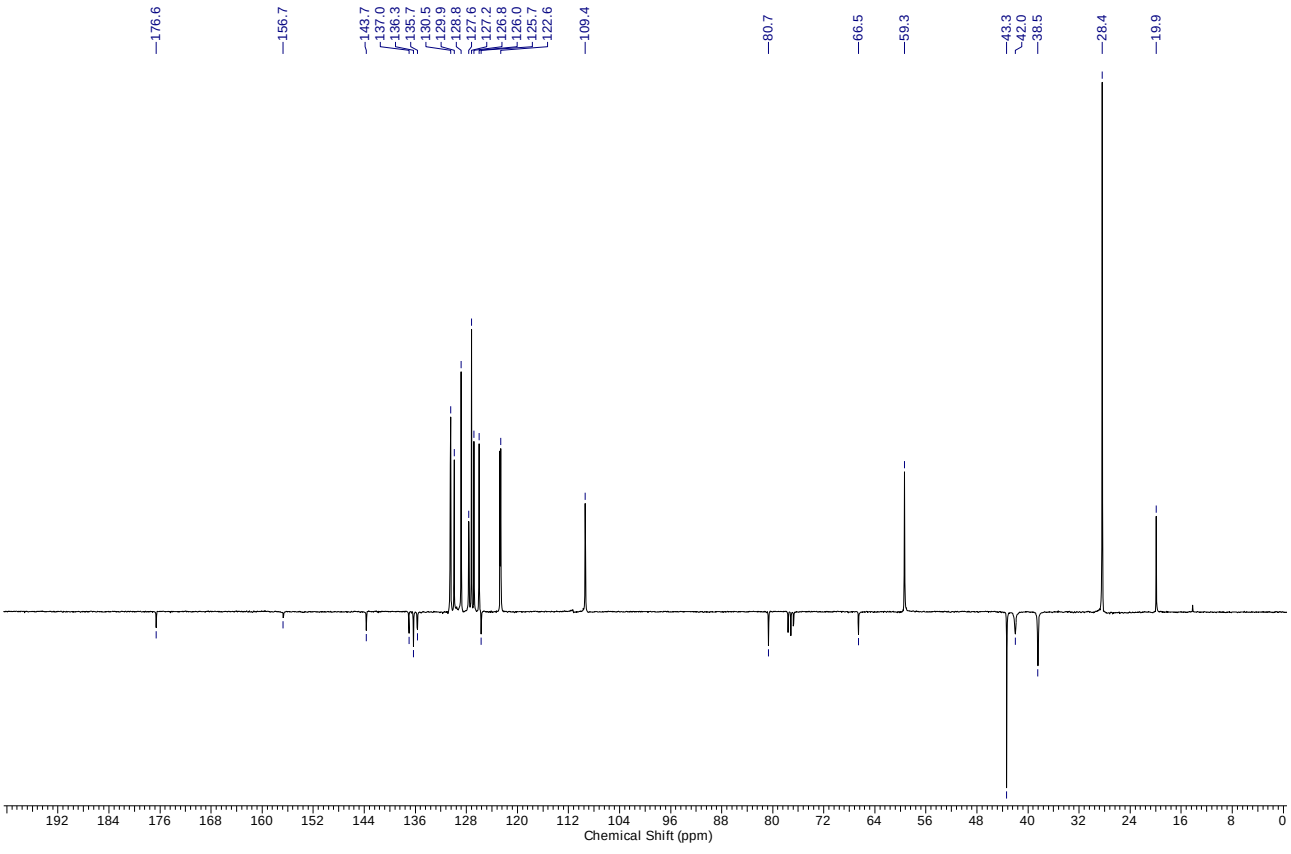

6f' ^{1}H NMR (300 MHz, $CDCl_3$):

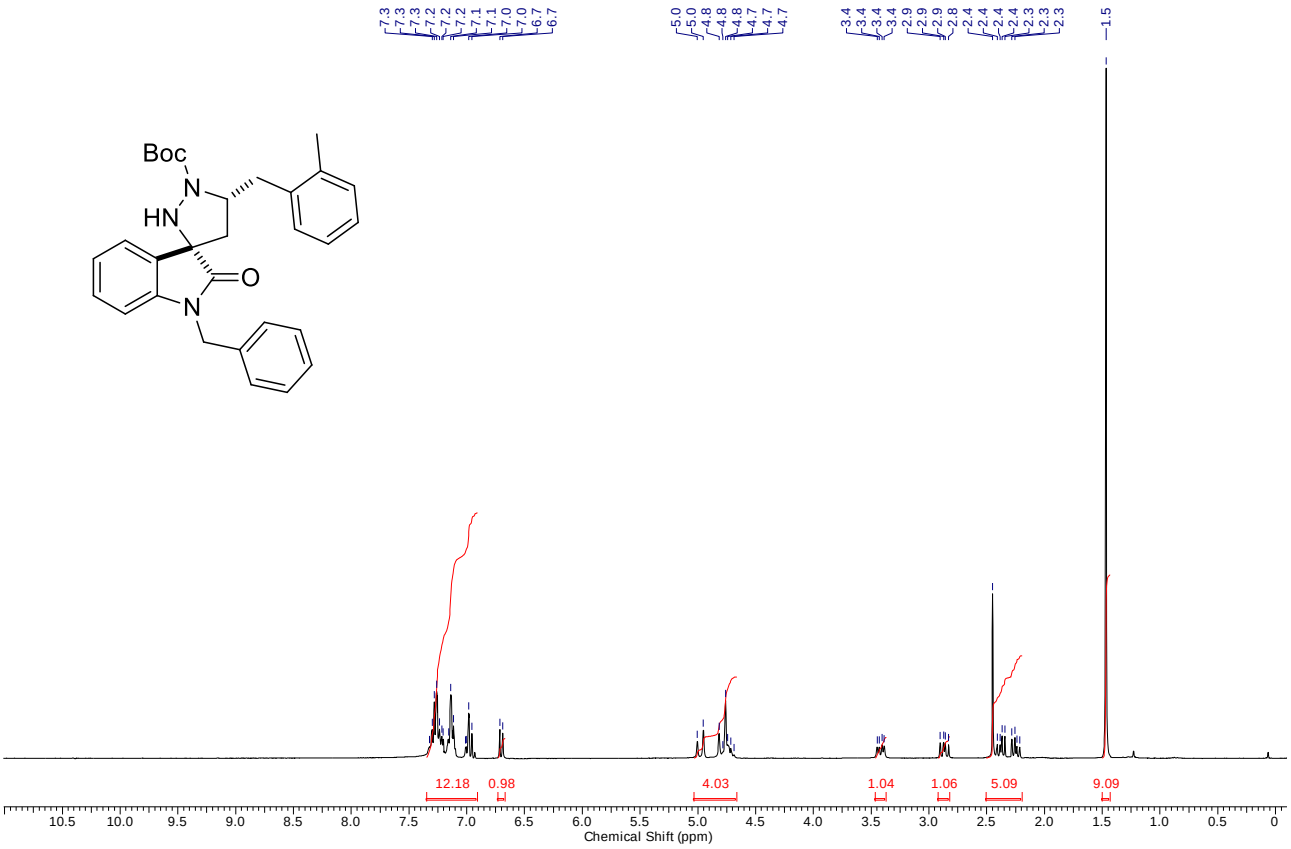

6f' ^{13}C NMR (75 MHz, ATP, $CDCl_3$):

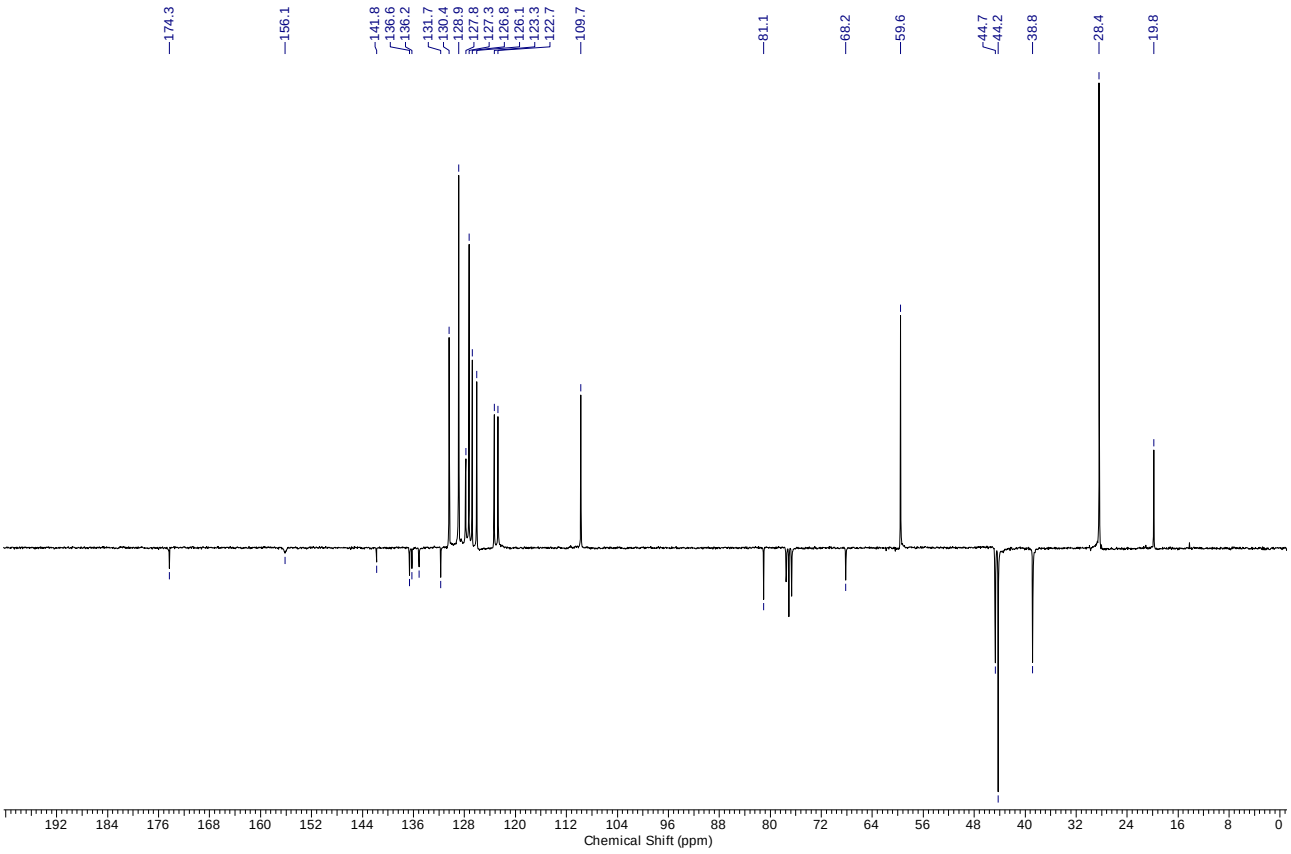

6g ^{1}H NMR (300 MHz, $CDCl_3$):

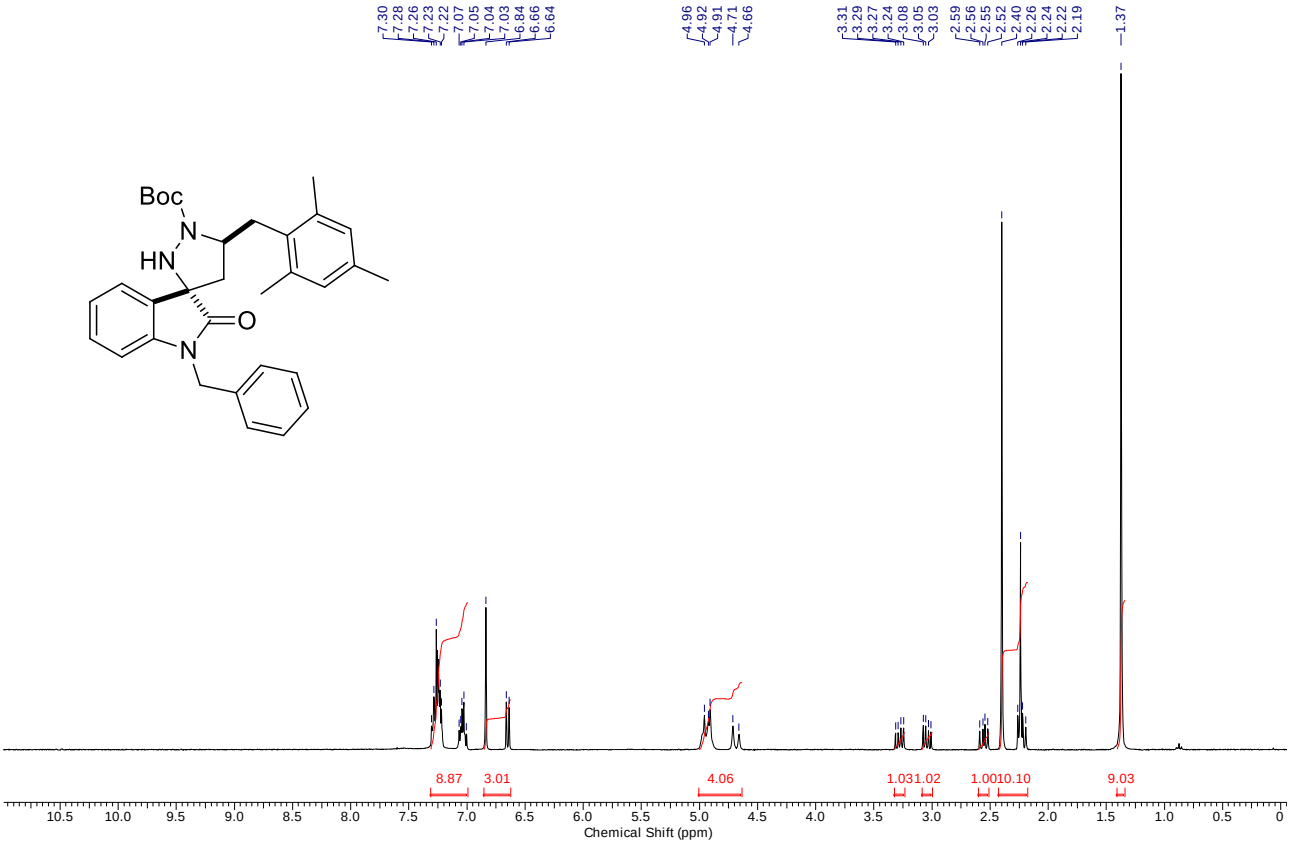

6g ^{13}C NMR (101 MHz, ATP, $CDCl_3$):

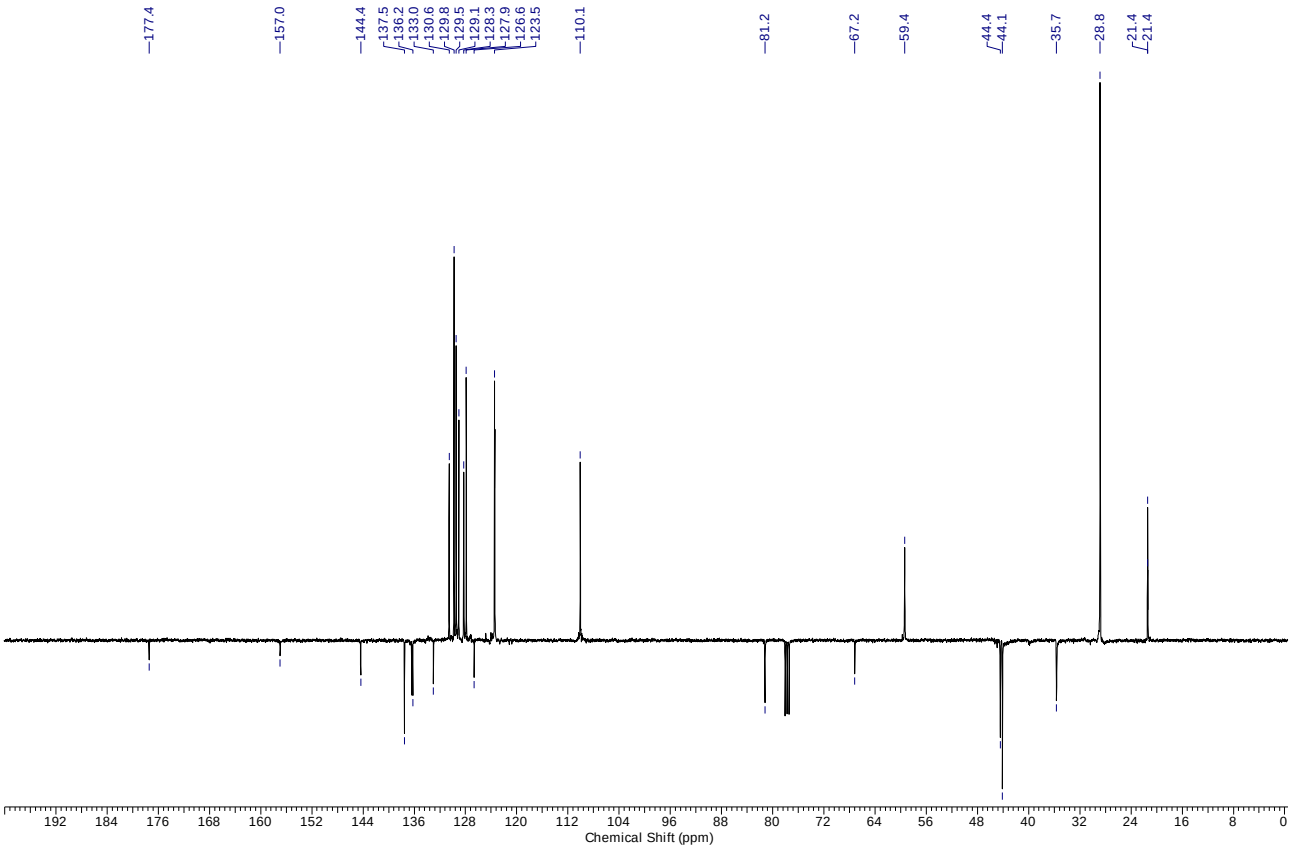

6g' ^{1}H NMR (300 MHz, $CDCl_3$):

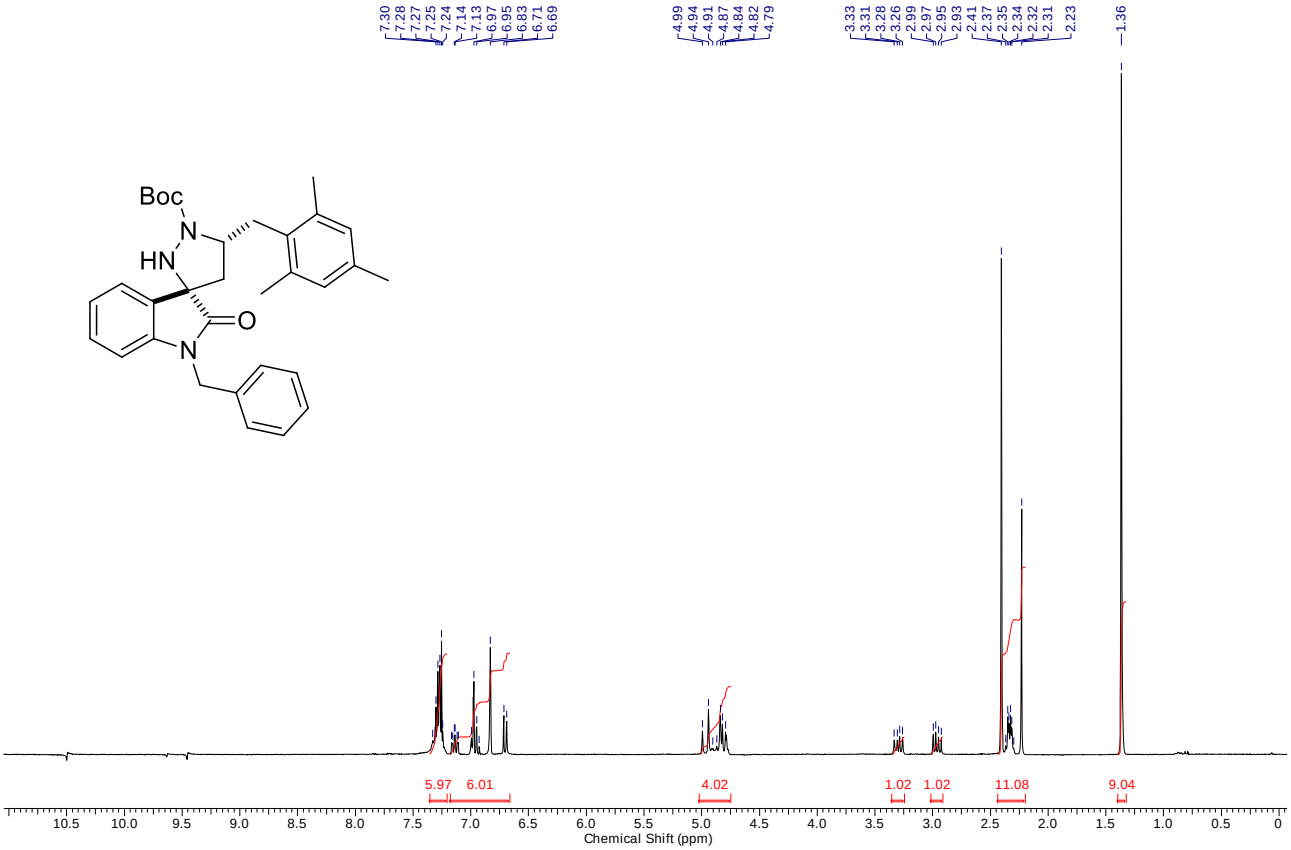

6g' ^{13}C NMR (101 MHz, ATP, $CDCl_3$):

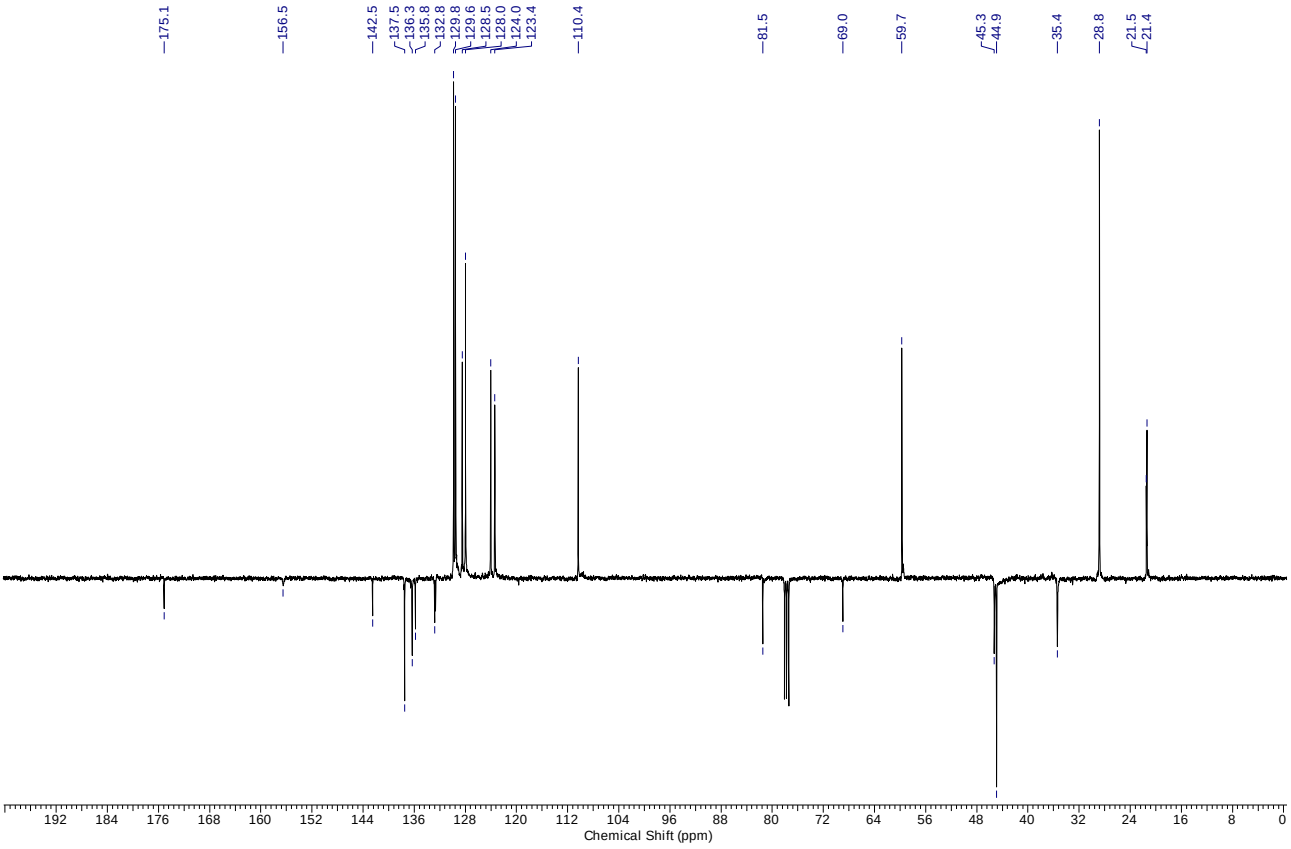

6h ^{1}H NMR (300 MHz, $CDCl_3$):

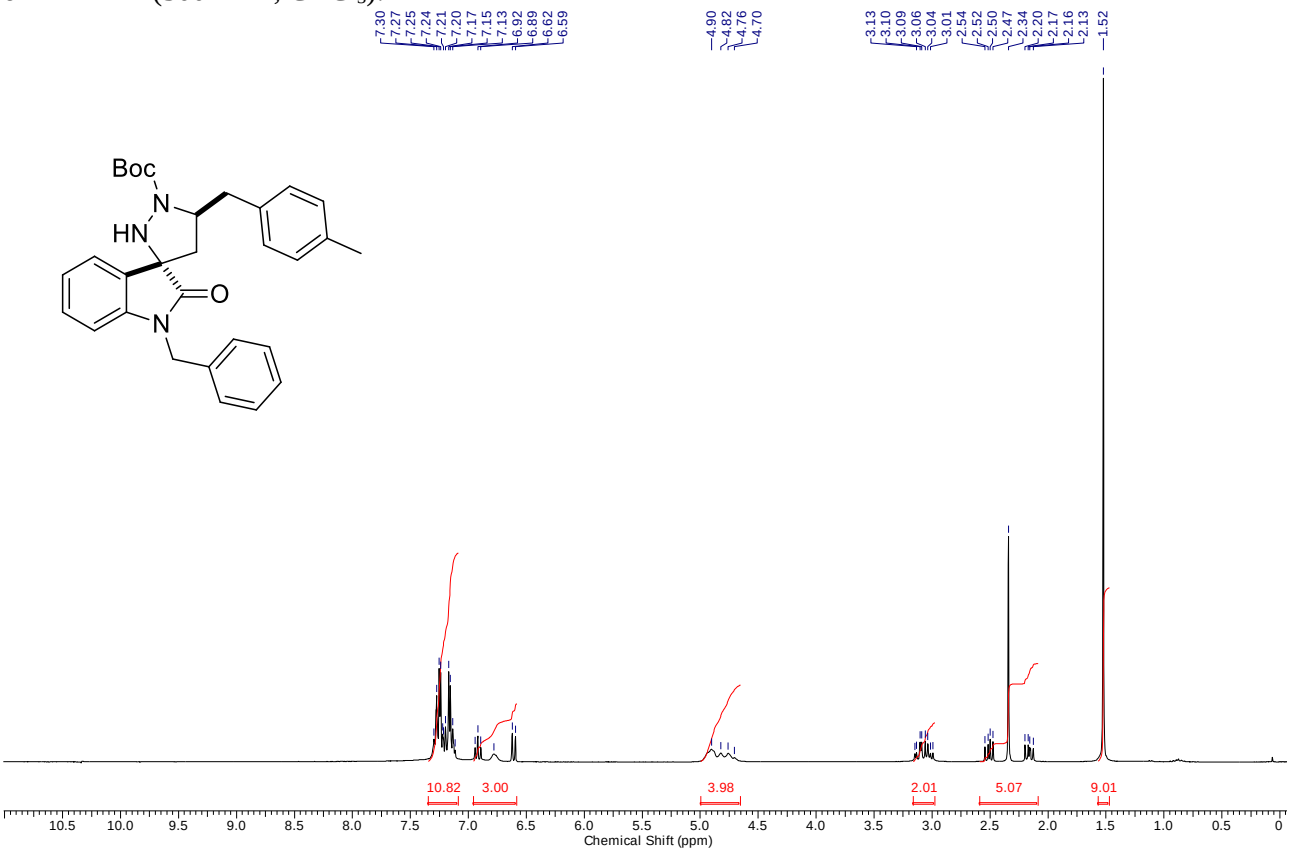

6h ^{13}C NMR (101 MHz, ATP, $CDCl_3$):

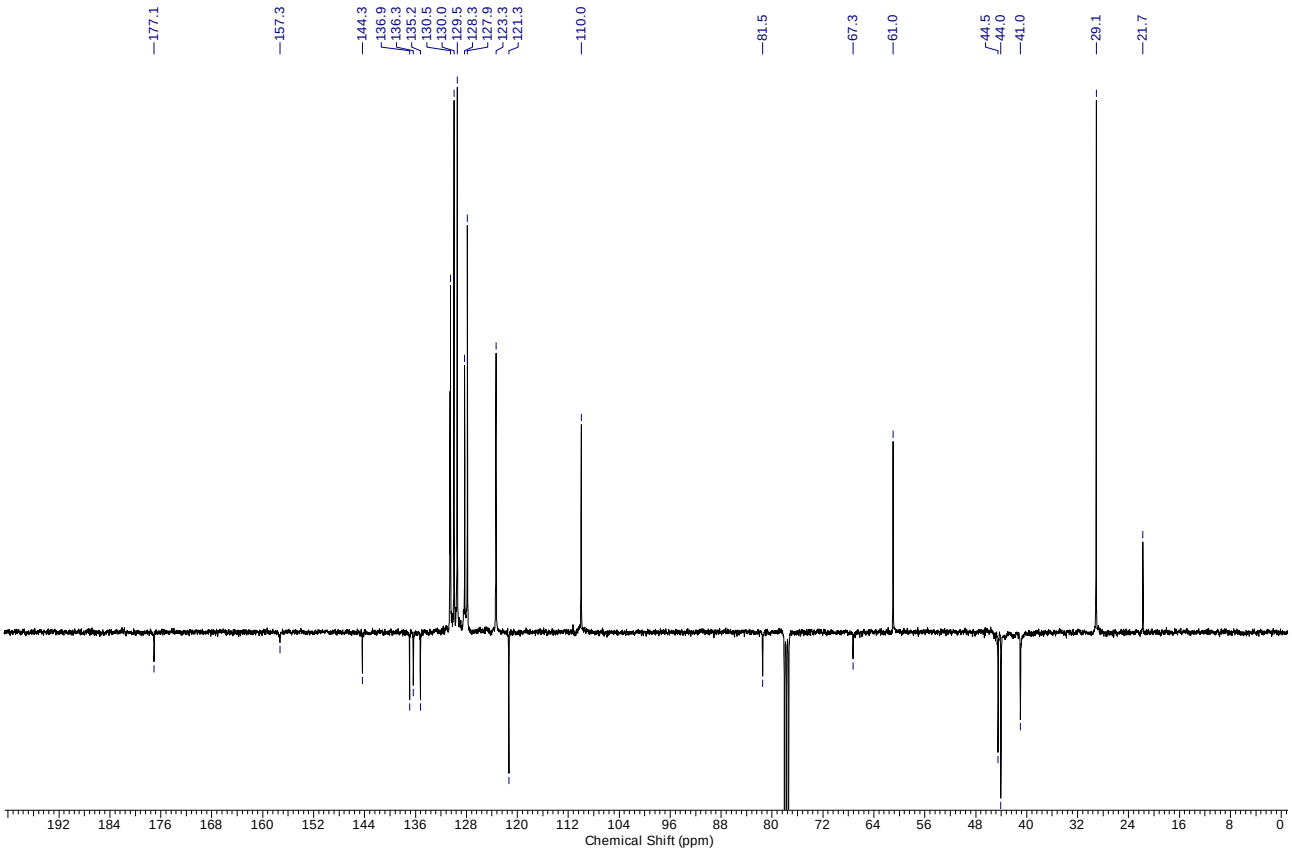

6h' ^{1}H NMR (400 MHz, $CDCl_3$):

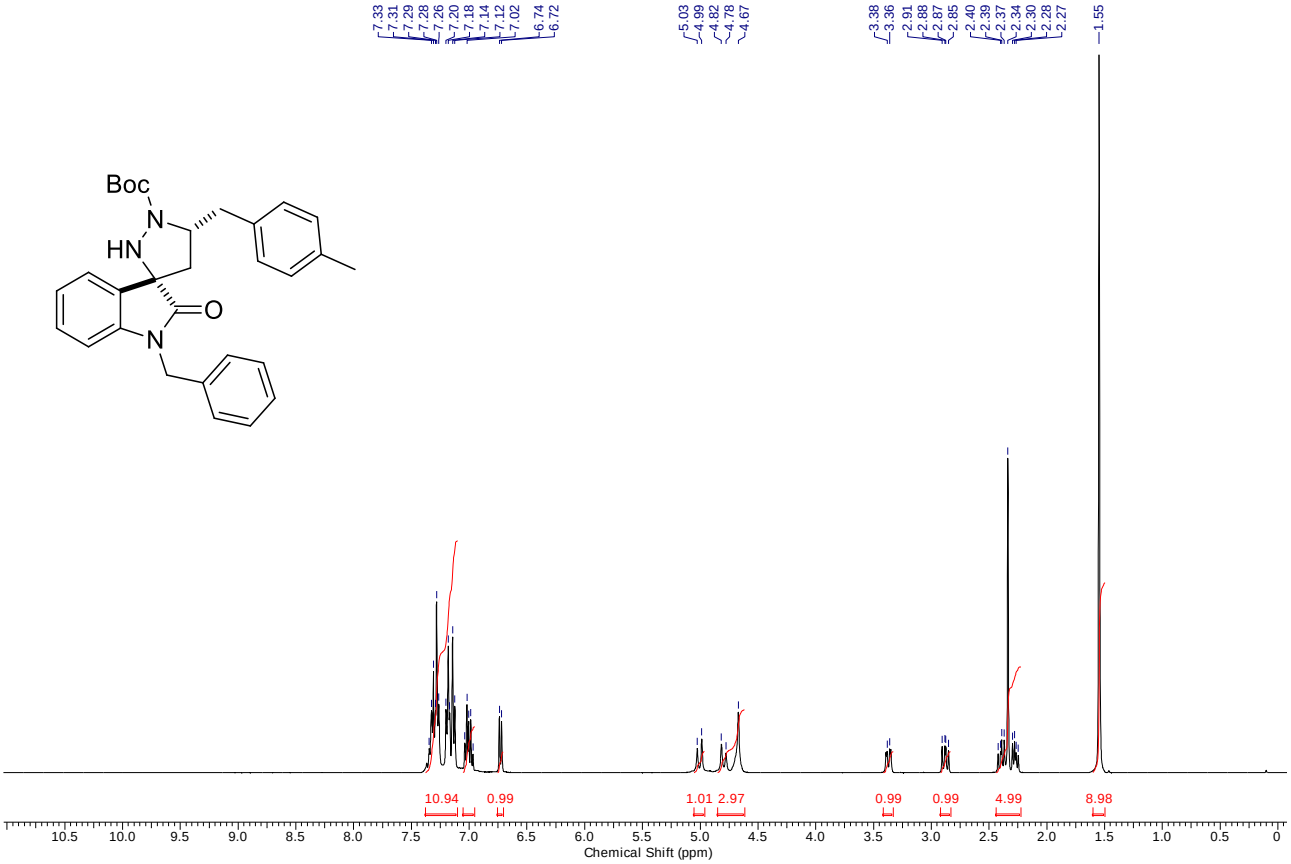

6h' ^{13}C NMR (101 MHz, ATP, $CDCl_3$):

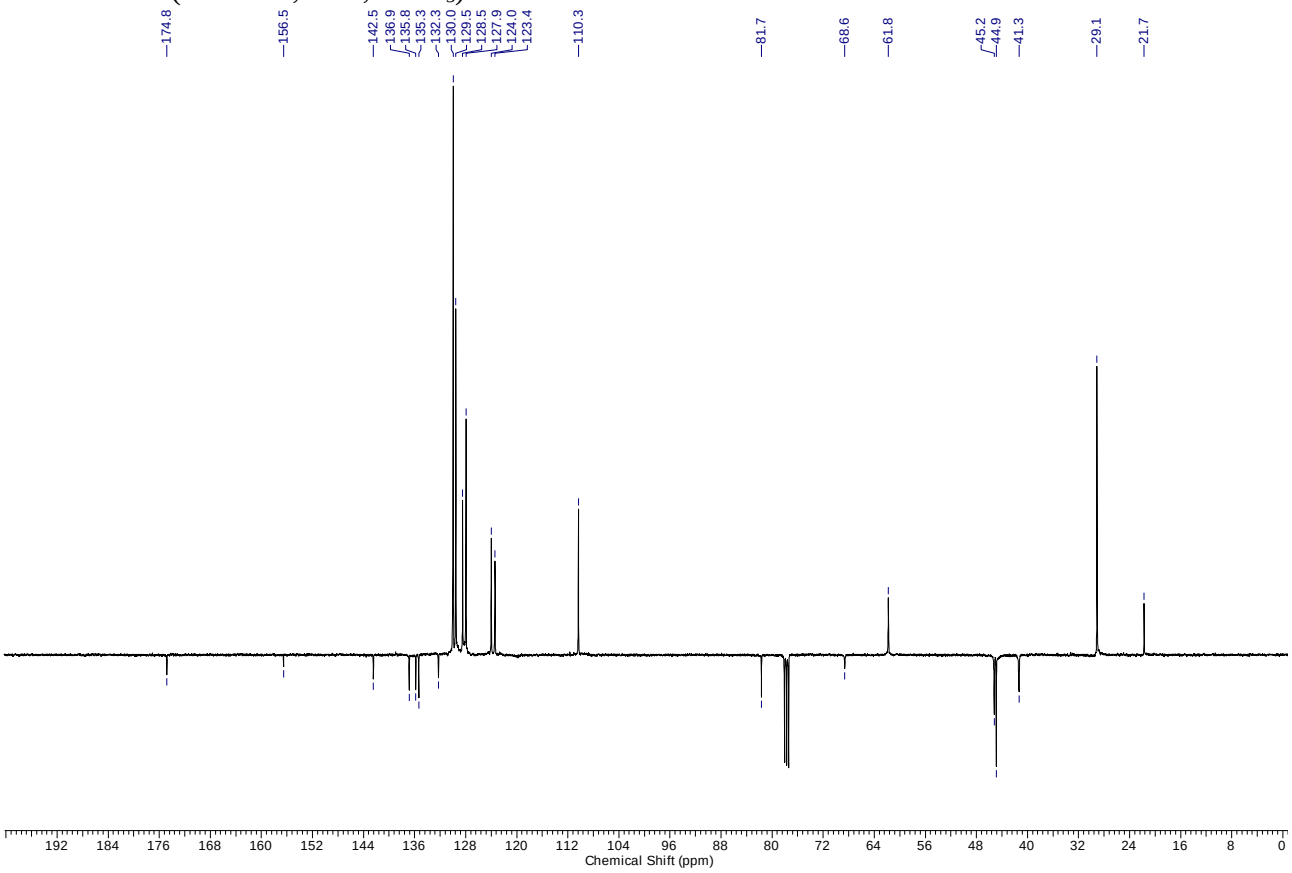

6i ^{1}H NMR (300 MHz, $CDCl_3$):

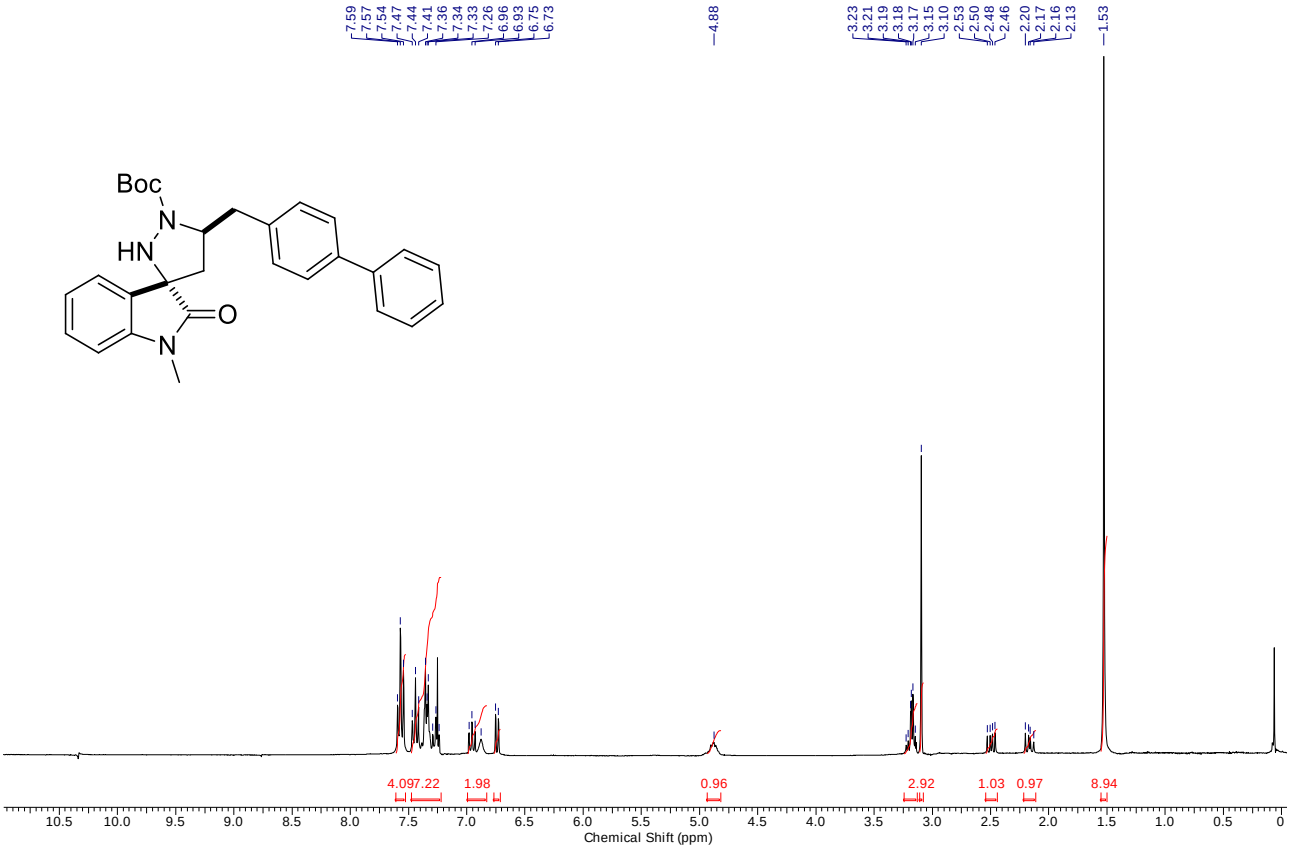

6i ^{13}C NMR (101 MHz, ATP, $CDCl_3$):

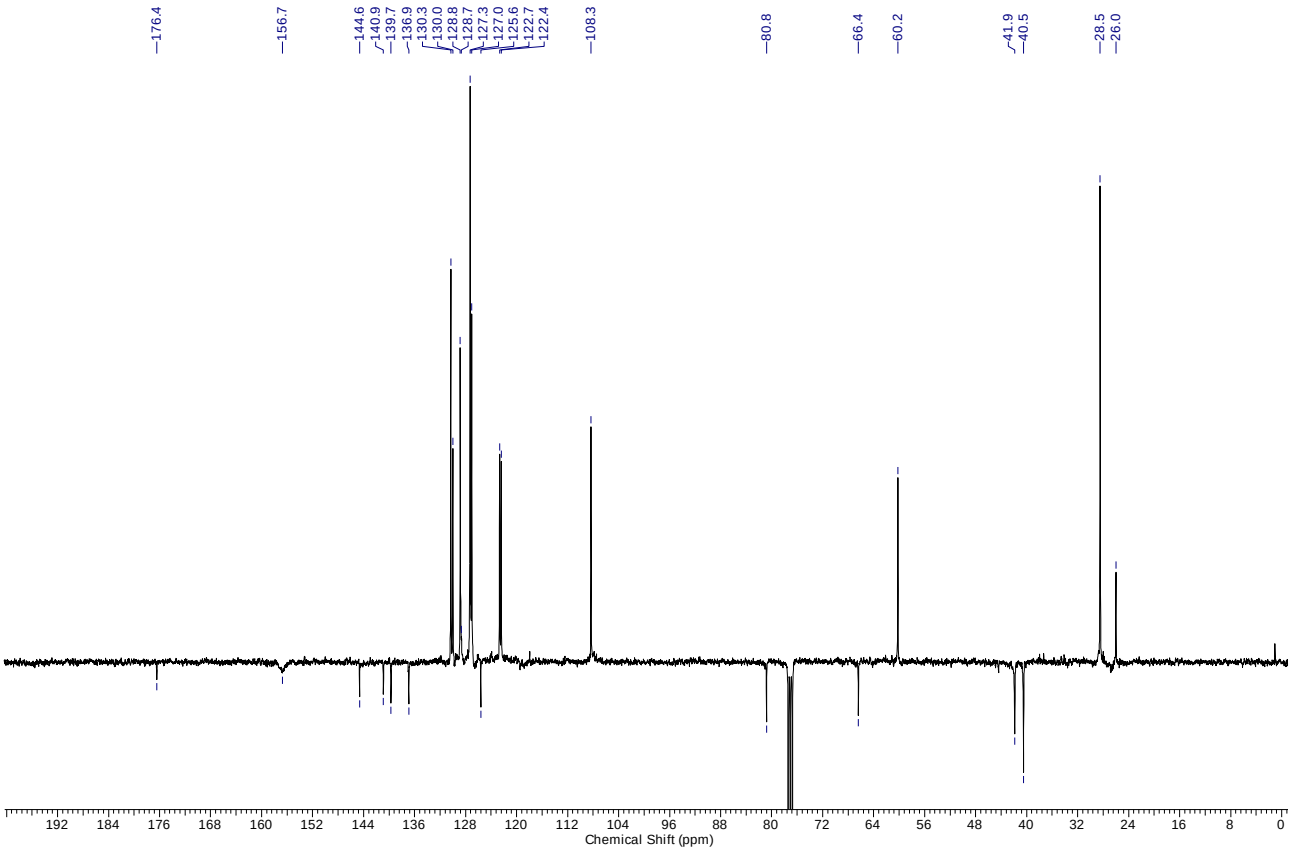

6i' ^{1}H NMR (300 MHz, $CDCl_3$):

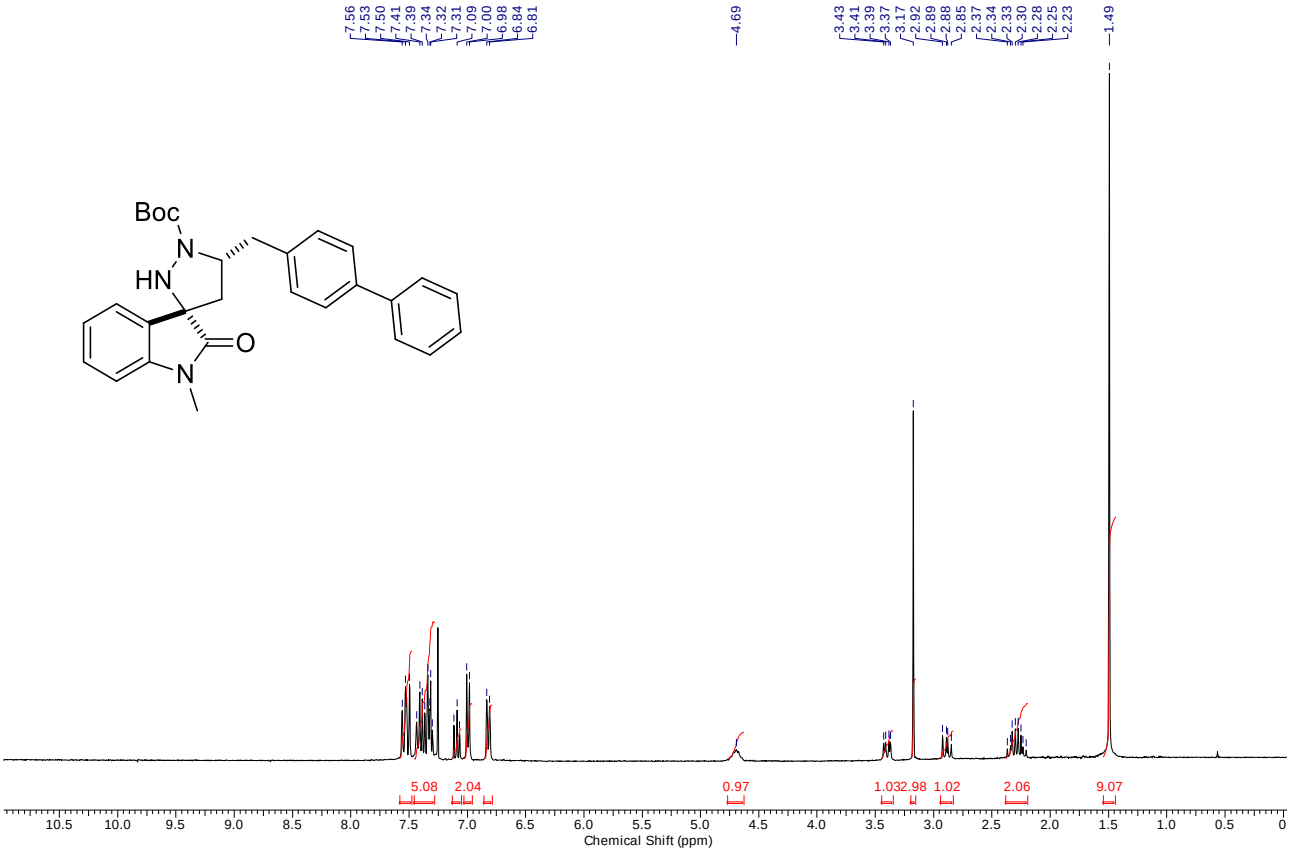

6i' ^{13}C NMR (101 MHz, ATP, $CDCl_3$):

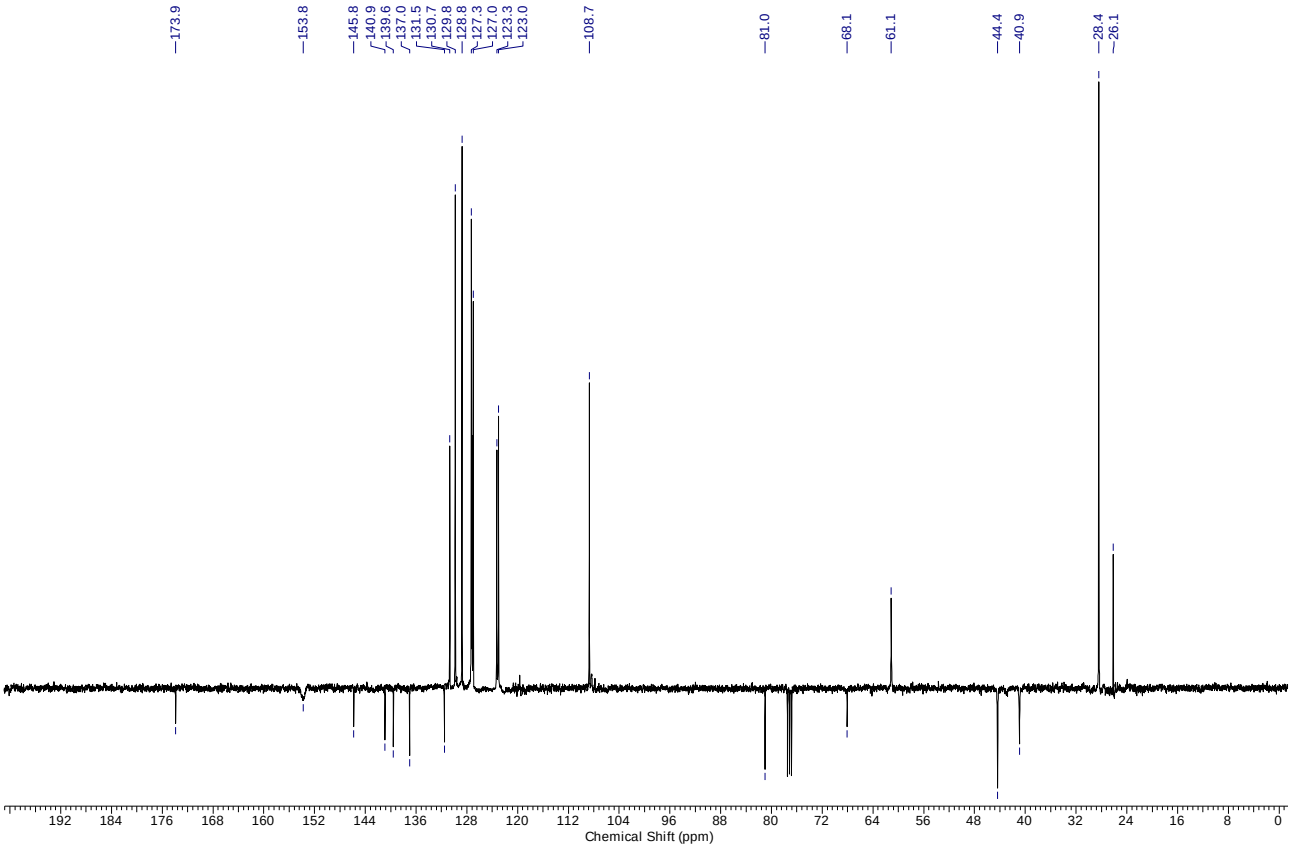

6j ^{1}H NMR (300 MHz, $CDCl_3$):

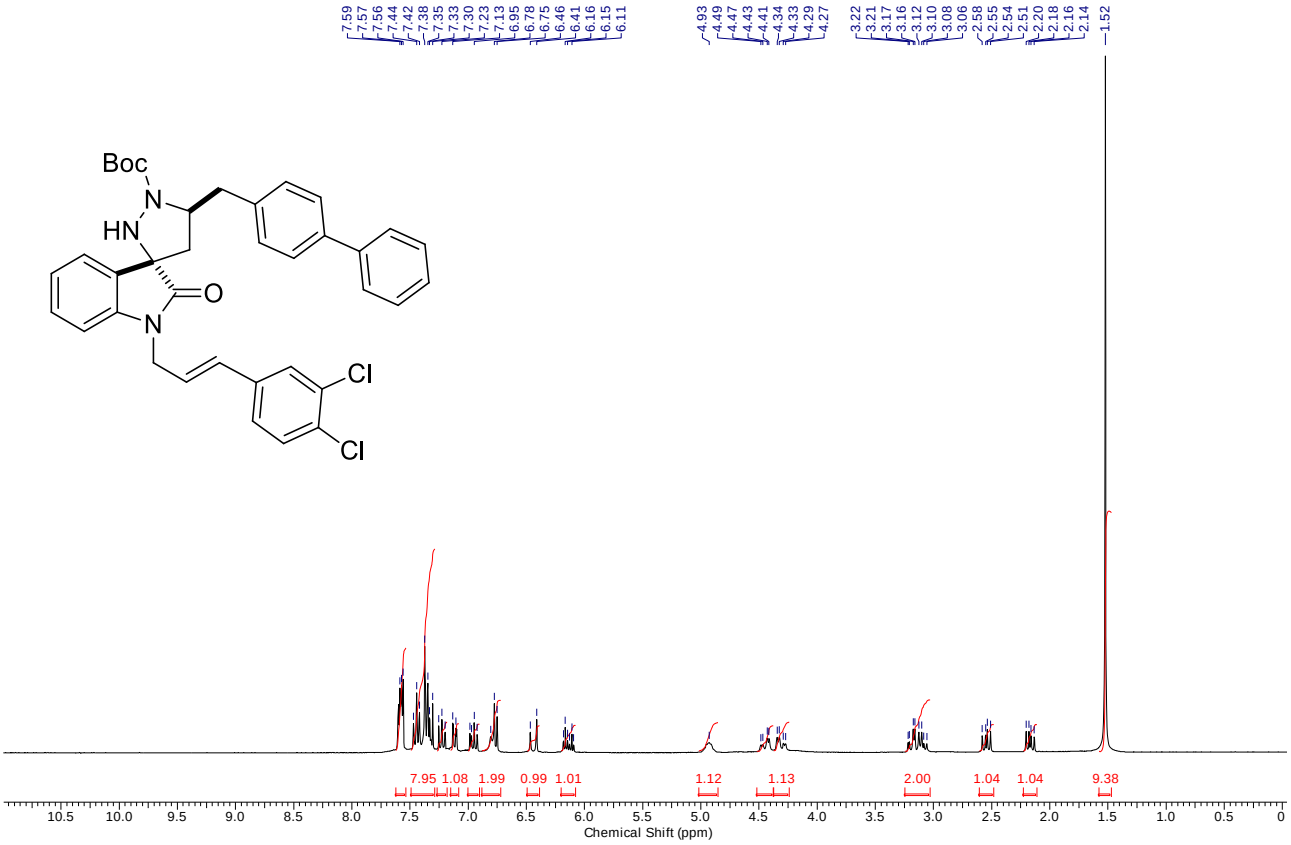

6j ^{13}C NMR (101 MHz, ATP, $CDCl_3$):

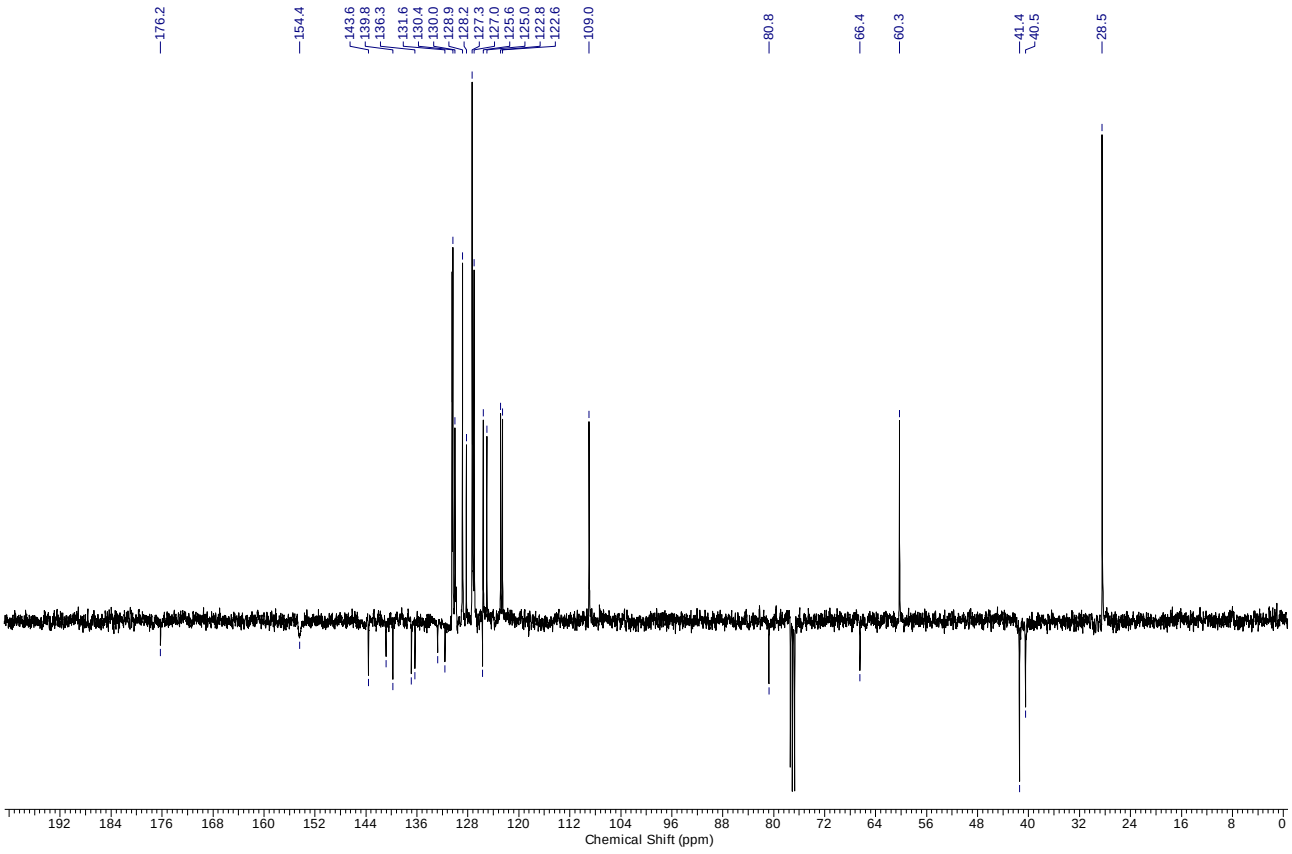

6j' ^{1}H NMR (300 MHz, $CDCl_3$):

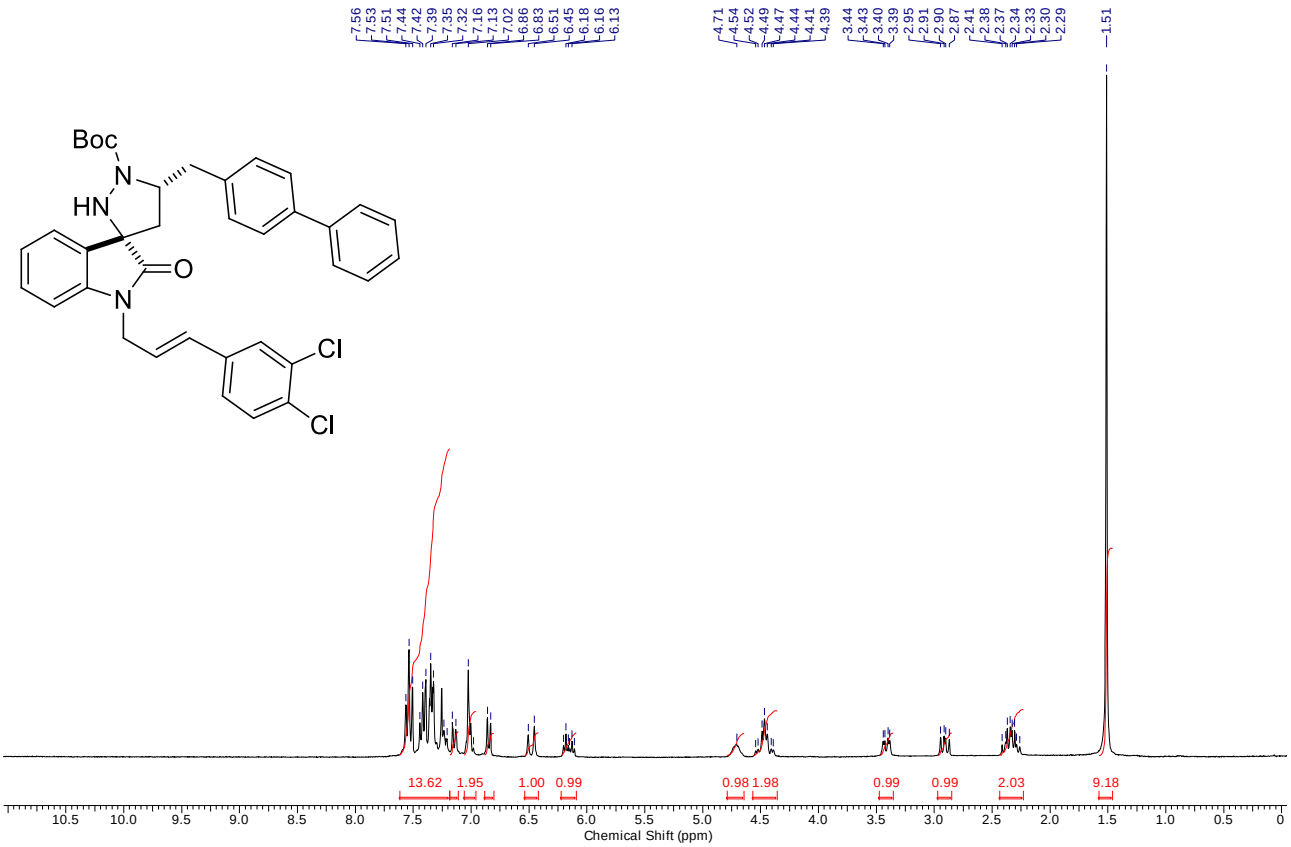

6j' ^{13}C NMR (101 MHz, ATP, $CDCl_3$):

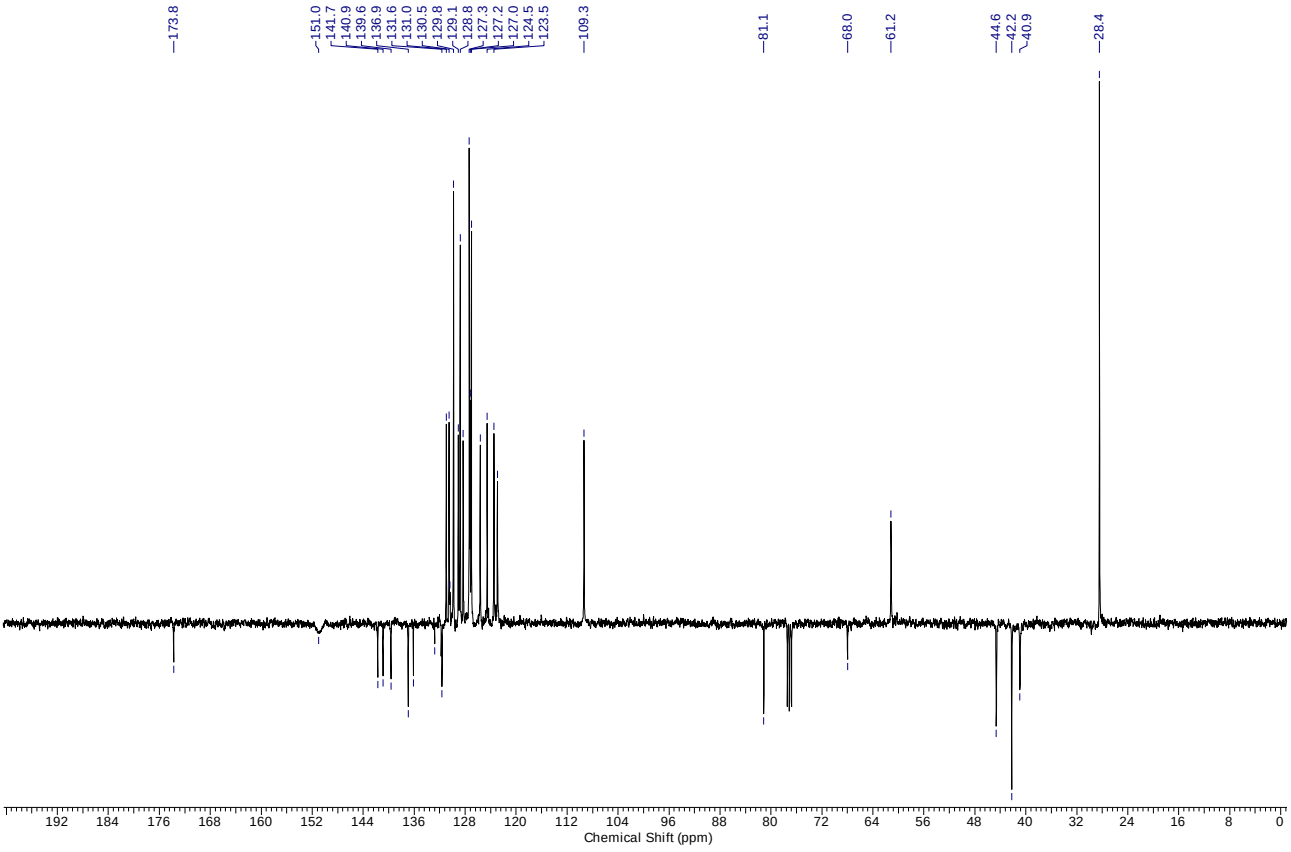

6k ^{1}H NMR (300 MHz, $CDCl_3$):

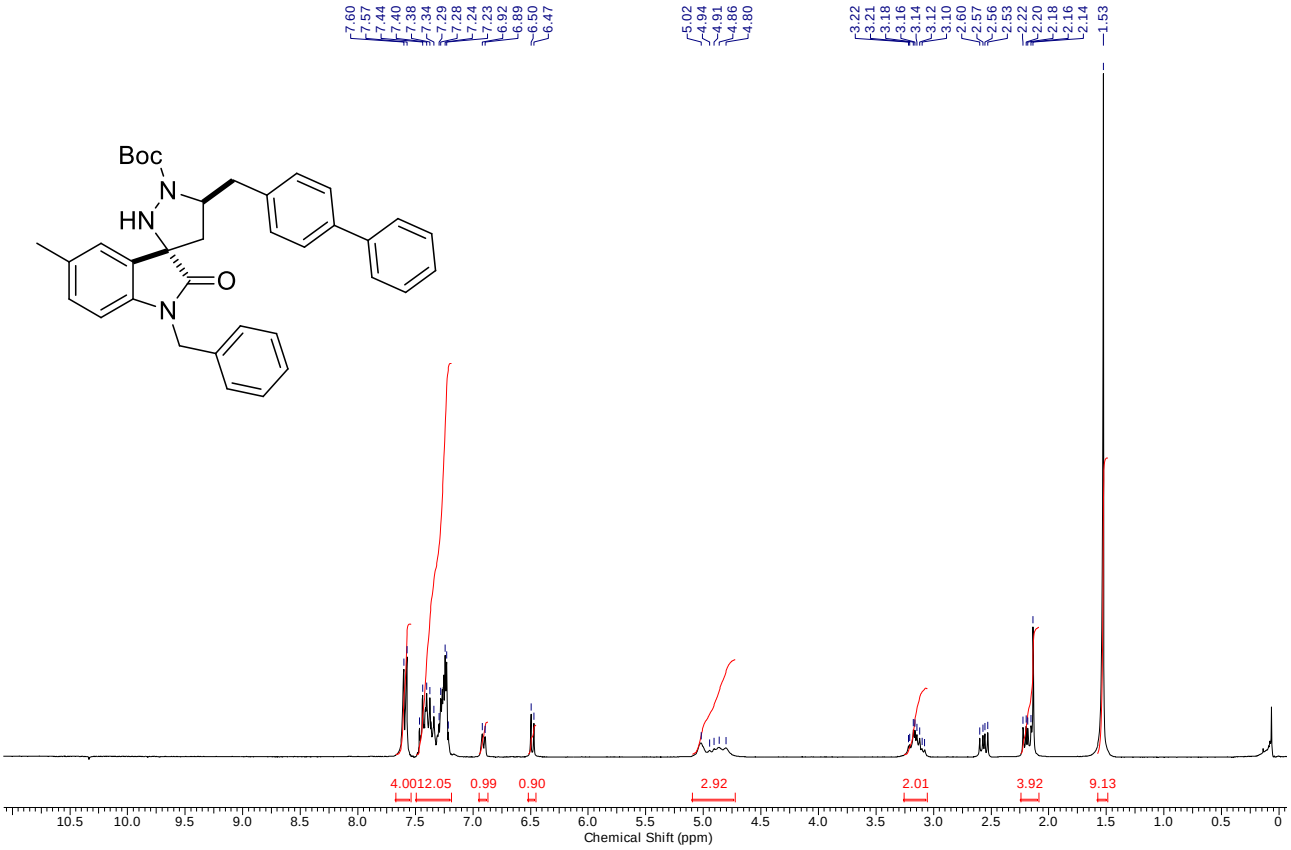

6k ^{13}C NMR (101 MHz, ATP, $CDCl_3$):

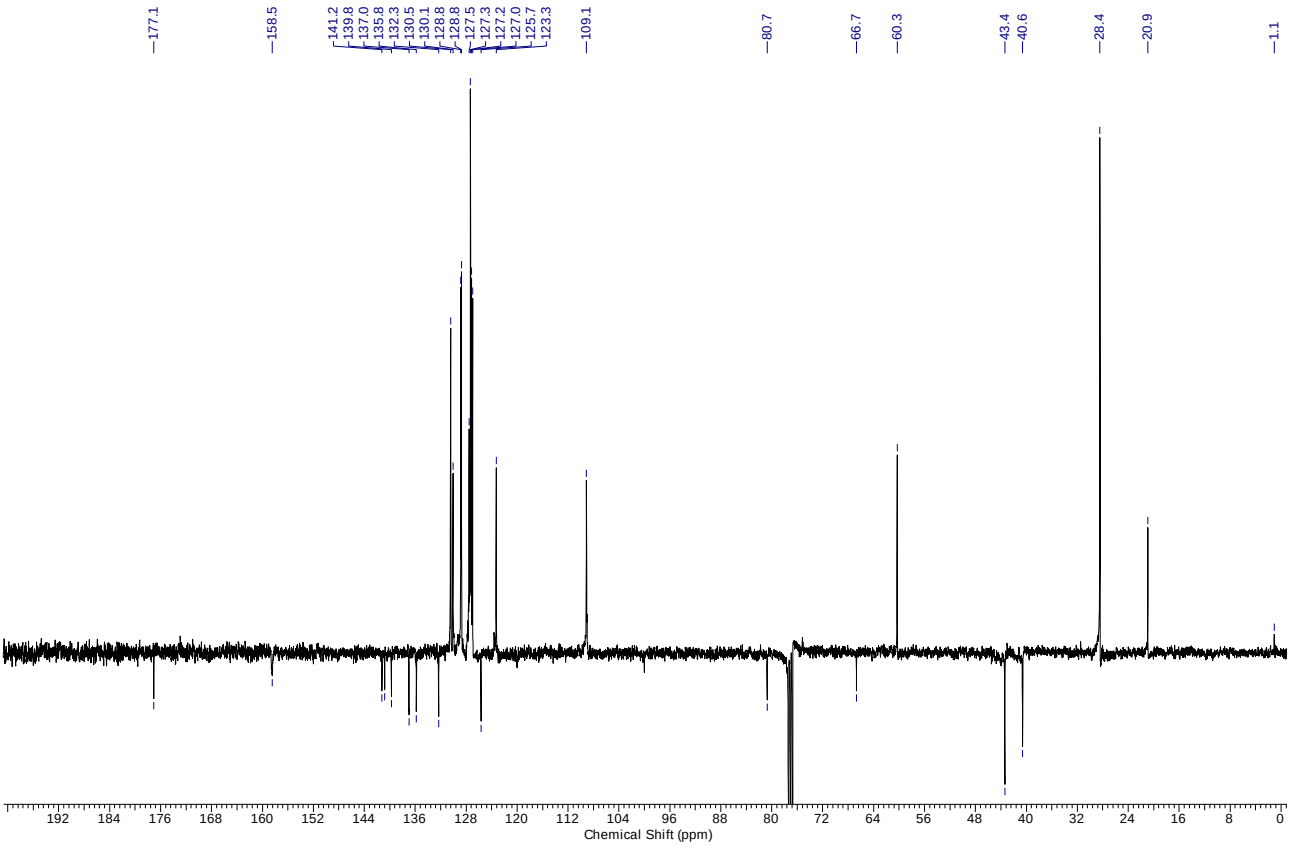

6k' ^{1}H NMR (400 MHz, $CDCl_3$):

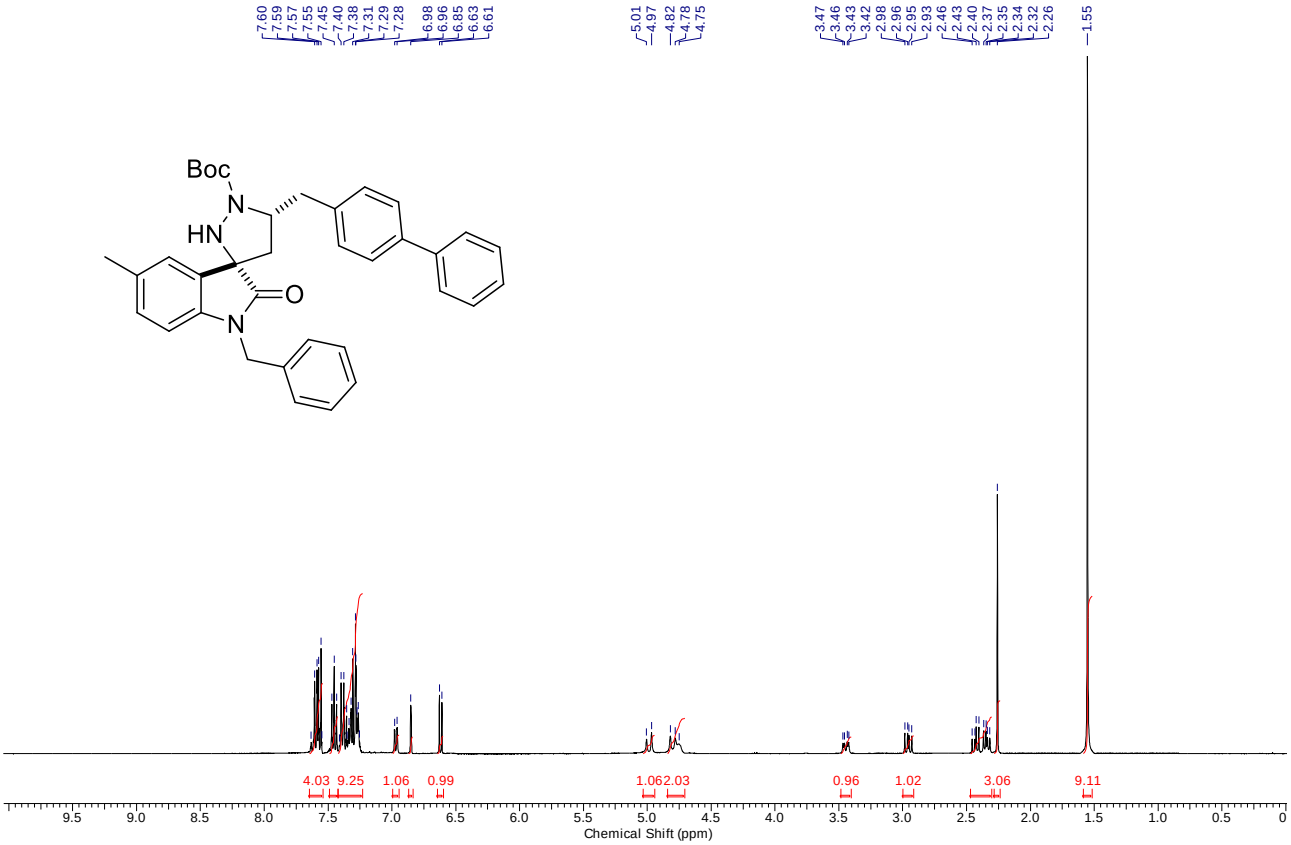

6k' ^{13}C NMR (101 MHz, ATP, $CDCl_3$):

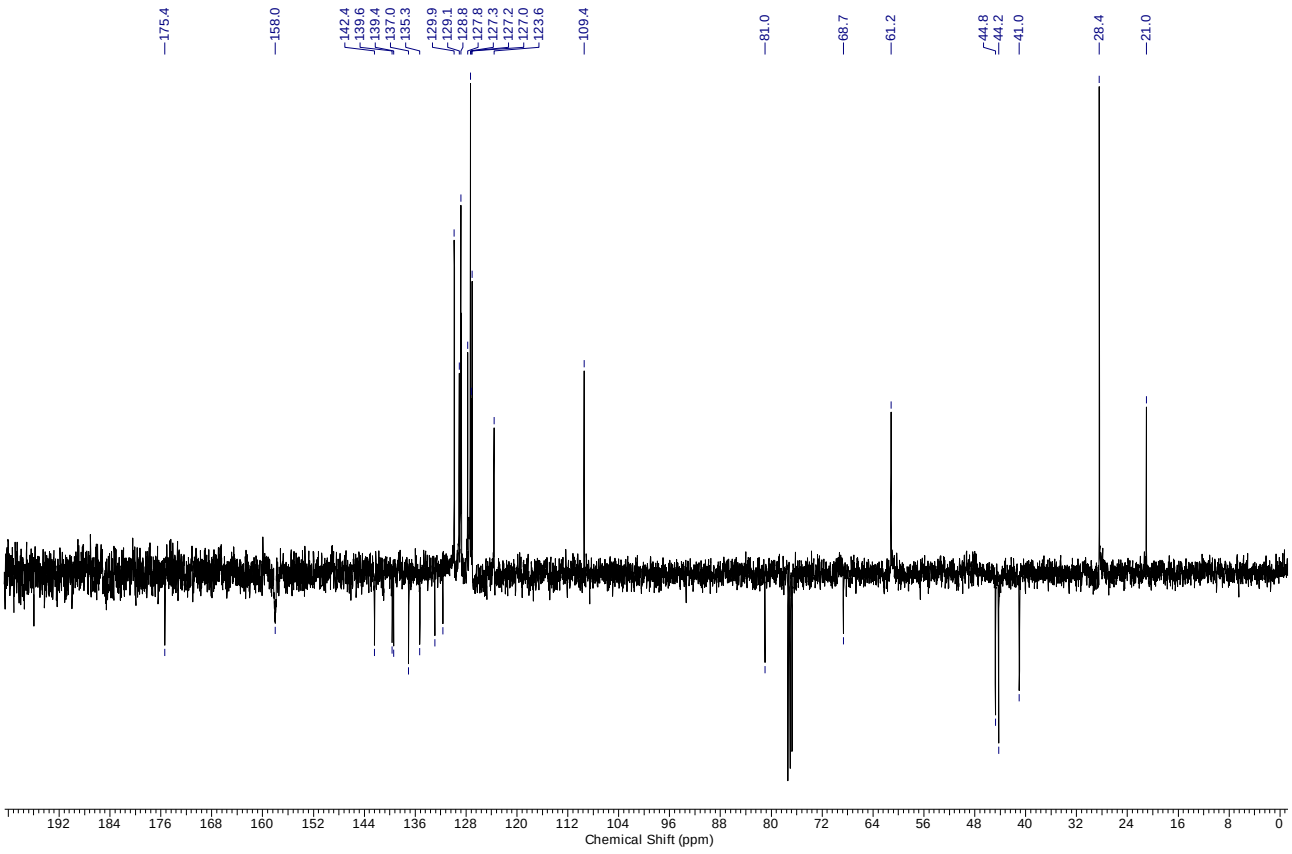

6l,6l' (*7:3 mixture of diastereoisomers*) ^{1}H NMR (400 MHz, $CDCl_3$):

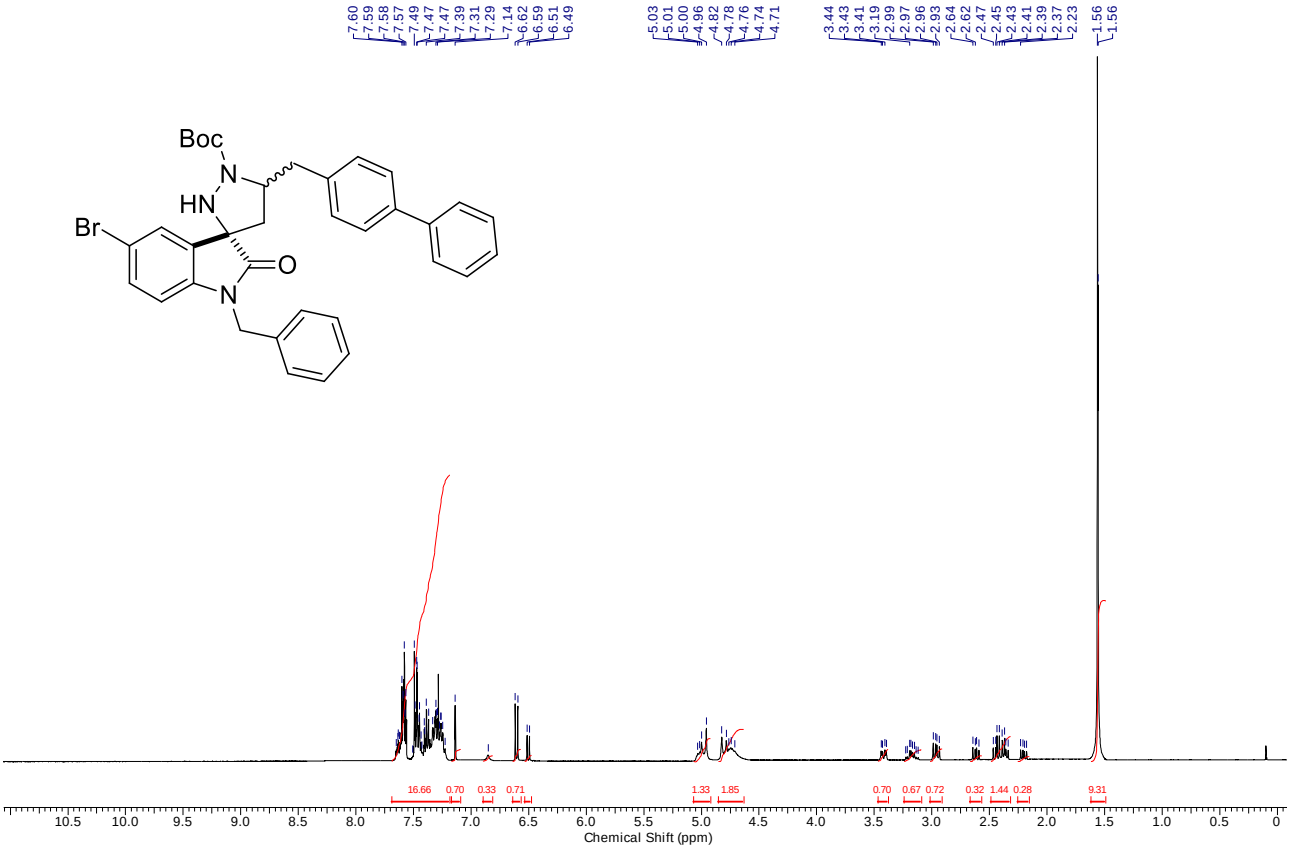

6l,6l' (*7:3 mixture of diastereoisomers*) ^{13}C NMR (101 MHz, ATP, $CDCl_3$):

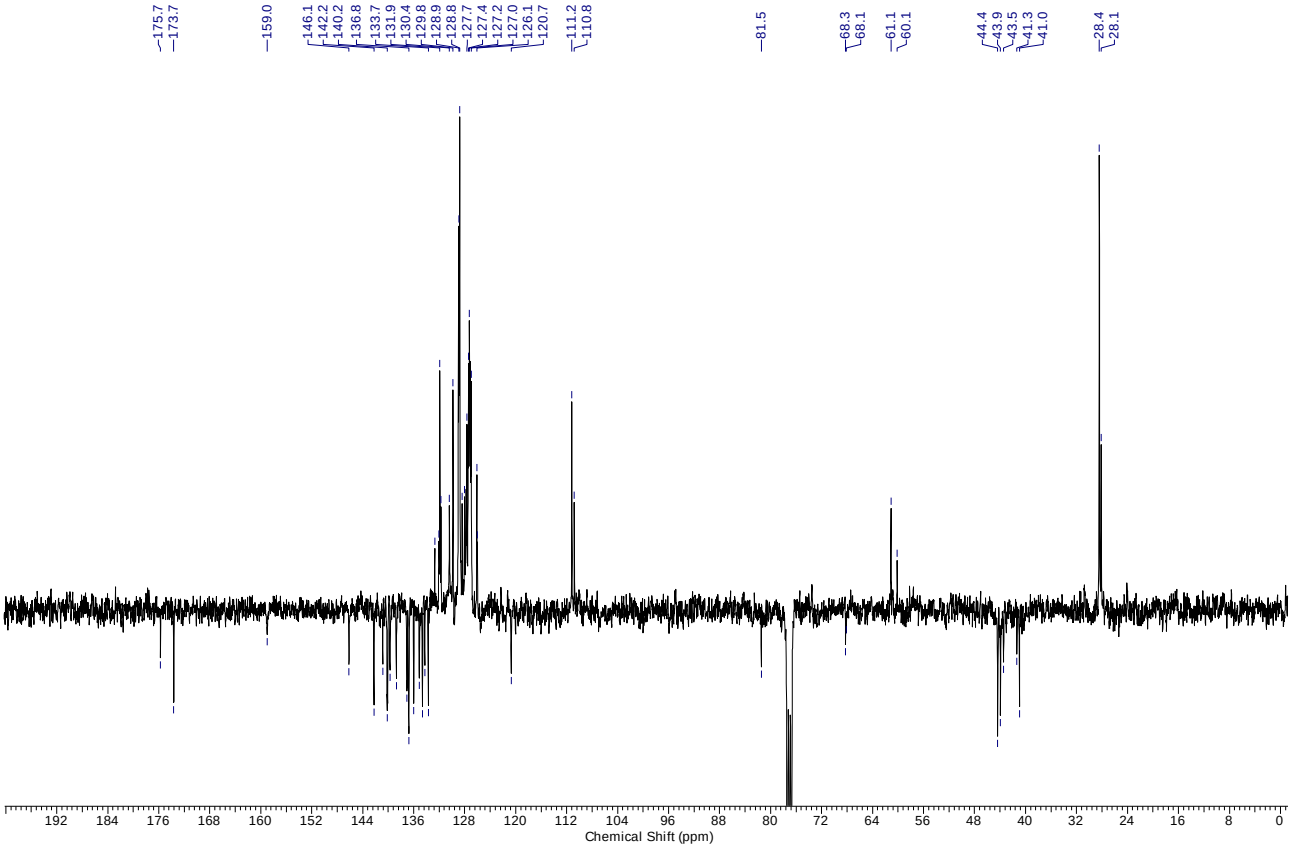

6m ^{1}H NMR (400 MHz, $CDCl_3$):

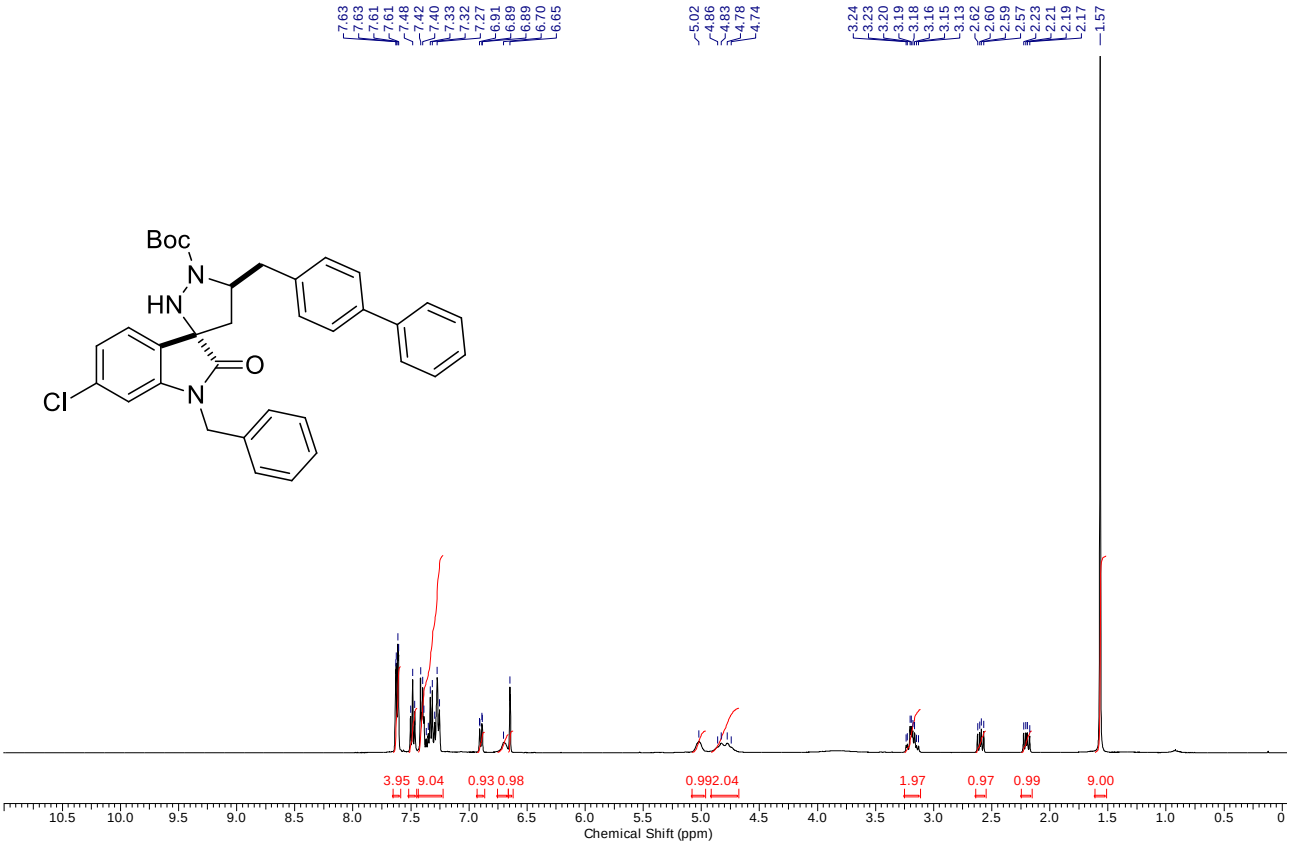

6m ^{13}C NMR (101 MHz, ATP, $CDCl_3$):

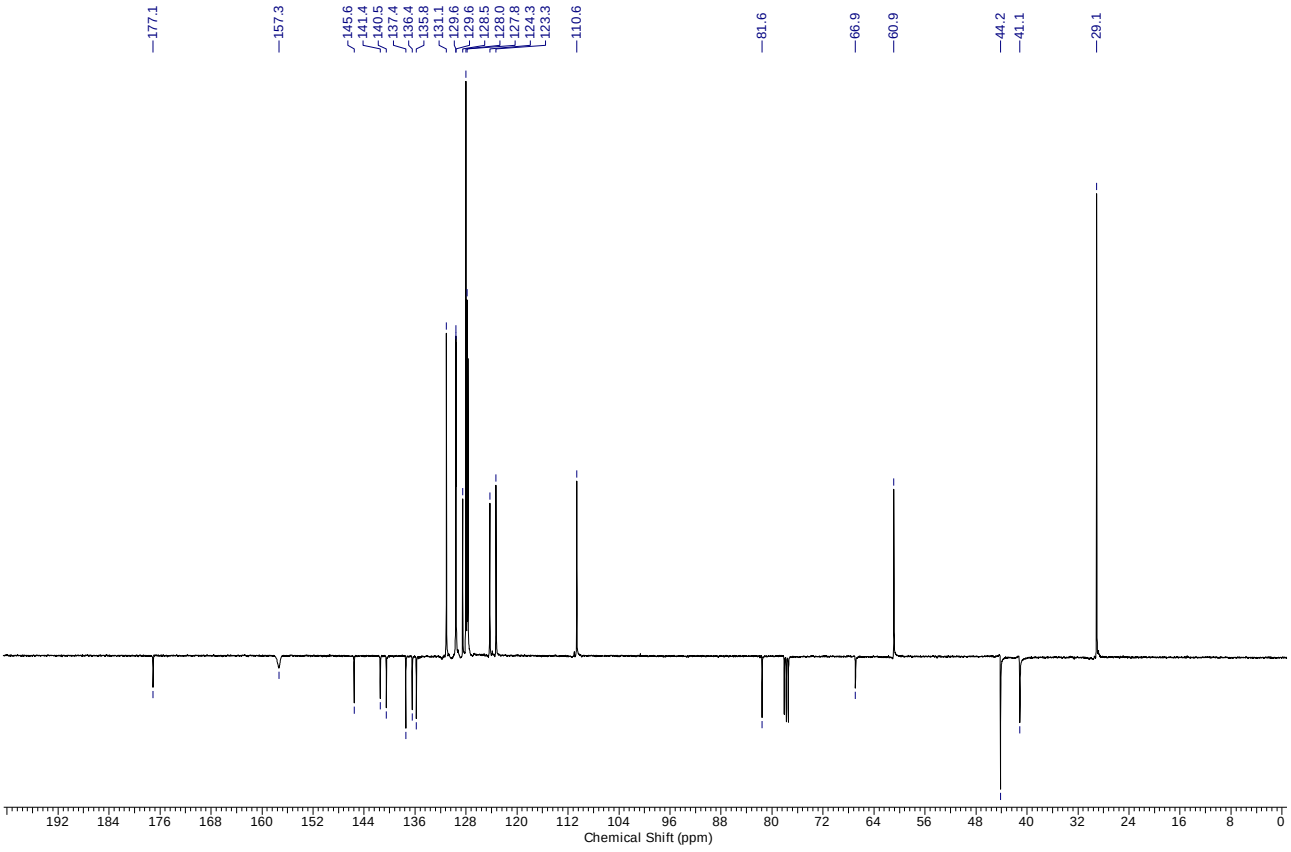

6m' ^{1}H NMR (300 MHz, $CDCl_3$):

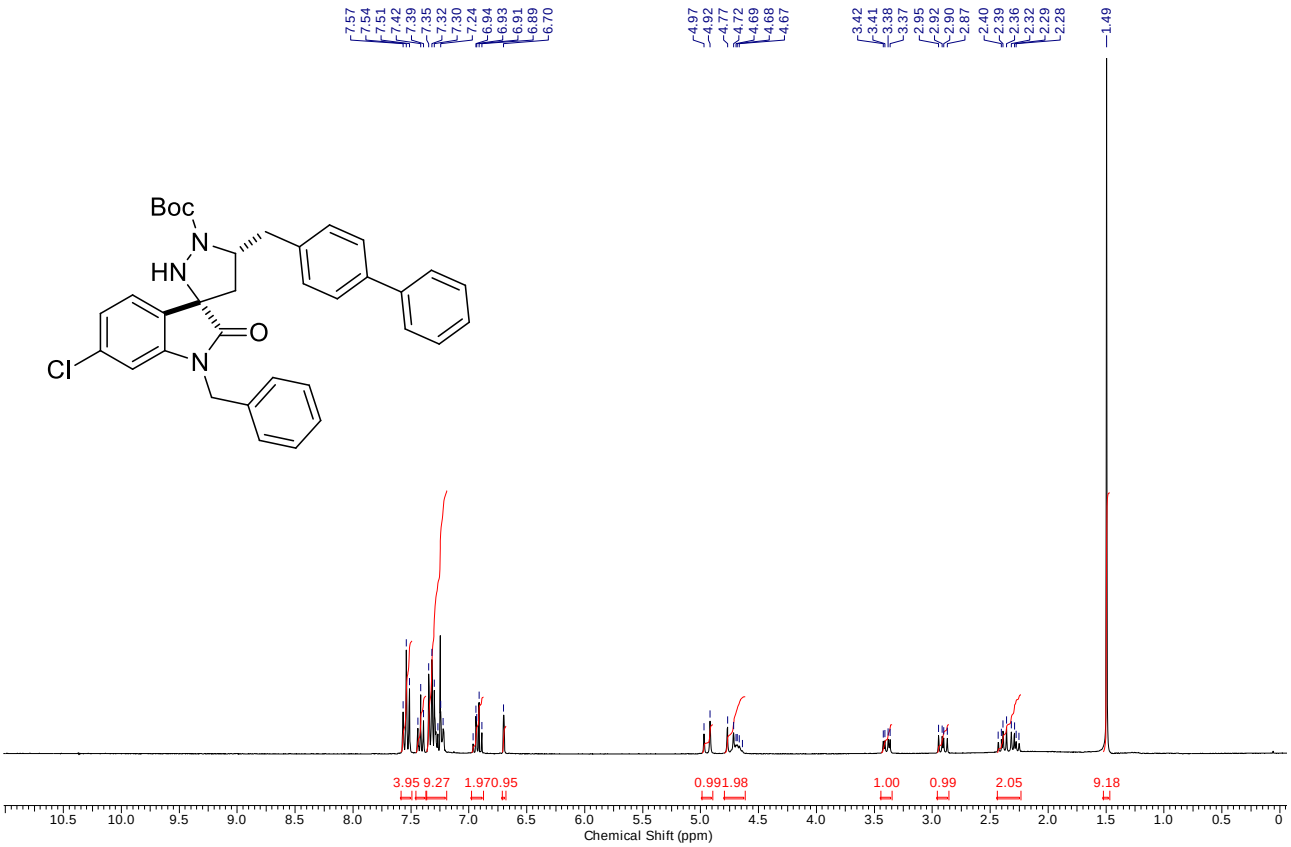

6m' ^{13}C NMR (101 MHz, ATP, $CDCl_3$):

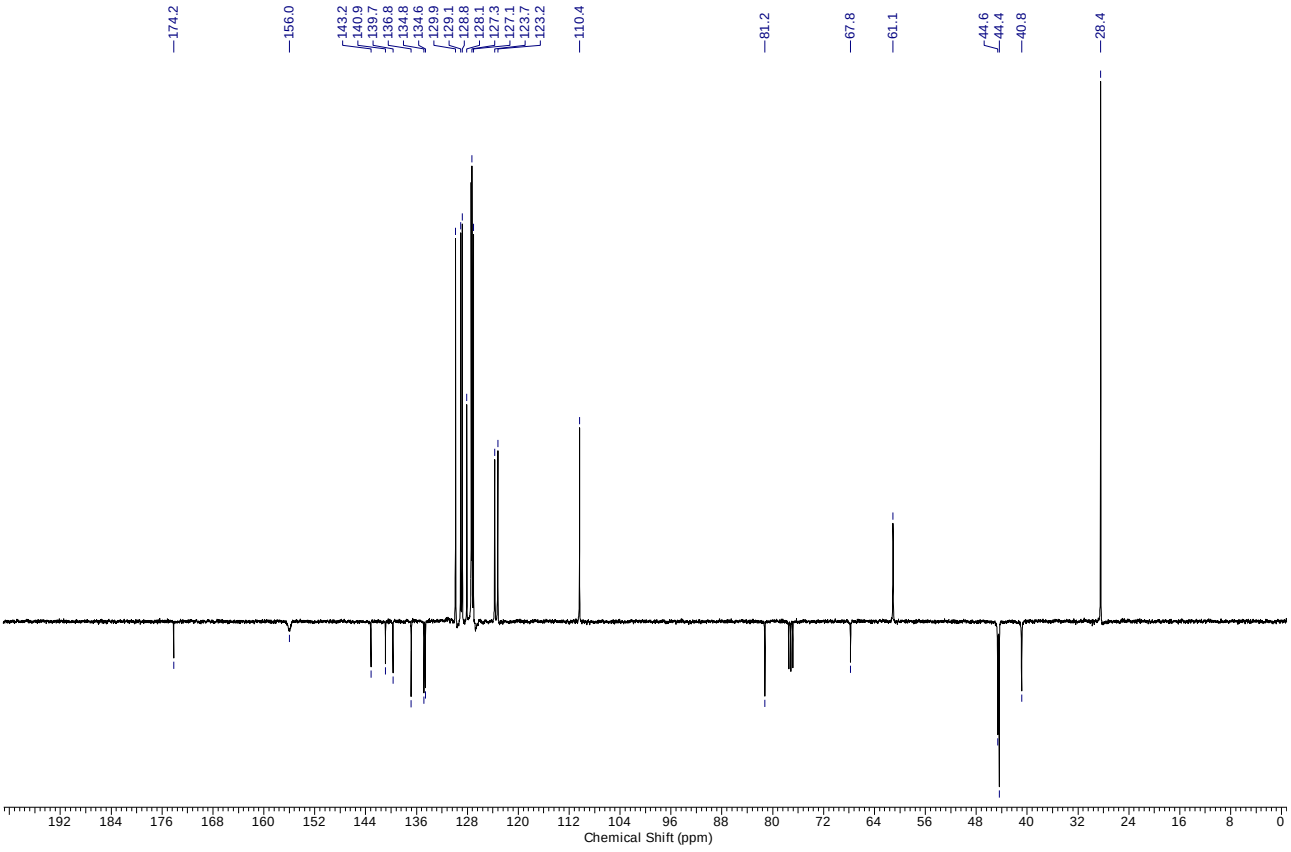

6n ^{1}H NMR (300 MHz, $CDCl_3$):

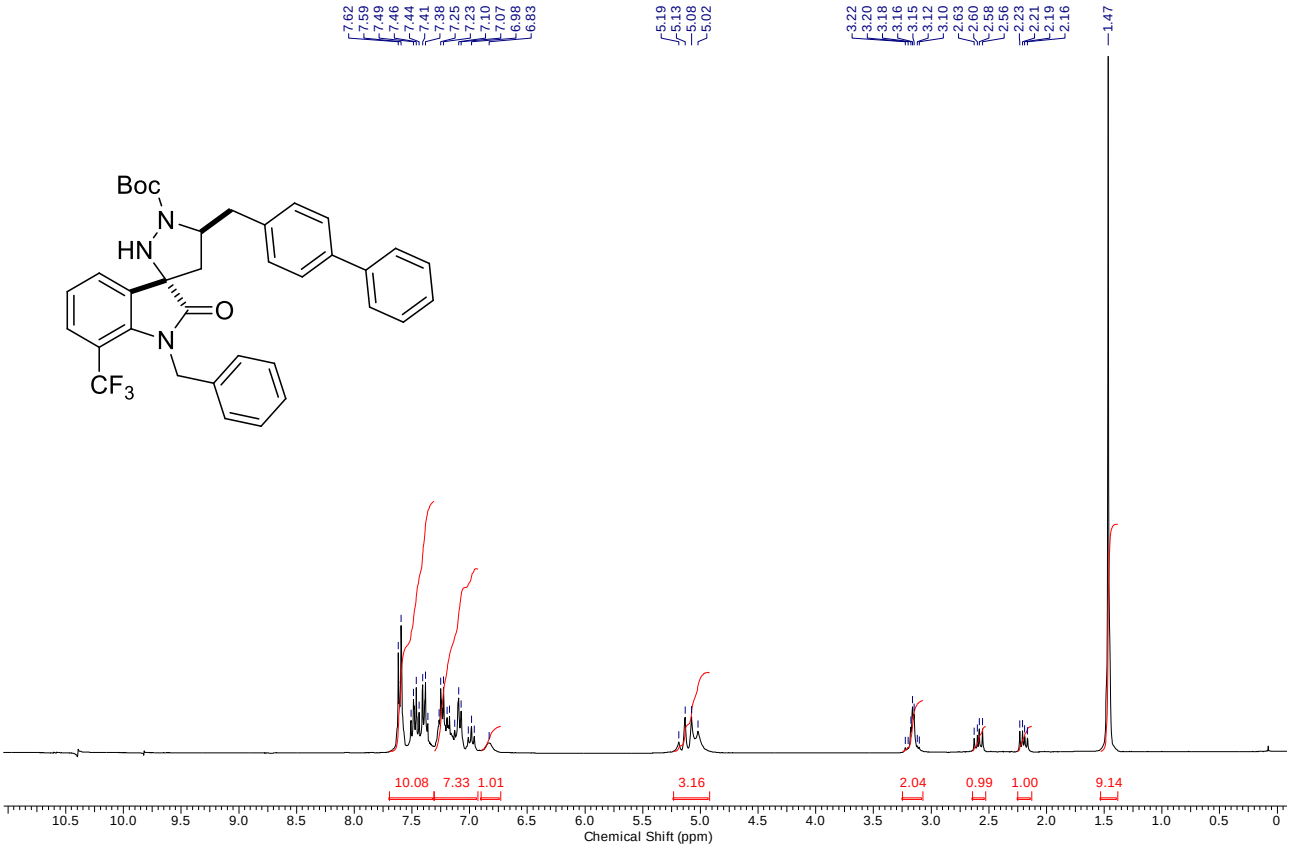

6n ^{13}C NMR (101 MHz, ATP, $CDCl_3$):

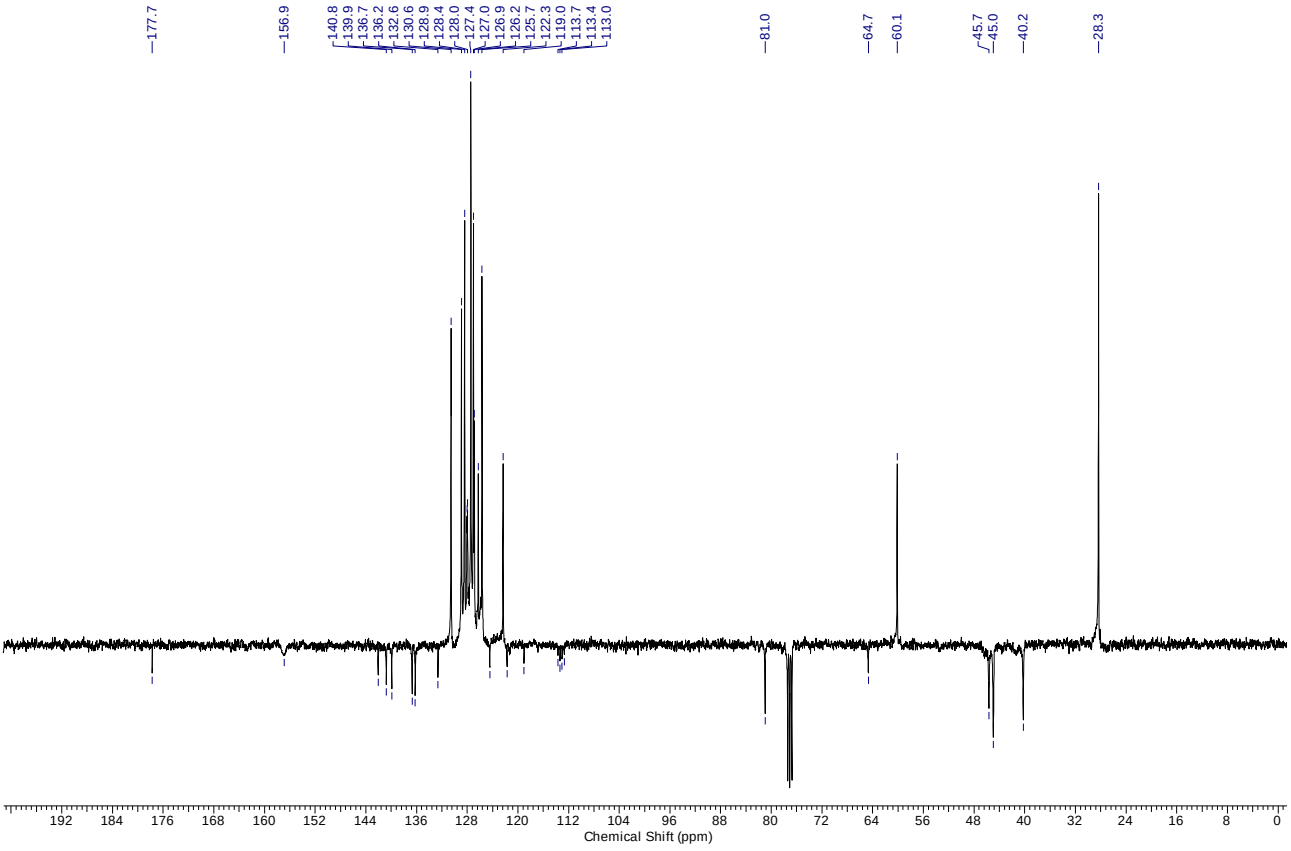

6n' ^{1}H NMR (300 MHz, $CDCl_3$):

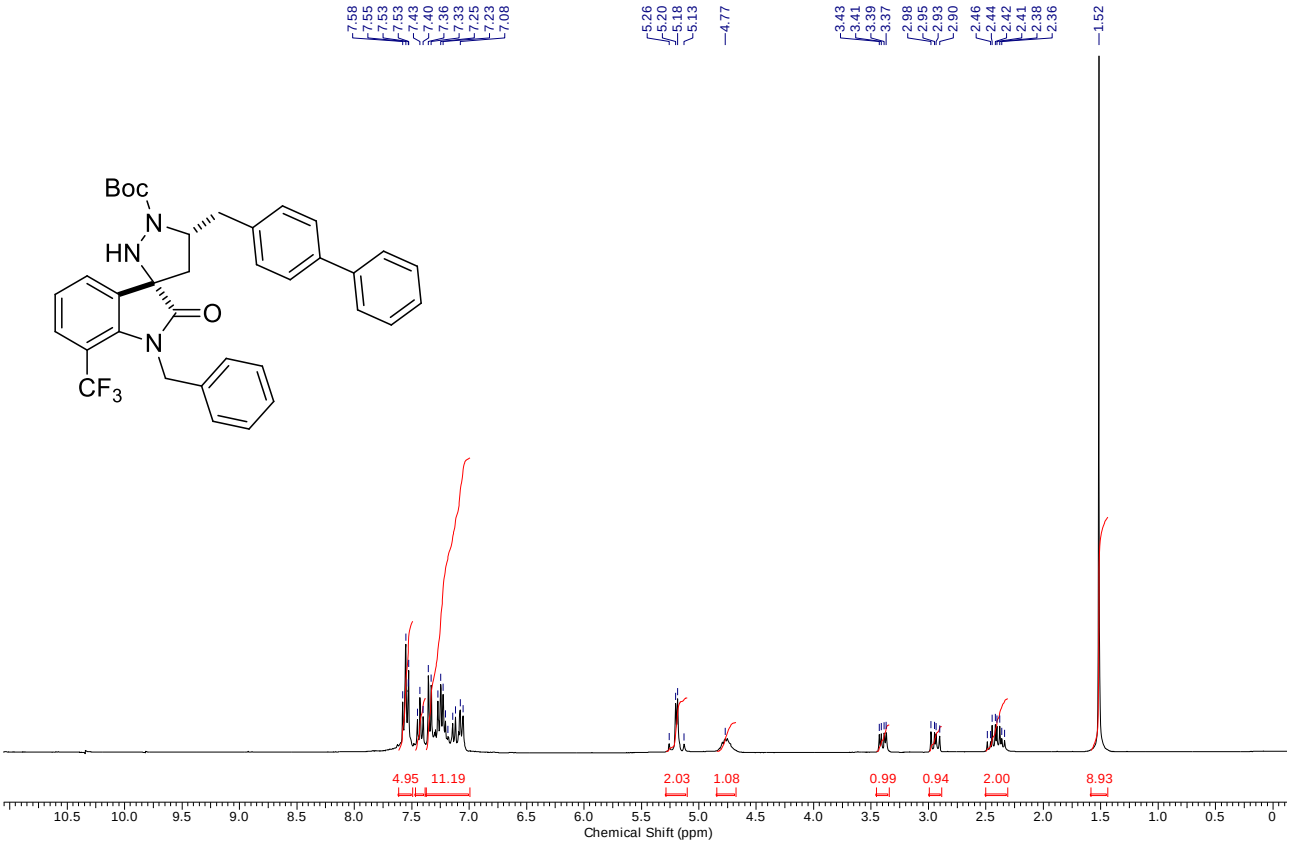

6n' ^{13}C NMR (101 MHz, ATP, $CDCl_3$):

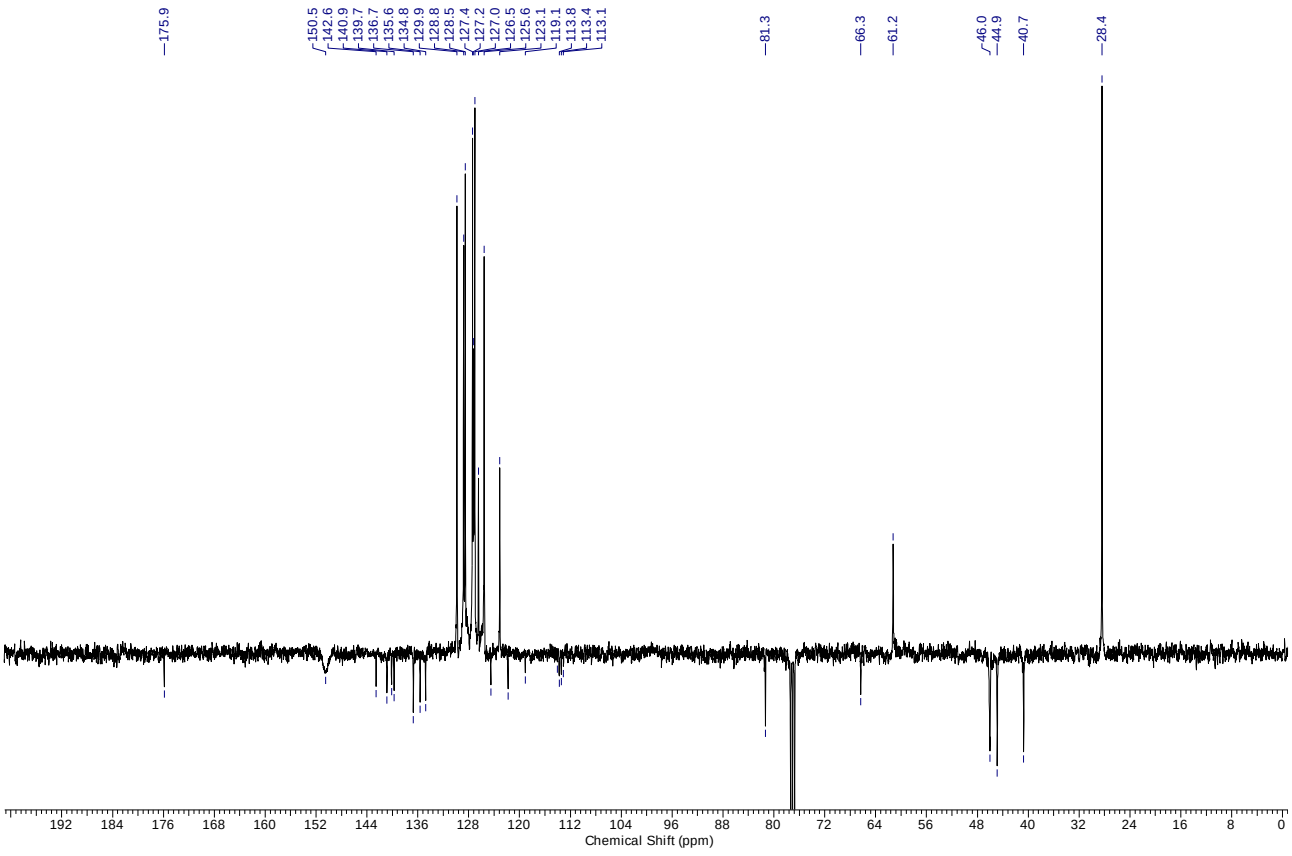

3b ^{1}H NMR (300 MHz, $CDCl_3$):

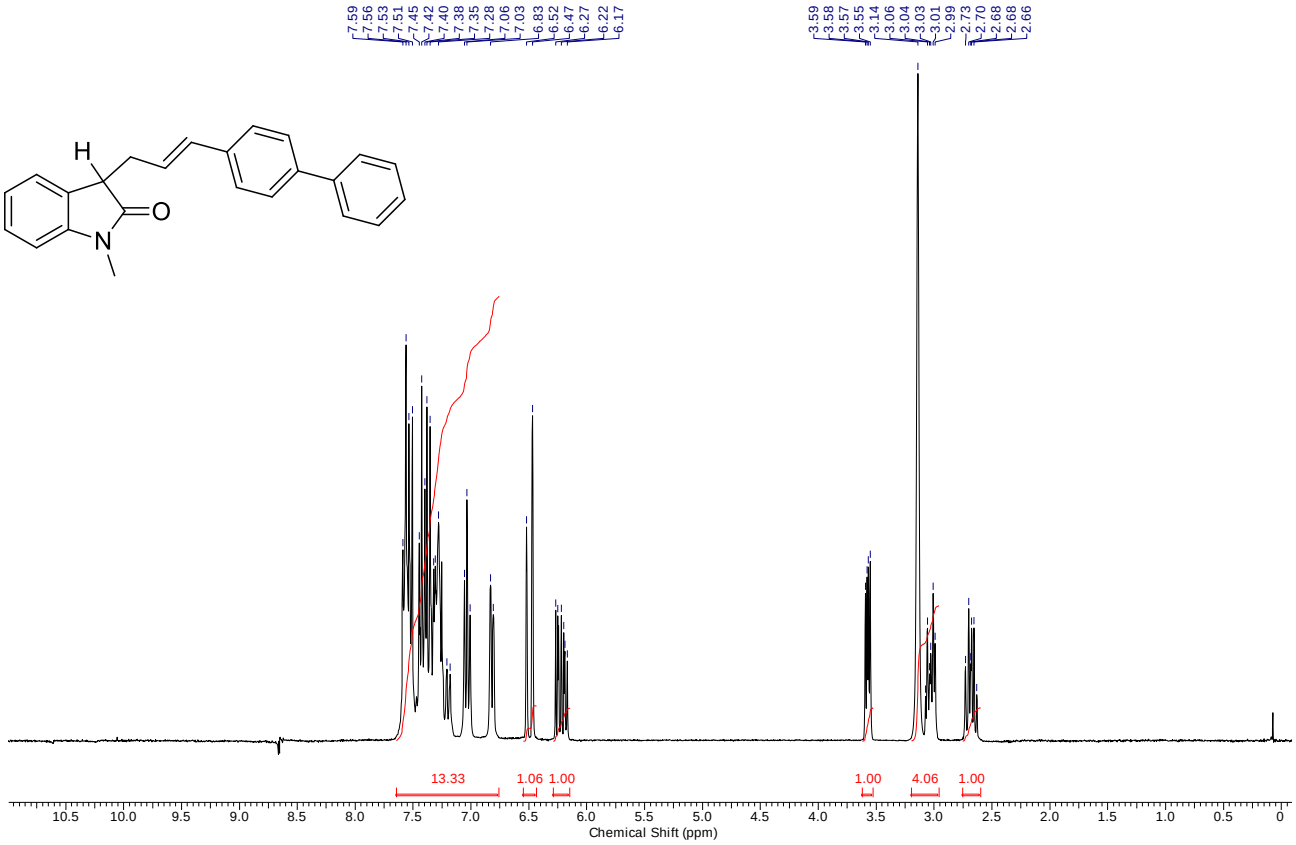

3b ^{13}C NMR (75 MHz, ATP, $CDCl_3$):

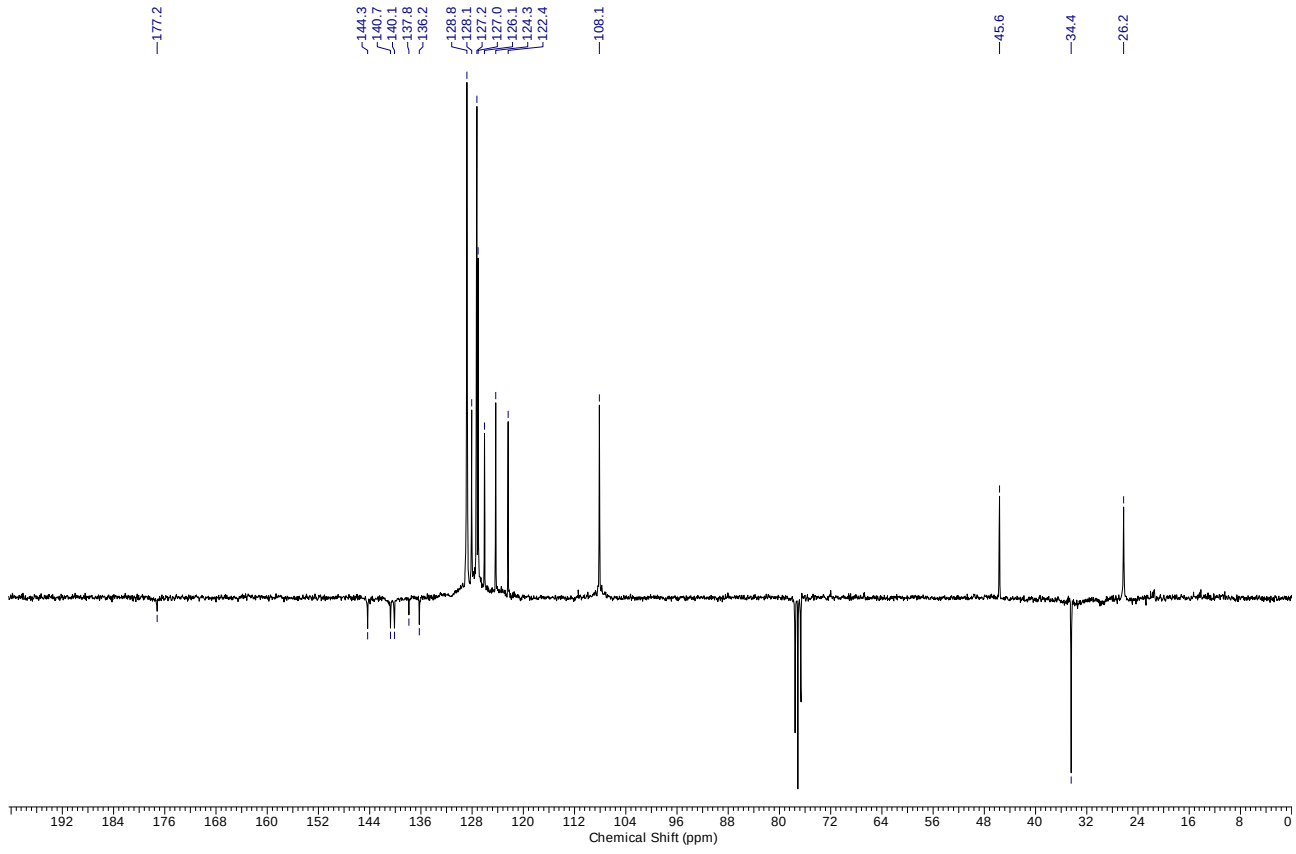

7 ^{1}H NMR (400 MHz, $CDCl_3$):

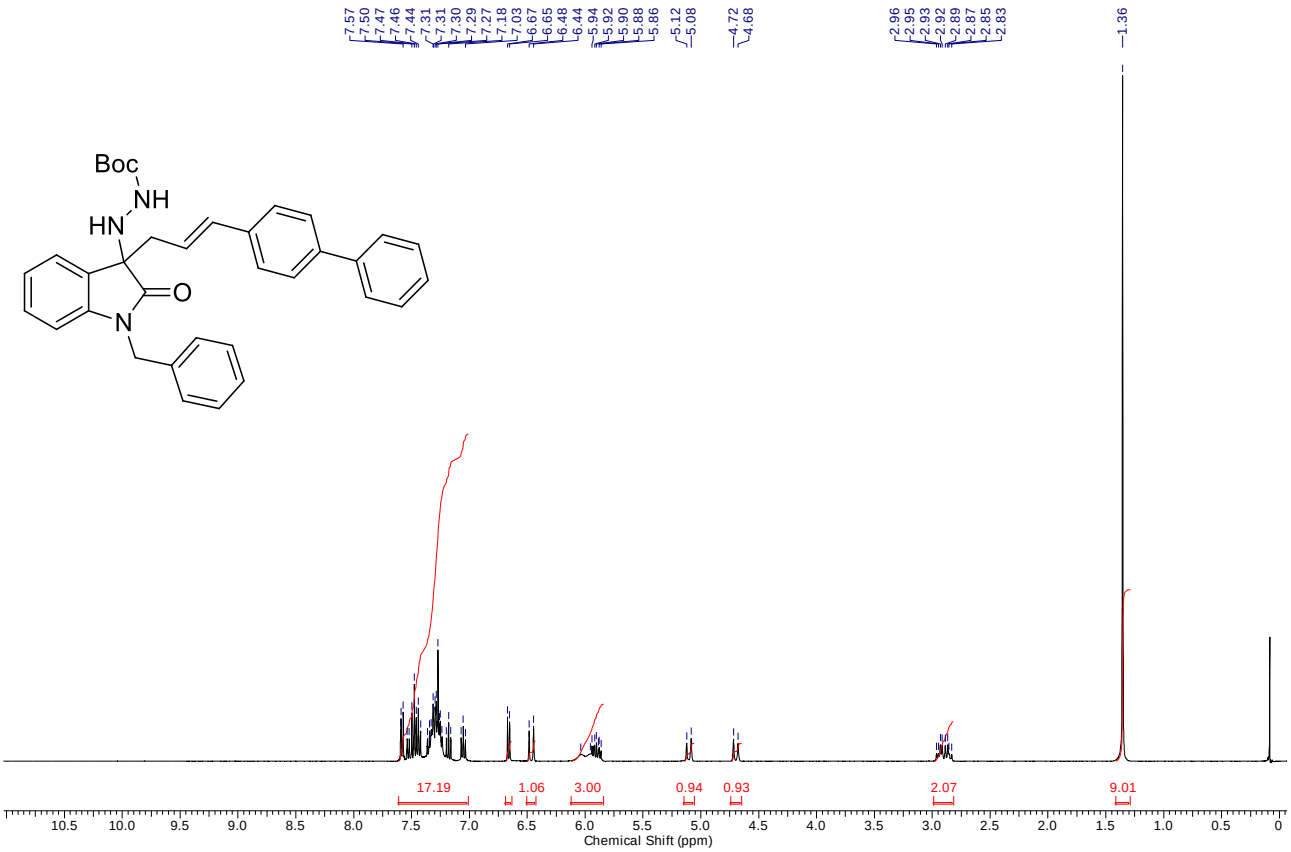

7 ^{13}C NMR (101 MHz, ATP, $CDCl_3$):

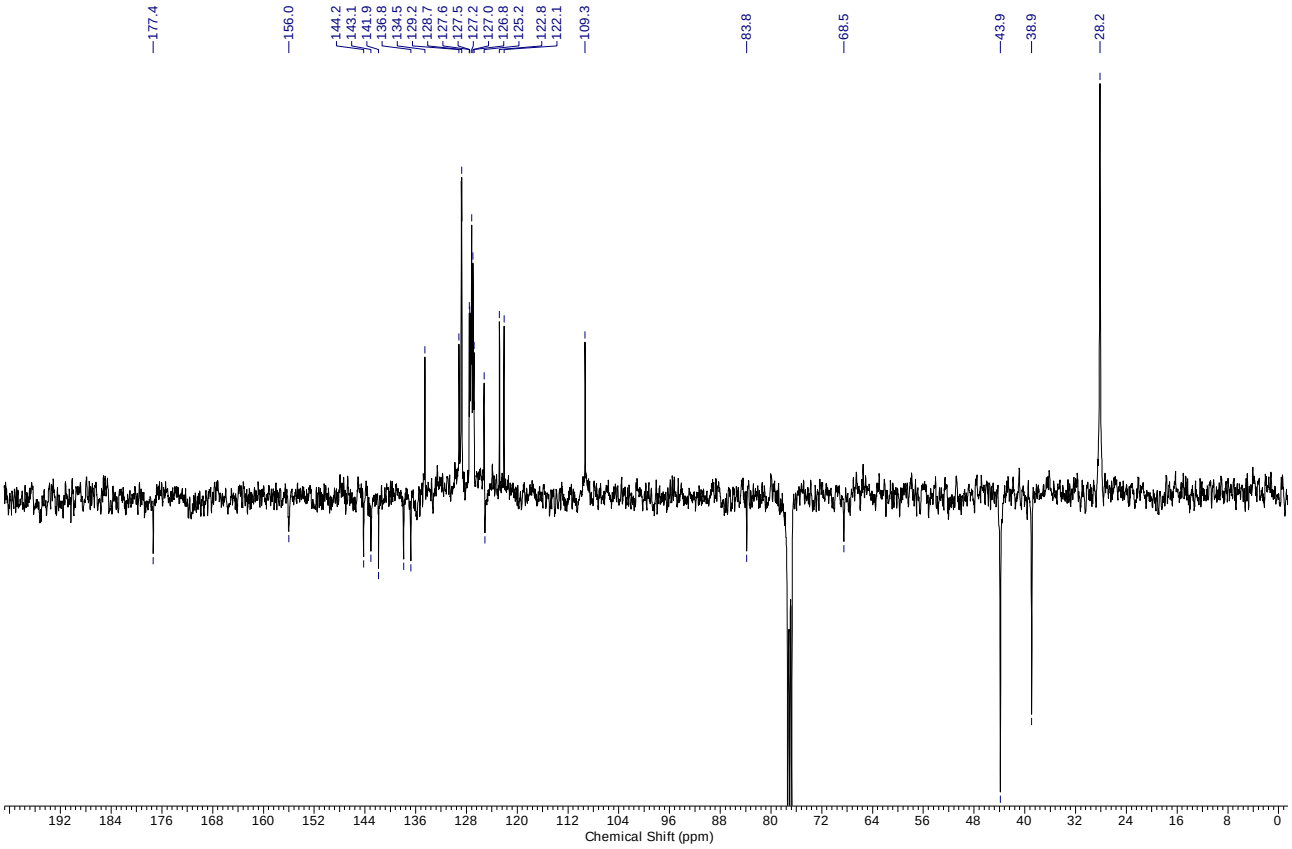

8 ^{1}H NMR (300 MHz, $CDCl_3$):

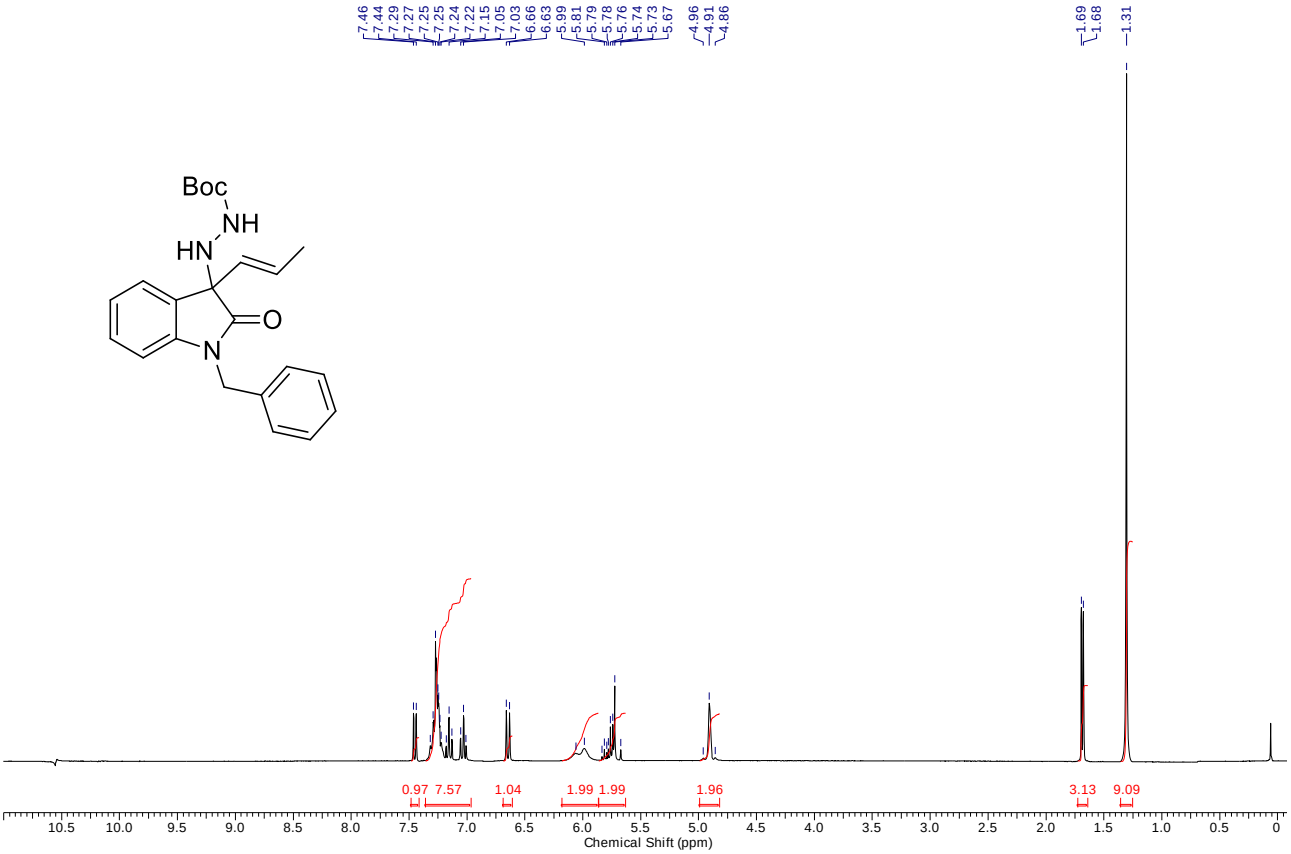

8 ^{13}C NMR (75 MHz, ATP, $CDCl_3$):

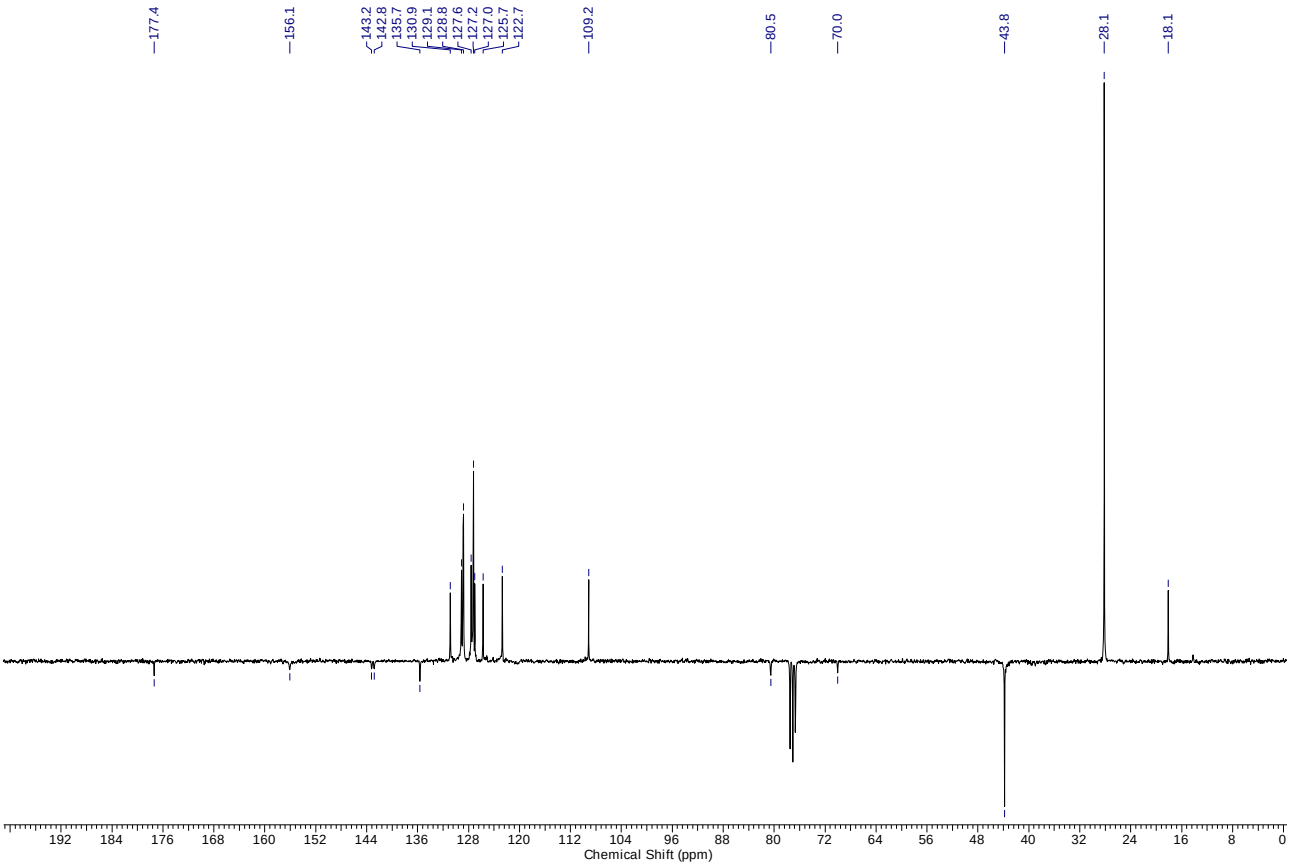

9 ^{1}H NMR (300 MHz, $CDCl_3$):

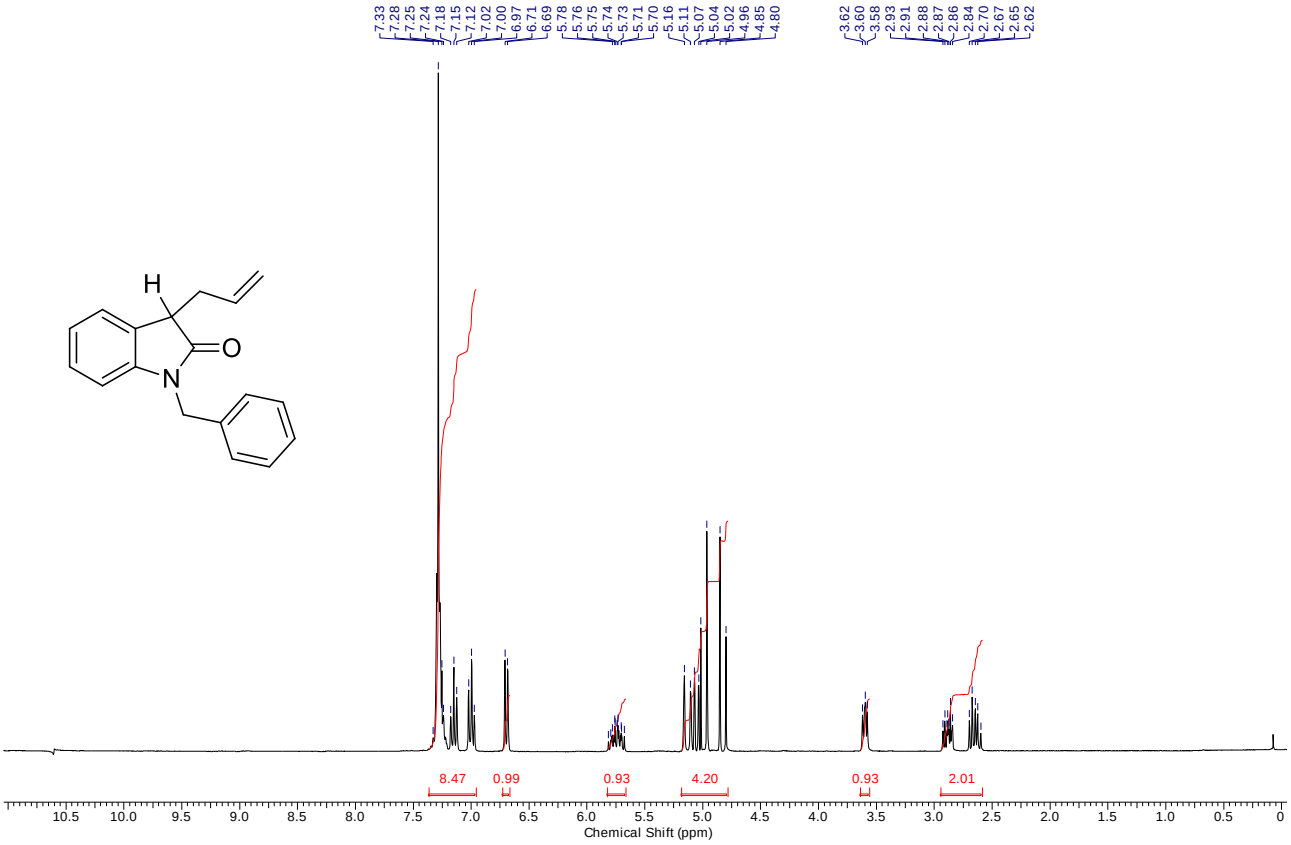

9 ^{13}C NMR (75 MHz, ATP, $CDCl_3$):

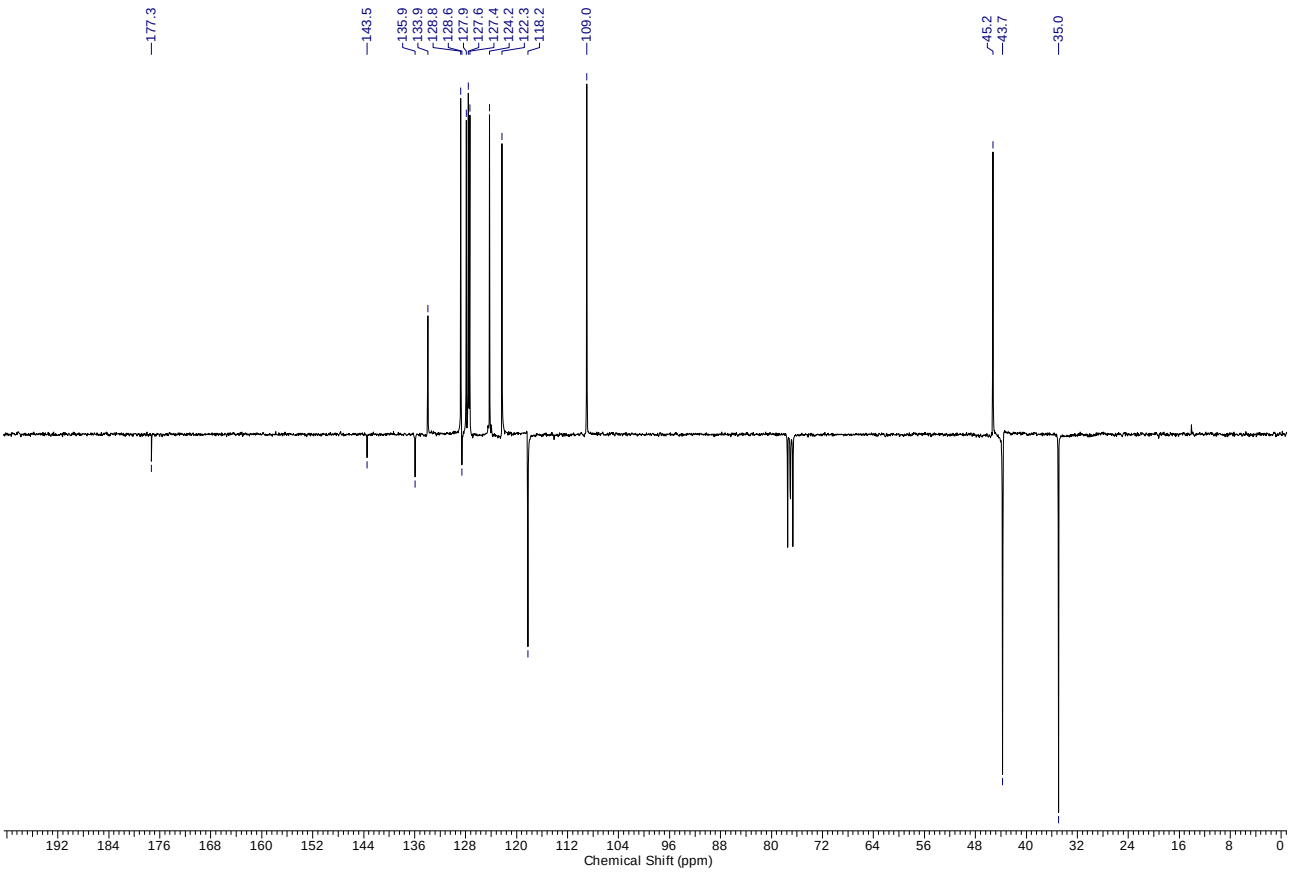

10 ^{1}H NMR (300 MHz, $CDCl_3$):

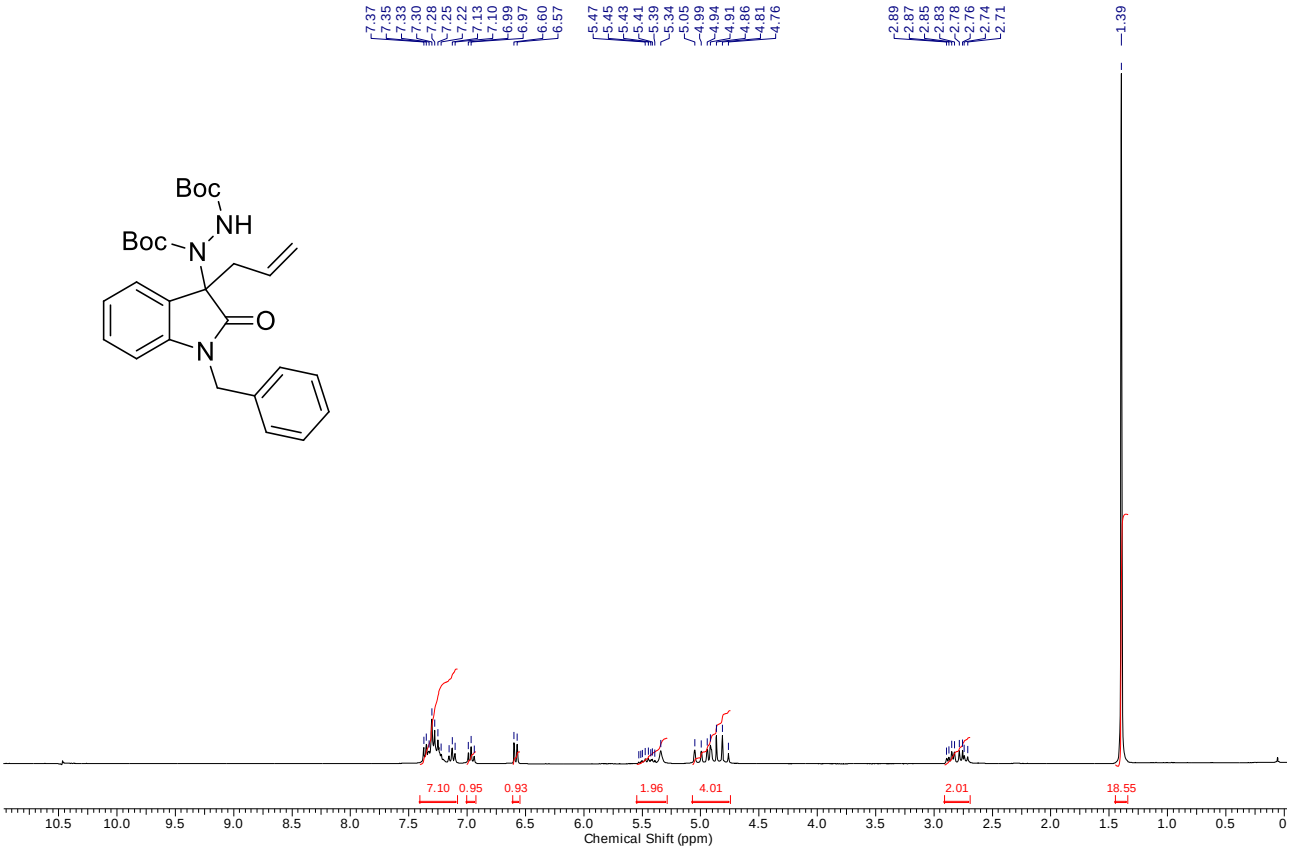

10 ^{13}C NMR (75 MHz, ATP, $CDCl_3$):

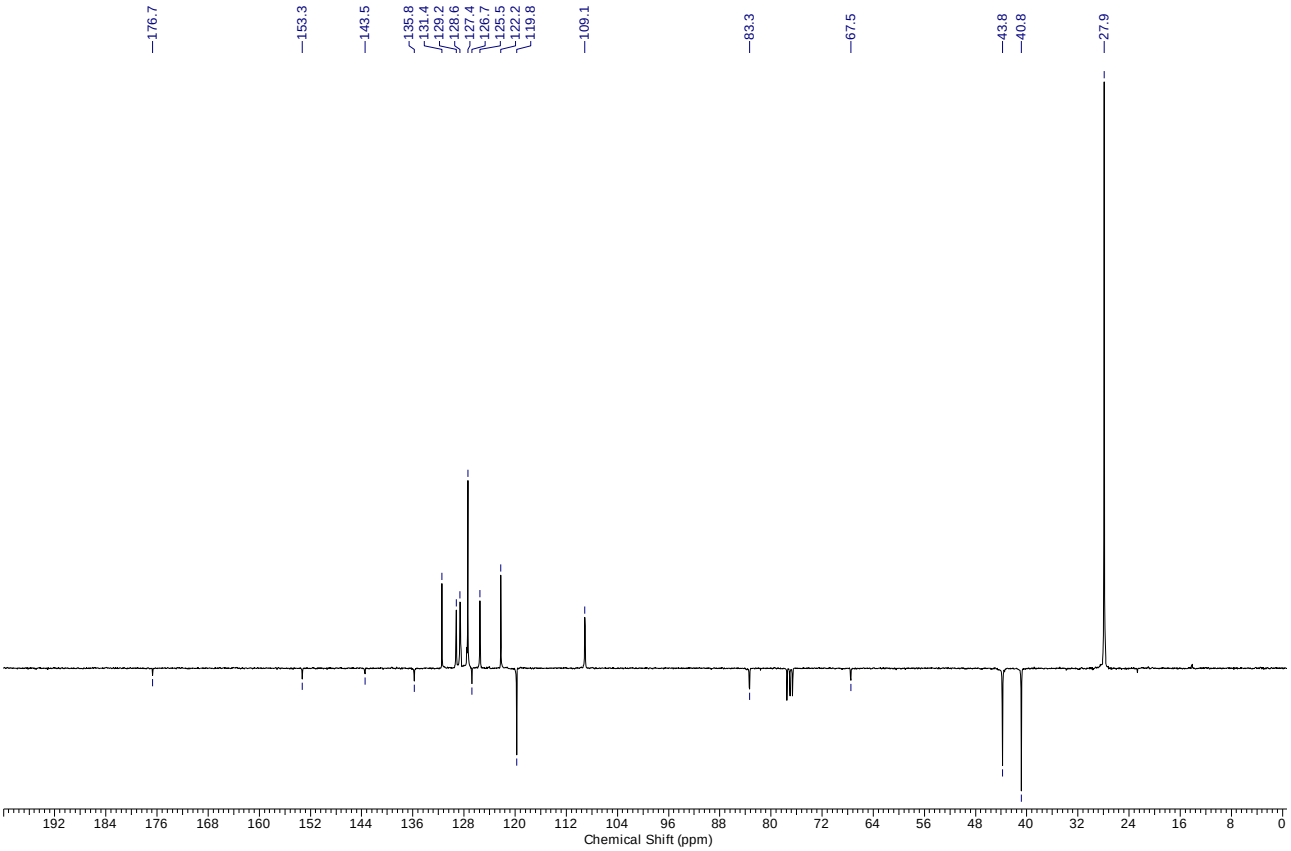

11 ^{1}H NMR (400 MHz, $CDCl_3$):

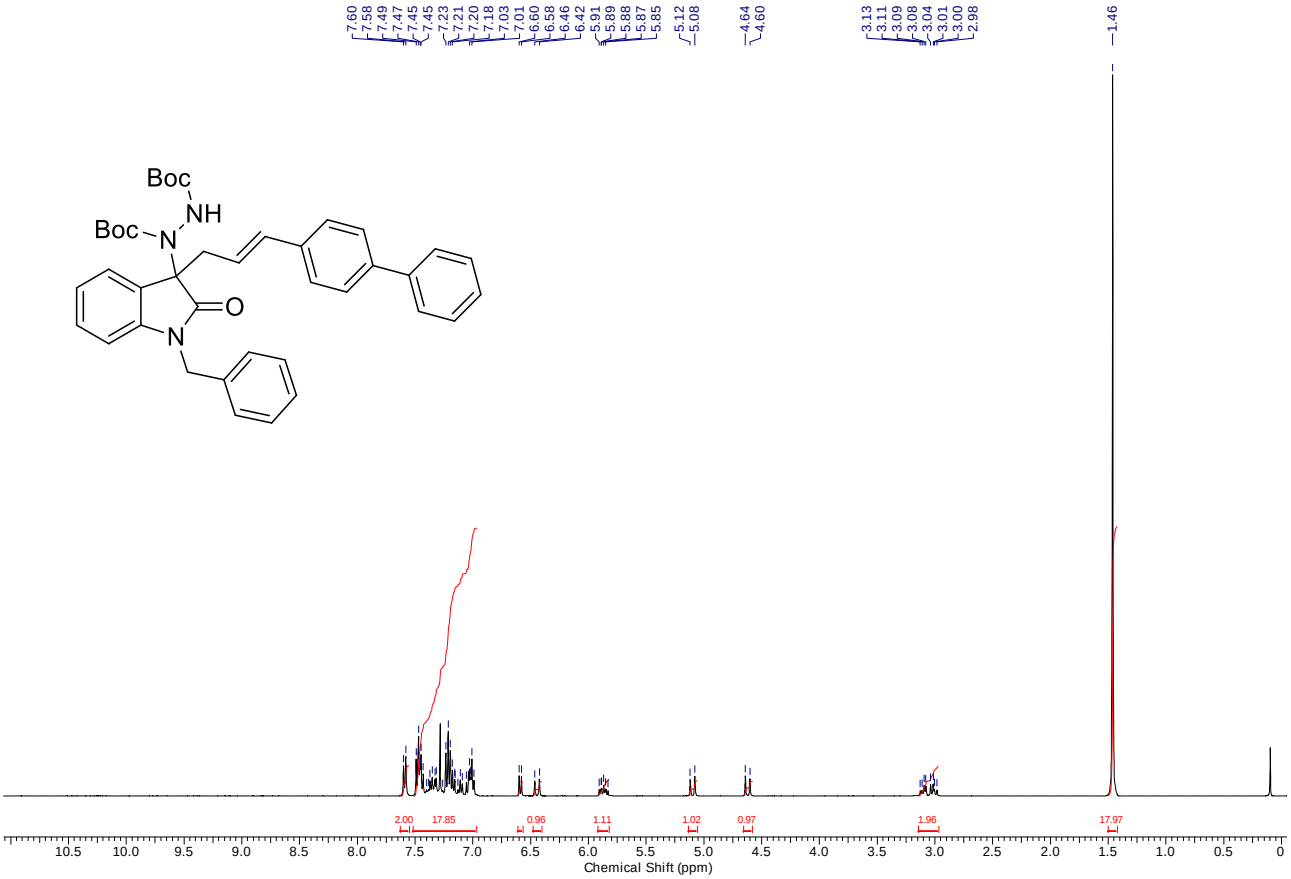

11 ^{13}C NMR (101 MHz, ATP, $CDCl_3$):

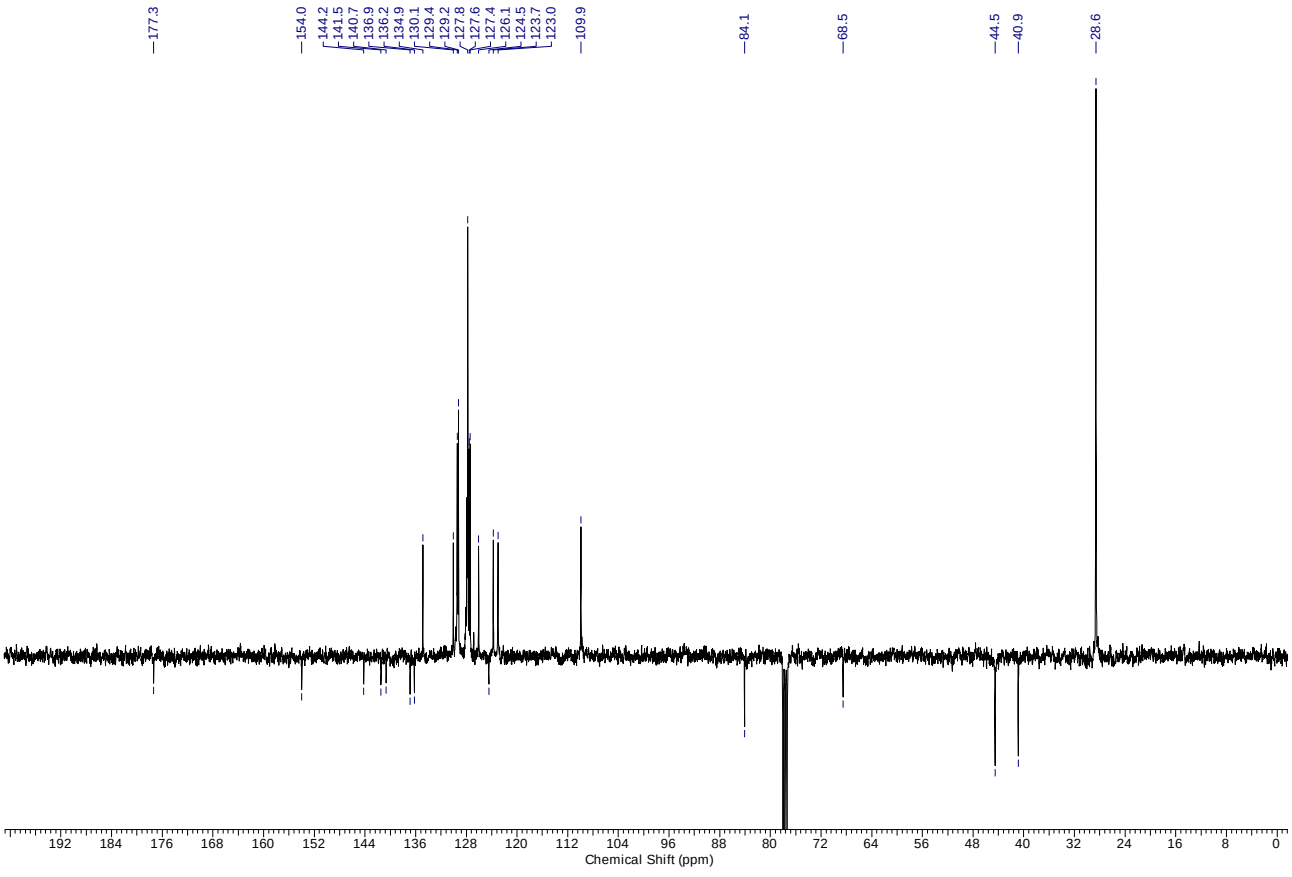

12 ^{1}H NMR (400 MHz, $CDCl_3$):

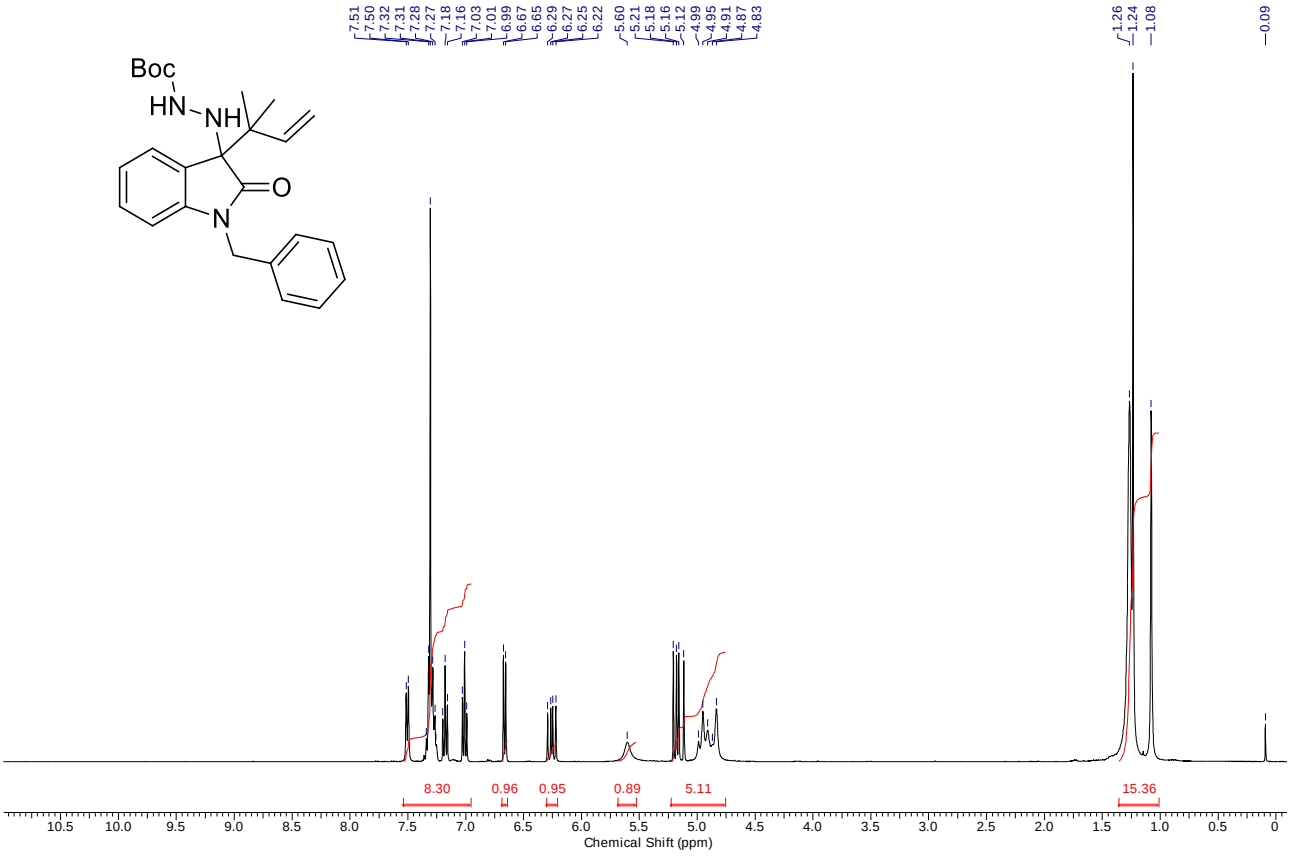

12 ^{13}C NMR (101 MHz, ATP, $CDCl_3$):

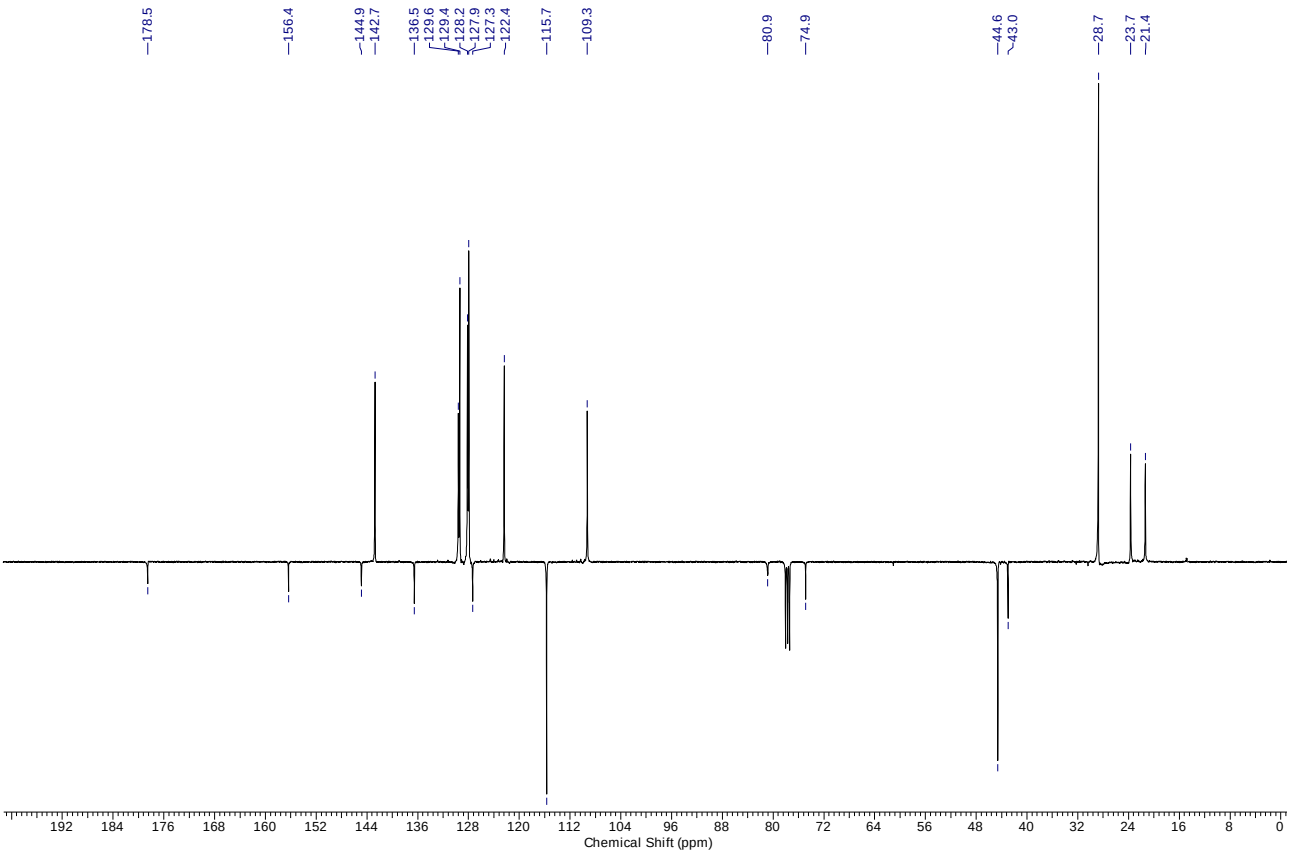

13 ^{1}H NMR (300 MHz, $CDCl_3$):

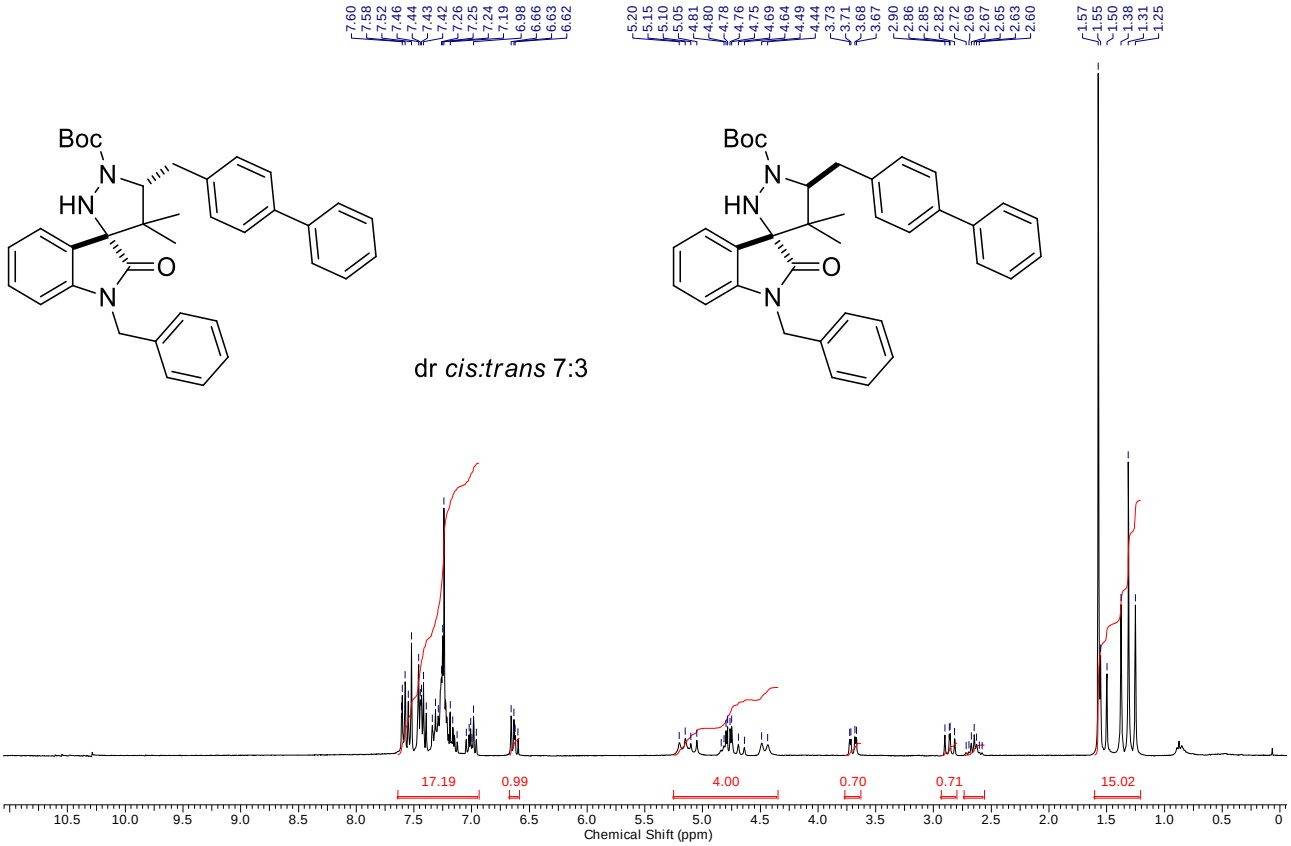

13 ^{13}C NMR (75 MHz, ATP, $CDCl_3$):

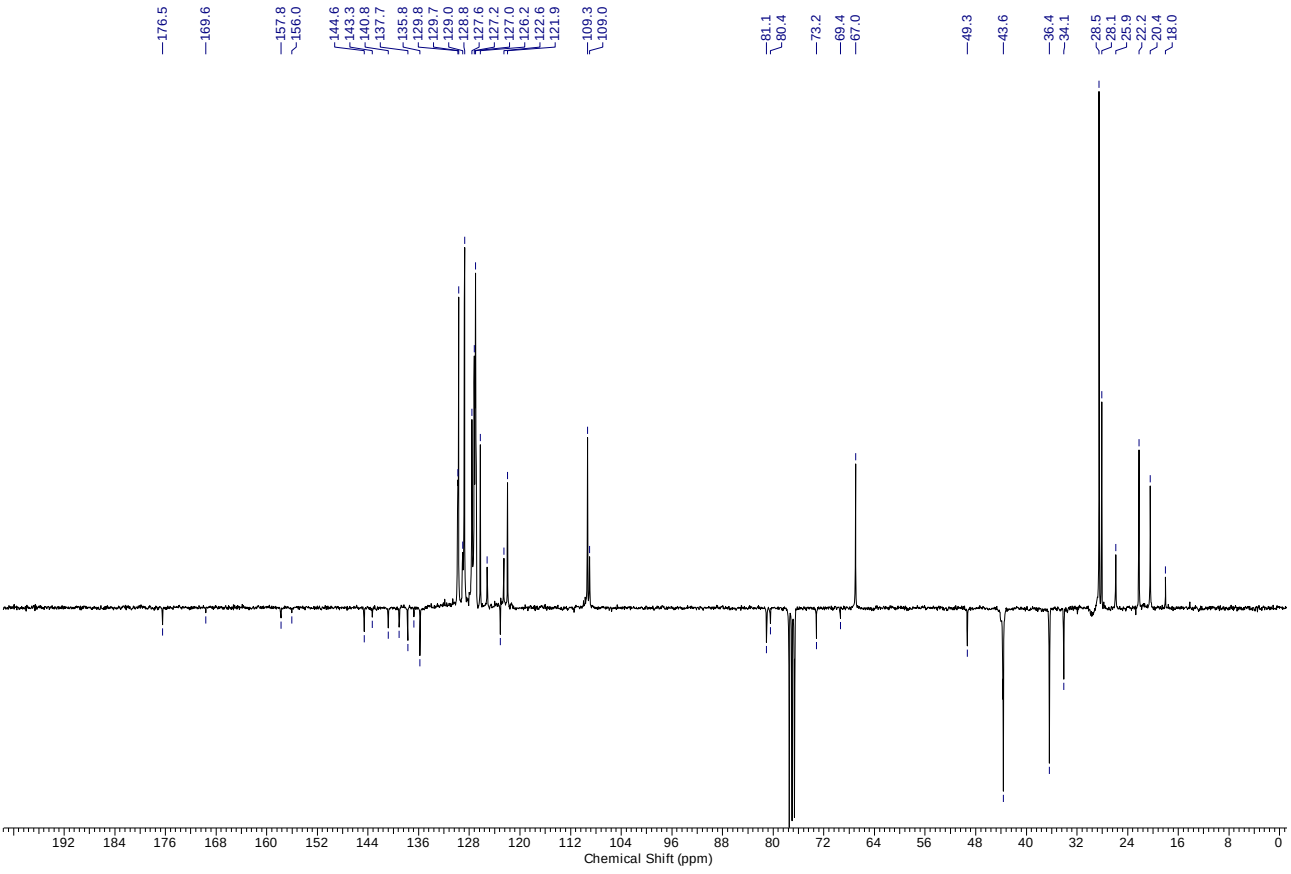

6a ^{1}H-^{1}H ROESY NMR (400 MHz, $CDCl_3$):

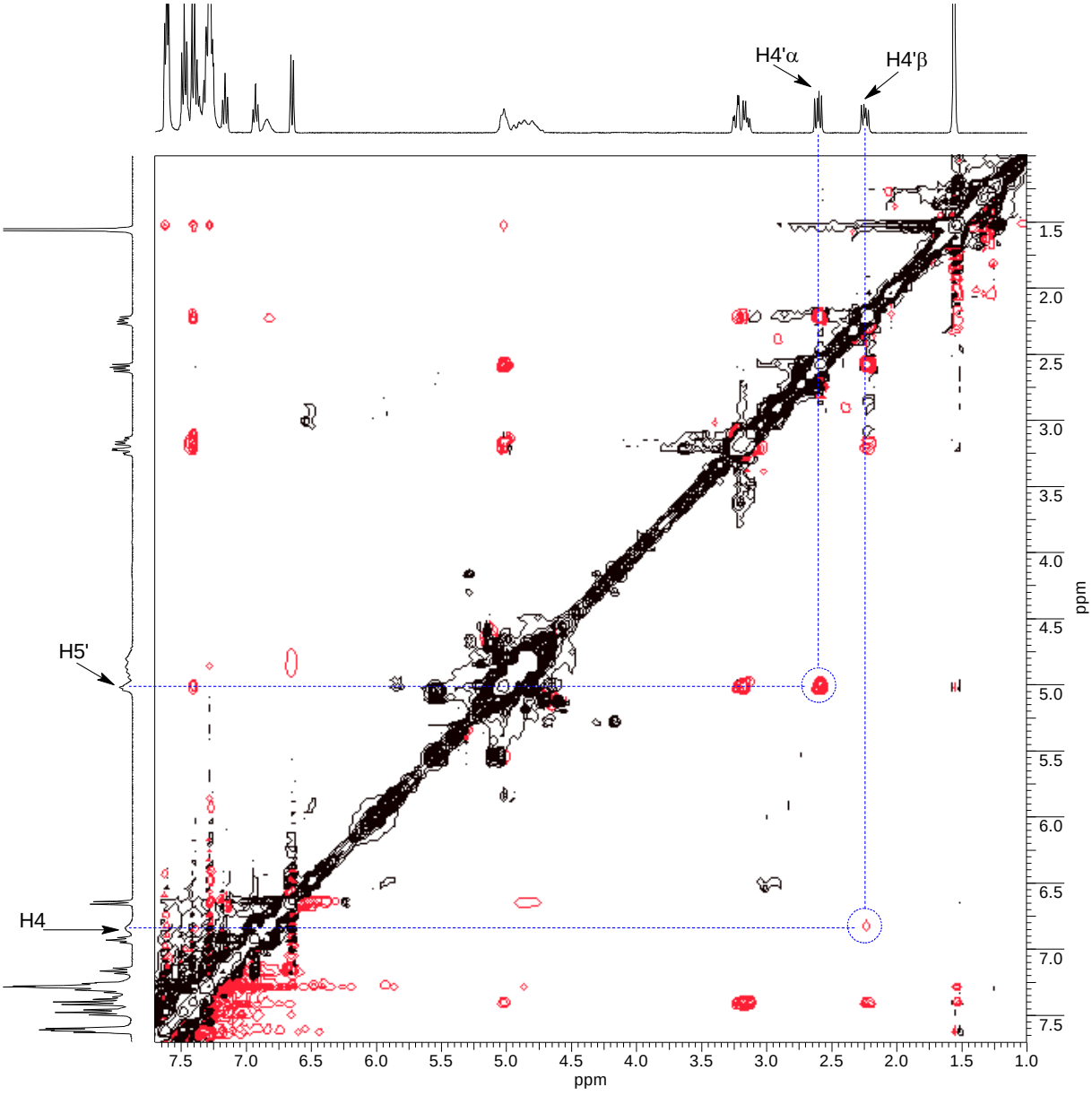

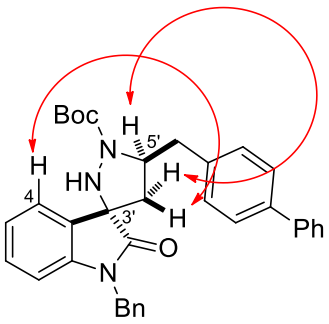

(3'-5'-*trans*)-**6a**

6a' ^{1}H-^{1}H ROESY NMR (400 MHz, $CDCl_3$):

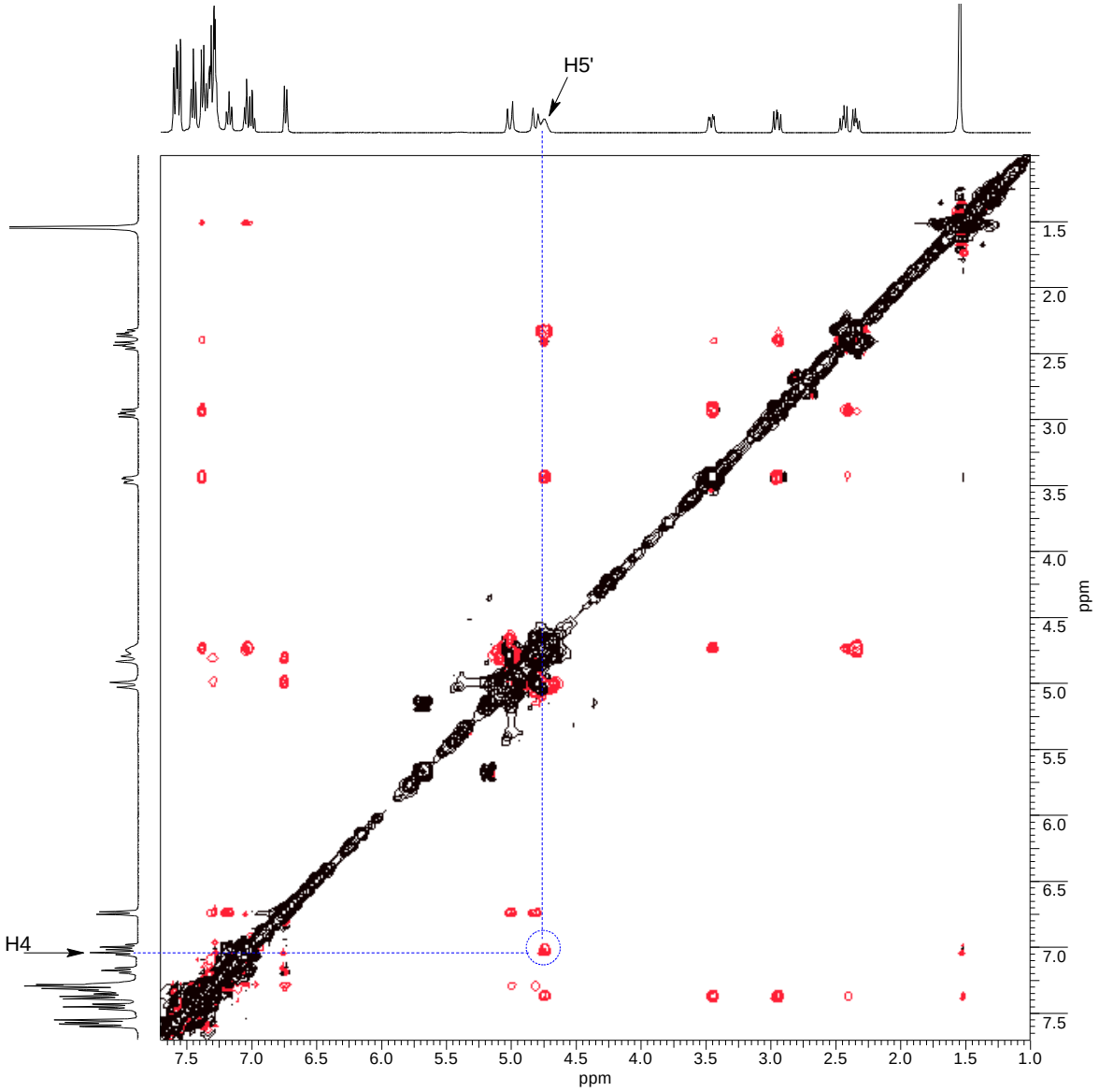

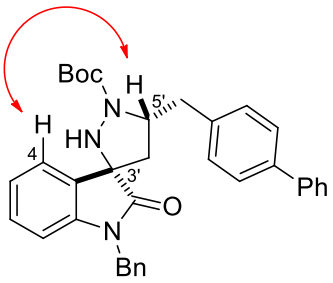

(3'-5'-*cis*)-**6a'**

Single–Crystal X-ray diffraction analysis of the compound 6f'

The specimen selected for the current diffraction experiment was a colourless and transparent prism, with dimensions 0.325 x 0.150 x 0.100 mm, cut from a larger aggregate with a stainless microblade and carefully polished into a drop of perfluorinated oil. The crystal was grown from MeOH by slow evaporation at room temperature (~24 h). The room temperature data collection was performed on a three–circle Bruker AXS Smart diffractometer at a nominal 50 kV x 30 mA power of the X-ray source, using a graphite–monochromatized Mo Kα probe (λ = 0.71073 Å). A 99.9 % complete full sphere of reflections was collected up to a maximum resolution of 0.72 $Å^{-1}$ in sinϑ/λ, obtaining 39704 unmerged reflections and 6051 independent data (4090 with $I > 2\sigma(I)$). The unit cell was determined by 4872 intense reflections among 5.16 and 40.18 deg of 2ϑ, obtaining the following estimates for the lattice parameters: a = 10.6314(2) Å, b = 24.1537(4) Å, c = 10.5798(2) Å, β = 103.6630(10) deg, V = 2639.9(1) $Å^3$, ρ = 1.217 g/cm^3.

Data collection and reduction were carried out with the software SAINT-plus (Bruker (2012). *Saint-plus*. Bruker AXS Inc., Madison, Wisconsin, USA), and raw data were subsequently corrected for beam anisotropy with SADABS (Bruker (2001). *SADABS*. Bruker AXS Inc., Madison, Wisconsin, USA). The structure was solved with direct methods and refined with the Shelx suite of programs (Sheldrick, G. M. (2015). *Acta Cryst.* C**71**, 3-8). The molecular model was developed through an unrestrained non–linear least–squares fit of the measured structure factor amplitudes.

Large librational motion affects rotatable terminal phenyl rings, which lie far from the main molecular inertial axes. As a consequence, the thermal motion of some atoms (C1, C2, C6, C20–C22, see Figure 3 in the main text for the atom numbering) is determined with low accuracy. The quality of the final least-squares estimates for the thermal motion of these atoms can be improved by performing low-T X-ray diffraction experiments. However, these problems did not hamper us from obtaining a fully satisfactory structural determination, securing in particular the relative configuration of the molecular steroecentres (see below).

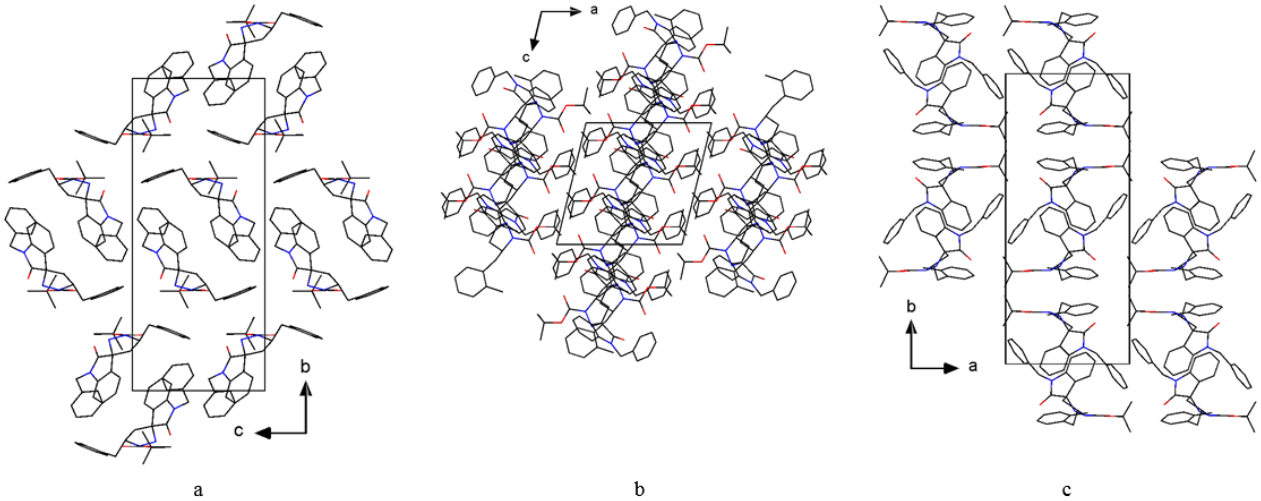

Figure S1. Wires-stick representation of the crystal packing of **6f'**, as seen (a) along the *a* cell axis; (b) the *b* cell axis; (c) the *c* cell axis. Hydrogen atoms are omitted for clarity.

The compound **6f'** is a racemate and crystallizes in the monoclinic centric space group $P2_1/c$ (nº 14) with one molecule per asymmetric unit. Figure 3 in the main text shows the absolute configuration of

the 2 chiral centres, which were unequivocally determined as 3'*S**,5'*R** [*S*(C9), *R*(C17), Figure 3 in the main text]. Note, however, that also the *R*(C9), *S*(C17) enantiomer is present in an exact 1:1 ratio.

The relatively uncommon N–N covalent bond in the N2–N3–C17–C16–C9 5-membred pyrazolidine ring (Figure 3, main text) has a $d_{N2–N3}$ length of 1.424(2) Å. This ring adopts an almost perfect envelope conformation, with puckering amplitude Q_2 = 0.360(2) Å and phase ϕ_2 = 152.7(3) deg (see Cremer & Pople, J. Am. Chem. Soc.1975, 976, 1354-1358).

Figure S1 above shows the main packing motifs of **6f'**. Overall, the substance adopts a folding that maximizes close packing. However, no strong hydrogen bond donors are present, so only a small number of weak CH···O contacts are set up (Table S1 and Figure S2). Moreover, no direct hydrogen bond interactions are found that involve the secondary amine at N2. This is not unexpected, as NH donors without close possible acceptors are common in organic crystals, especially for molecules with complex foldings. Inversion-ralated molecules are arranged in a head-to-tail fashion (Figure S1a), allowing the stacking of facing indole–like rings along roughly the direction [1/3 1/3 –1], with a ~ 5.1 Å large spacing.

Table S1. Geometric parameters for the hydrogen-bonded contacts in **6f'** at room temperature. Only contacts with $d_{H\cdots A} \leq 3.0$ and DHA angles in the 120–180º angular range were deemed as significant. Values in Å / deg, with standard deviations reported in parentheses. See Figure 4 for the atom labels.

C–H···O	D-H	H···A	D···A	D-H···A	Symmetry operation
C29–H29A···O1	1.00(2)	2.77(2)	3.699(4)	155(1)	–1+x, y, z
C29–H29C···O2	1.00(1)	2.78(2)	3.738(4)	160(1)	x, ½–y, ½+z
C22–H22···O1	1.09(2)	2.69(2)	3.581(4)	138(1)	x, y, –1+z

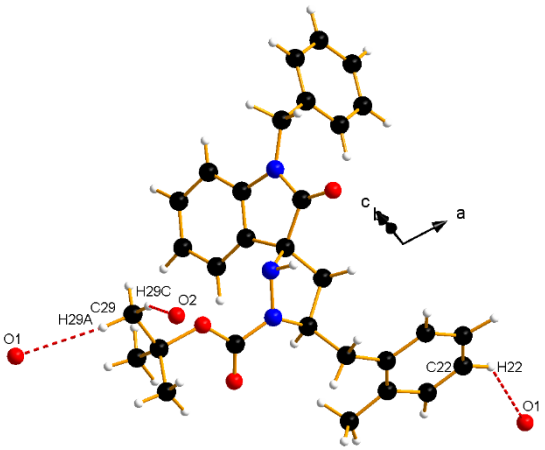

Figure S2. Interaction geometry of the **6f'** asymmetric unit. See Table S1 for the geometrical parameters of hydrogen-bonded contacts.

CCDC 1938731 contains the supplementary crystallographic data for this paper. These data can be obtained free of charge from The Cambridge Crystallographic Data Centre via www.ccdc.cam.ac.uk/structures.